

Electronic Thesis and Dissertation Repository

7-27-2015 12:00 AM

Quantitative Estimation of P-glycoprotein-Mediated Drug Transport by Mechanistically Modeled Intrinsic Clearance

Alex D. Morgan
The University of Western Ontario

Supervisor
Dr. Rommel Tirona
The University of Western Ontario

Graduate Program in Pharmacology and Toxicology
A thesis submitted in partial fulfillment of the requirements for the degree in Master of Science
© Alex D. Morgan 2015

Follow this and additional works at: <https://ir.lib.uwo.ca/etd>

 Part of the [Pharmacology Commons](#)

Recommended Citation

Morgan, Alex D., "Quantitative Estimation of P-glycoprotein-Mediated Drug Transport by Mechanistically Modeled Intrinsic Clearance" (2015). *Electronic Thesis and Dissertation Repository*. 2961.
<https://ir.lib.uwo.ca/etd/2961>

This Dissertation/Thesis is brought to you for free and open access by Scholarship@Western. It has been accepted for inclusion in Electronic Thesis and Dissertation Repository by an authorized administrator of Scholarship@Western. For more information, please contact wlsadmin@uwo.ca.

QUANTITATIVE ESTIMATION OF P-GLYCOPROTEIN-MEDIATED DRUG
TRANSPORT BY MECHANISTICALLY MODELED INTRINSIC CLEARANCE

(Thesis format: Integrated Article)

by

Alex D. Morgan

Graduate Program in Pharmacology and Toxicology

A thesis submitted in partial fulfillment
of the requirements for the degree of
Master of Science

The School of Graduate and Postdoctoral Studies
The University of Western Ontario
London, Ontario, Canada

© Alex D. Morgan 2015

Abstract

P-glycoprotein (P-gp/*ABCB1*) is an important efflux drug transporter affecting the disposition of 50% of marketed drugs. Cell monolayer permeability assays are the gold standard for assessing P-gp-drug interactions *in vitro*, but inter-laboratory assay differences produce heterogeneous results. We compared the validity and sensitivity of traditional assay metrics of efflux transport (unidirectional apparent permeability and efflux ratio) with a modeled clearance metric, CL_{P-gp} and hypothesized that CL_{P-gp} would be superior. Cell monolayers heterologously transfected with *ABCB1*, and 1,25(OH)₂D₃-modulated *ABCB1* in cells served as experimental models. P-gp expression was quantified by western blot and bidirectional [³H]-digoxin transcellular flux was measured. Linear regression analyses were performed for P-gp expression versus each P-gp activity metric. The validity and sensitivity of modeled clearance was comparable to traditional metrics within a cell type, but was superior across different cell types. In conclusion, CL_{P-gp} offers a physiologically-relevant and universally acceptable metric for efflux transport activity.

Keywords

P-glycoprotein, P-gp, modeled clearance, intrinsic clearance, apparent permeability, efflux ratio, monolayer permeability assay, efflux transporter, Caco-2, LLCPK, LMDR1

Co-Authorship Statement

For the integrated article thesis entitled “Quantitative Estimation of P-glycoprotein-Mediated Drug Transport by Mechanistically Modeled Intrinsic Clearance”, the following contributions were made:

Alex D Morgan and Dr. Rommel G Tirona designed the experiments. Alex D Morgan conducted the experiments. Alex D Morgan and Rommel G Tirona analyzed and interpreted the data. Alex D Morgan and Rommel G Tirona wrote the integrated article thesis.

Acknowledgments

I would like to thank my supervisor Dr. Rommel Tirona for giving me the opportunity to pursue my masters and for his continuous professional and emotional support and guidance throughout the entire process. I would not be where I am today without him.

I would like to thank the past and present members of the Kim/Tirona Lab for their support, advice and friendship during my time spent in the lab, including: Dr. Wendy Teft, Dr. Inna Gong, Dr. Marrienne Degorter, Ms. Sarah Woolsey, Mr. Colin Suen, Ms. Sara Mansell LeMay, Mr. Cameron Ross, Ms. Matilde Leon-Ponte, Dr. Ute Schwarz, Mr. David Sheshelidz, Dr. Daisuke Sugiyama, Dr. Hidenori Takada, Dr. Murray Cutler, Dr. Crystal Schmerk, Mr. Peter Yin, Mr. Markus Gulilat, Ms. Cheynne Mclean, Ms. Mandy Li and especially Dr. Michael Knauer, to whom I owe so much of my success.

I would like to thank my advisory committee, Dr. Richard Kim, Dr. Timothy Regnault, Dr. Sean Cregan and Dr. David Freeman for their guidance throughout this process.

Finally, words cannot express my gratitude towards my parents, Dunstan and Beverley, my siblings Cynthia and Anthony, and my dearest friends Sarah Chung and Ashbeel Roy. They have been my strength and continue to support me in all of my endeavors.

Table of Contents

Abstract.....	ii
Co-Authorship Statement.....	iii
Acknowledgments.....	iv
Table of Contents.....	v
List of Tables.....	ix
List of Figures.....	x
Abbreviations.....	xii
Chapter 1.....	1
Introduction.....	1
1.1 Pharmacokinetics.....	1
1.1.1 Absorption, distribution, metabolism and elimination (ADME).....	1
1.1.2 Interindividual variation in ADME.....	3
1.2 Transporters.....	4
1.2.1 Transporters.....	4
1.2.1.1 Physiological and pharmacological role.....	4
1.2.1.2 Structure and function.....	5
1.2.2 P-glycoprotein/MDR1.....	6
1.2.2.1 Discovery and Cloning of P-gp.....	6
1.2.2.2 Biochemistry (structure, substrates and function).....	7
1.2.2.3 Tissue expression and role in absorption, distribution and elimination.....	8
1.2.2.4 Gene regulation.....	9
1.2.2.5 Relevance of P-gp to clinical pharmacology.....	10
1.2.2.6 Relevance to drug development.....	18

1.2.2.7	Animal models.....	18
1.3	In vitro to in vivo (IVIV) prediction of pharmacokinetics	20
1.3.1	General scheme	20
1.3.2	Quantitative IVIVE.....	20
1.3.2.1	Intrinsic clearance in PK modeling	23
1.3.2.2	Facilitated (Carrier-mediated) transport kinetics.....	26
1.3.3	In vitro systems for estimating metabolism and transport	27
1.3.3.1	Hepatocytes, recombinant cells, and membrane vesicles.....	27
1.3.3.2	The cell monolayer permeability assay for efflux transport.....	30
1.3.4	In vitro estimation of drug efflux activity in the monolayer permeability assay	32
1.3.4.1	Directional apparent permeability	32
1.3.4.2	Efflux ratio.....	33
1.3.4.3	Modeled intrinsic transport clearance	33
1.3.5	Current recommendations for in vitro assessment of efflux transporter activity.....	35
1.4	Digoxin	37
1.4.1	Historical perspectives	37
1.4.2	Indications and use in Canada.....	38
1.4.3	Clinical pharmacology	39
1.4.4	Discovery as a P-gp substrate	39
1.4.5	Digoxin pharmacokinetics	40
1.4.6	Digoxin as a model P-gp substrate.....	41
1.5	Rationale	42
1.6	Objectives	44
1.7	Hypothesis.....	44
1.8	References.....	45

3.1 Study Objective.....	117
3.2 Monolayer permeability assay metrics of P-gp activity	117
3.3 Standardizing monolayer permeability assays.....	119
3.4 Applying monolayer permeability assay data to drug discovery and development	120
3.5 Applying monolayer permeability assay data to IVIVE.....	121
3.6 Limitations of the experimental approach to estimate CL_{P-gp} (model assumptions)	122
3.7 Recommendations/future studies	123
3.8 Overall conclusion	124
3.9 References.....	125
Curriculum Vitae	131

List of Tables

Table 1.1 P-glycoprotein substrates	11
Table 1.2 P-gp substrates and inhibitors	13
Table 1.3 Clinical genetic polymorphisms in MDR1	15
Table 2.1 Transwell monolayer inulin permeabilities	78
Table 2.2 Transwell monolayer P-gp and Actin expression levels.....	85
Table 2.3 Calculated P_{app} , EfR, and CL values for LLCPK and LMDR1 monolayers.	96
Table 2.4 Caclculated P_{app} , EfR and CL values for Caco-2 (0 nM), (10 nM), and (100 nM) monolayers.....	97
Table 2.5 Summary of goodness of fit (r^2) and regression slopes (m) for regression analyses of different estimates of P-gp activity with P-gp expression.....	107

List of Figures

Figure 1.1. Simplified general scheme of quantitative IVIVE.	Error! Bookmark not defined.
Figure 1.2. Schematic depiction of the physiological model for liver clearance described by Sirianni and Pang, 1997	25
Figure 1.3 The cell monolayer permeability assay	31
Figure 1.4 Schematic depiction of cytochrome P450-expressing Caco-2 cell monolayer under linear conditions described by Tam <i>et al.</i> , 2003.	34
Figure 1.5. Putative transporters expressed in cultured Caco-2 cells	36
Figure 2.1 Schematic presentation of our compartmental model	71
Figure 2.2 The cytotoxic effect of vitamin D (1,25(OH) ₂ D ₃) on cultured Caco-2 cells.....	79
Figure 2.3 [³ H]-Digoxin bidirectional flux across LLCPK and LMDR1 monolayers.	80
Figure 2.4 [³ H]-Digoxin bidirectional flux across Caco-2 (0 nM), (10 nM), and (100 nM) monolayers	81
Figure 2.5 P-gp western blots for LLCPK, LMDR1, and Caco-2 (0 nM), (10 nM), and (100 nM) experiment monolayers	83
Figure 2.6 [³ H]-Digoxin A-B and B-A apparent permeability values for LLCPK, LMDR1, and Caco-2 (0 nM), (10 nM), and (100 nM) monolayers	87
Figure 2.7 [³ H]-Digoxin efflux ratio LLCPK, LMDR1, and Caco-2 (0 nM), (10 nM), and (100 nM)	88
Figure 2.8 Model fitting of inulin transport across LLCPK, LMDR1, and Caco-2 (0 nM), (10 nM), and (100 nM) monolayers	90

Figure 2.9 Model fits of [³ H]-digoxin transwell transport across LLCPK and LMDR1 cell monolayers	92
Figure 2.10 Model fits of [³ H]-digoxin transwell transport across Caco-2 (0 nM), (10 nM), and (100 nM) cell monolayers	93
Figure 2.11 Modeled CL_{P-gp} , CL_{A-C} , CL_{C-B} , and CL_{A-B} of bidirectional [³ H]-digoxin transport across LLCPK, LMDR1, and Caco-2 (0 nM), (10 nM), and (100 nM) monolayers	95
Figure 2.12 Normalized $P_{app(A-B)}$ coefficients vs. normalized P-gp expression for LLCPK and LMDR1 data alone, for Caco-2 (0 nM), (10 nM) and (100 nM) data alone, and for all data combined.....	100
Figure 2.13 Normalized $P_{app(B-A)}$ coefficients vs. normalized P-gp expression for LLCPK and LMDR1 data alone, for Caco-2 (0 nM), (10 nM) and (100 nM) data alone, and for all data combined.....	102
Figure 2.14 Normalized EfR coefficients vs. normalized P-gp expression for LLCPK and LMDR1 data alone, for Caco-2 (0 nM), (10 nM) and (100 nM) data alone, and for all data combined.....	104
Figure 2.15 Normalized CL_{P-gp} coefficients vs. normalized P-gp expression for LLCPK and LMDR1 data alone, for Caco-2 (0 nM), (10 nM), and (100 nM) data alone, and for all data combined.....	106

Abbreviations

<i>ABCB1</i>	ATP-binding cassette, subfamily B, member 1
ADME	Absorption, distribution, metabolism, elimination
AUC	Area under the curve
BCRP	Breast cancer resistance protein
BBB	Blood-brain barrier
BSP	Bromosulfophthalein
C_u	Unbound (free) drug concentration
Caco-2	Human colorectal adenocarcinoma cell line
Caco-2 (0 nM)	Untreated Caco-2 cells
Caco-2 (10 nM)	Caco-2 cells treated with 10 nM 1,25(OH) ₂ D ₃
Caco-2 (100 nM)	Caco-2 cells treated with 100 nM 1,25(OH) ₂ D ₃
Calcitriol	1,25-dihydroxycholecalciferol or 1,25-dihydroxyvitamin D ₃
CAR	Constitutive androstane receptor
CL	Clearance
CL _{int}	Intrinsic clearance
CL _{int(Metabolism)}	Intrinsic metabolic clearance
CL _{int(Transport)}	Intrinsic carrier-mediated clearance
CL _{P-gp}	P-gp intrinsic clearance
CL _{plasma}	Systemic plasma clearance

C_{\max}	Peak serum concentration
CNS	Central nervous system
CNV	Copy number variation
C_p^{ss}	Steady-state plasma concentration
CYP	Cytochrome P450
DDD	Drug discovery and development
DDI	Drug-drug interaction
DME	Drug metabolizing enzyme
DMEM	Dulbecco's modified Eagle's medium
DMSO	Dimethyl sulfoxide
EfR	Efflux ratio
F	Bioavailability
FBS	Fetal bovine serum
FDA	Food and Drug Administration
FXR	Farnesoid X receptor
GST	Glutathione S-transferase
HPT1	Human peptide transporter 1
IV	Intravenous
IVIVE	<i>In vitro</i> to <i>in vivo</i> extrapolation
KHB	Krebs-Henseleit Bicarbonate Buffer

K_m	Michaelis-Menten constant
LLCPK	Porcine kidney epithelial cell line
LMDR1	LLCPK overexpressing MDR1
m	Slope
MATE	Multidrug and toxin extrusion transporter
MDCK	Madin-Darby canine kidney cell line
MDR1	Multi-drug resistance protein 1
MRP	Multidrug resistance-associated protein
MTT	Thiazolyl blue tetrazolium bromide
NEAA	Nonessential amino acids
NCE	New chemical entity
NDA	New drug application
OAT	Organic anion transporter
OATP	Organic anion-transporting polypeptide
OCT	Organic cation transporter
OST α	Organic solute transporter α
OST β	Organic solute transporter β
P_{app}	Apparent permeability
$P_{app(A-B)}$	Apical to basolateral apparent permeability
$P_{app(B-A)}$	Basolateral to apical apparent permeability

PBPK	Physiologically-based pharmacokinetics
PBS	Phosphate-buffered saline
PepT1	Peptide transporter 1
P-gp	P-glycoprotein
PK	Pharmacokinetic(s)
P.O.	Per os/Oral ingestion
PXR	Pregnane X receptor
RXR	Retinoic acid receptor
SLC	Solute-carrier group of membrane transporters
SNP	Single nucleotide polymorphism
TEER	Transepithelial electrical resistance
V_d	Volume of distribution
VDR	Vitamin D receptor

Chapter 1

Introduction

1.1 Pharmacokinetics

Pharmaceuticals agents act on various molecular targets throughout the body. A particular concentration of unbound drug must be achieved at a given site of action for a drug to produce its intended pharmacological effect. However, a much lower level of drug will not produce the desired therapeutic effect and a much higher level can be associated with toxicity. Therefore, drug concentration present at different sites is a critical determinant of the pharmacological efficacy of any drug therapy.

Pharmacokinetics (PK) is a branch of pharmacology that examines the interplay between drug properties and physiological processes in the body to dictate circulating drug levels over time.

1.1.1 Absorption, distribution, metabolism and elimination (ADME)

The pharmacokinetic processes can be broken down into absorption, distribution, metabolism, and elimination (excretion), given the common acronym ADME. *Absorption* refers to the pharmacokinetic processes involved in the movement of administered drugs into the systemic circulation and the bioavailability of a drug describes the fraction of an administered dose that actually reaches the systemic circulation unchanged. Any drug that is not injected directly into the blood stream by intravenous (IV) administration must cross at least one cell membrane barrier to enter the circulation. Permeability across any cell membrane is a function of the physiochemical properties of both the drug (i.e. molecular size, shape, ionization, and lipid solubility) and the membrane (e.g. protein channels and drug transporters). Drug movement may occur via passive diffusion through the lipid membrane and/or via carrier-mediated transport. Many primary active transporter proteins show unidirectional transport activity and depending on their orientation in polarized epithelia, they may either facilitate or oppose absorption from the GI tract and other body compartments. Since the vast majority of drugs are administered by oral dose (per os), factors affecting GI drug absorption are of particular therapeutic concern.

During the *distribution* phase, a drug achieves a certain concentration in the blood (C_{Plasma}), which changes over time. Transporters expressed in various tissues of the body may play a role in the selective accumulation and distribution of drugs into target tissues. The term volume of distribution (V_d) describes overall how well a drug distributes from the blood into body tissues.

Chemical modification, or *metabolism*, of parent drugs occurs primarily in the liver to produce metabolites of increased polarity. Many of the metabolic reactions are mediated by a class of heme-containing enzymes found in the hepatocyte endoplasmic reticulum, which are known as the cytochrome P450 superfamily of oxygenases (CYP). There are 57 genes and over 59 pseudogenes in humans, divided among 18 families and 43 subfamilies by sequence homology (1). The CYP 1 to 3 families are the biggest contributors to drug metabolism in humans. In particular, cytochrome P450 family 3, subfamily A, member 4 (CYP3A4) metabolizes as many as 50 percent of drugs on the market and is the most clinically relevant of the CYP isoforms (1;2).

Polar parent drugs and metabolites are *eliminated* by passive filtration into the urine or by carrier-mediated transport into the urine or stool. Plasma clearance (CL_{plasma}) represents the irreversible removal of a drug from the plasma, as a volume cleared per unit time, and it is the summation of elimination processes in the body. CL_{plasma} can be determined from the area under the plasma concentration curve (AUC) following a single IV dose as Dose/AUC . The half-life ($t_{1/2}$) of a drug – the amount of time it takes for drug concentrations in blood to decline by 50 percent – also relates to the plasma clearance and volume of distribution by the following relationship:

$$t_{1/2} = 0.693 \times \frac{V_d}{CL} \quad [1.1]$$

For multiple dosing, C_{Plasma} oscillates with each dose until an average steady-state plasma concentration (C_p^{ss}) is reached when the rate of administration is equal to the rate of elimination.

At steady state:

$$\frac{D}{\tau} = CL \times C_p^{ss} \quad [1.2]$$

where,

$$\text{Rate of drug administration} = \frac{D}{\tau} \quad [1.3]$$

$$\text{Rate of drug elimination} = CL_{\text{plasma}} \times C_p^{ss} \quad [1.4]$$

The drug dose (D) and dosing frequency (τ) are selected inversely proportional to the CL_{plasma} , such that the C_p^{ss} of a drug remains within the therapeutic range.

1.1.2 Interindividual variation in ADME

As suggested in Section 1.1.1, drug transporters and drug metabolizing enzymes (DMEs) play a critical role in ADME processes. Accordingly population variations in these ADME proteins can account for striking differences observed in the way that certain individuals or populations handle a particular drug (3; 4). For many drugs, pharmacokinetics and thus optimal dosing can vary significantly between patients; the standard dosing regimen may fail to reach a therapeutic level in some individuals or may exhibit dose-dependent toxicity in others. This is of particular concern for drugs with a narrow therapeutic index (the ratio between the therapeutic dose and the toxic dose).

Both genetic and environmental factors can contribute to the variations in ADME protein activity and expression that are responsible for population pharmacokinetic variability. Genetic polymorphisms are DNA sequence variants that naturally occur at a given genome locus in more than 1% of the population and are not due to recurrent mutations. They may be in the form of a single substituted, inserted or deleted nucleotide base (a single nucleotide polymorphism or SNP), or a larger segment of DNA that is present in irregular frequency (copy number variation or CNV). Polymorphisms appear broadly throughout the human genome and many polymorphic sites have been shown to impact the expression and/or function of a variety of gene products, including several key drug metabolizing enzymes and transporters (4-6).

Exposure to xenobiotics can also produce significant interindividual variation in the activity and expression of drug metabolizing enzymes and drug transporters. A drug interaction is said to have occurred when the presence of foods, dietary supplements, other drugs or drug diluents cause variation in drug response. Co-administered compounds may bind an enzyme or transporter to cause a concentration-dependent decrease in enzyme or transporter activity. They may also inhibit or induce ADME protein activity by modulating gene expression via transcriptional mechanisms involving nuclear hormone receptors. Those interactions that result specifically from the presence of a second drug, termed drug-drug interactions (DDIs), have been a recognized obstacle to successful drug therapy since the 1960s (7; 8).

As a result of the ever-growing list of clinically relevant genetic polymorphisms and drug-drug interactions, many drug regulatory agencies, including the FDA, offer recommendations for routine assessment and management of polymorphisms and DDIs during drug discovery, drug development and clinical drug use. Pharmacogenomic and drug-drug interaction studies have become critical in the selection of new chemical entities with desirable pharmacokinetics and in elucidating the mechanisms underlying observed preclinical and clinical drug levels. It is important to know how extensively particular polymorphisms and DDIs alter the expression and or activity of ADME proteins and to know how this information translates into the clinical setting.

1.2 Transporters

1.2.1 Transporters

1.2.1.1 Physiological and pharmacological role

Transporters are transmembrane proteins that are expressed in the various tissues of the body to facilitate the movement of important endogenous compounds across the cell plasma membrane. Endogenous substrates include inorganic ions, amino acids, sugars and nucleotides. However, substrate specificity is not limited to physiological compounds. Many transporters, in fact, recognize a variety of structurally diverse xenobiotics including environmental compounds, dietary compounds, drugs and drug metabolites. Transporters can thus have an important role in pharmacokinetics and

therapeutic efficacy and can be a mechanism for interindividual variability, interspecies variability and drug-drug interactions.

1.2.1.2 Structure and function

Due to their hydrophobic nature, relatively low abundance, and inherently flexible structure, molecular identification of transporters was difficult to accomplish until the development of modern expression cloning techniques in the early 1990s. Three dimensional crystal structures have only been achieved at atomic resolution for a limited number of transporters thus far. Nonetheless, drug transporters can be categorized molecularly into two major groups: the ATP-binding cassette (ABC) and the solute carrier (SLC) superfamilies of transporters. In humans, the ABC superfamily is comprised of 7 families with 48 known members (9; 10). These transporters have an ATP-binding domain that binds and hydrolyzes ATP to power active transport of substrates against a concentration gradient. The most well characterized members of this superfamily are the *ABCB1* and *ABCG2* members known as P-glycoprotein/multidrug resistance protein 1 (MDR1) and breast cancer resistance protein (BCRP) respectively. The SLC superfamily is comprised of 55 families, with approximately 362 known members (11). These transporters do not have an ATP-binding domain, but instead use an ion gradient to power active transport of their substrates. Important SLC drug transporters are the organic anion-transporting polypeptide 1B1 (OATP1B1), the organic anion-transporting polypeptide 1B3 (OATP1B3), the organic anion transporter 1 (OAT1) the organic anion transporter 3 (OAT3), and the organic cation transporter 2 (OCT2) (12). Respectively, these transporters are the *SLCO1B1*, *SLCO1B3*, *SLC22A6*, *SLC22A8*, and *SLC22A2* members of the solute-carrier transporter family.

In addition to molecular categorization, transporters can also be grouped by their function. Uptake transporters move substrates from the extra cellular space into the cell cytoplasm. This is more common among SLC drug transporters. Conversely, efflux transporters extrude substrates into the extracellular environment, which is more common among, but not limited to, the ABC drug transporters. Quite often, uptake and efflux transporters coordinate activity for the asymmetrical transport of endogenous compounds, drugs, or toxins across an epithelial or endothelial barrier of cells (13). This kind of

vectorial transport is how polarized cells can facilitate passage of both hydrophilic and lipophilic compounds across biological membranes to contribute to drug absorption, distribution and elimination, as alluded to in Section 1.1.1.

Vectorial transport is possible because of overlap in the substrate specificities of different uptake and efflux transporters. For example, in a model of the blood to bile hepatic secretion of organic anions, Cui *et al.* showed vectorial transport of sulfobromophthalein (BSP) across a membrane of polarized Madin-Darby canine kidney (MDCK) cells that were double-transfected with organic anion transporter 1B3 (*OATP1B3*; SLC member *SLCO1B3*) and multidrug resistance-associated protein 2 (*MRP2*; ABC member *ABCC2*) (14). The cells demonstrated basolateral *OATP1B3* uptake and subsequent apical *MRP2* efflux of BSP. For highly lipophilic compounds with sufficient membrane permeability, unidirectional ABC efflux transporters are able to achieve vectorial transport across a polarized plasma membrane without coordinated influx by an uptake transporter (15). But, coordination of uptake and efflux transporters is necessary for the vectorial transport of more hydrophilic compounds. Consequently, a variety of different uptake and efflux transporters are expressed on either membrane of the polarized epithelial or endothelial cells of several organs. This includes intestinal epithelia, hepatocyte epithelia, kidney proximal tubule epithelia, and endothelial cells of the blood-brain barrier.

1.2.2 P-glycoprotein/MDR1

The role of transporters in pharmacokinetics is a maturing area of investigation and the important pharmacokinetic impacts of many transporters have yet to be fully elucidated. P-glycoprotein was among the first transporters to be studied; it is the most well characterized transporter to date and it was the first transporter protein recommended for regular pharmacokinetic testing by the FDA (16-18).

1.2.2.1 Discovery and Cloning of P-gp

In 1960, acquired resistance to actinomycin D was reported in HeLa cell lines (19) and then later in Chinese hamster ovary cells (20). These cells were shown to possess multidrug resistance and subsequently Dano *et al.* demonstrated active efflux of daunomycin in the cells by a proposed efflux pump (21). Juliano and Ling named the

pump permeability-glycoprotein (P-glycoprotein or P-gp), for its ability to alter the permeability of mutant cells (22). In the following decade, Riordan and his group were the first to clone the gene for P-glycoprotein (23). By 1987, it became apparent that P-gp is physiologically expressed in normal human excretory and barrier tissues, such as the intestine, liver, kidney and the blood brain barrier (24-34). Ultimately, P-gp was defined as a primary efflux pump that uses the energy from ATP hydrolysis to actively extrude its substrates from cells (35). The gene for the transporter was originally called multidrug resistance gene (MDR1) because of the multidrug resistance phenotype it conferred to tumour cells, but has since been classified as *ABCB1* (member 1 of the B subfamily in the ATP-binding cassette transporter superfamily). In 2009, the P-gp x-ray crystal structure was revealed for better characterization of substrate-binding and solute translocation mechanism of this key drug transporter (36). Today, P-gp remains the most well studied and well characterized drug transporter in humans.

1.2.2.2 Biochemistry (structure, substrates and function)

P-gp is a 170 kDA protein composed of 1280 amino acids. Its quaternary protein structure is organized as 2 homologous halves, each with an intracellular nucleotide binding domain and a bundle of 6 hydrophobic transmembrane α -helices (36-39). N-glycosylation occurs at the first extracellular loop and the 2 halves are linked by a highly charged and phosphorylated region. The linking region contains signature motifs that are characteristic of the ABC transporter family. Collectively, the transmembrane segments form a central internal cavity where multiple sites are found for substrate and modulator binding (36). This binding pocket is substantially larger than most transporters and can even accommodate 2 substrates simultaneously (40). Additionally, substrate binding in the pocket produces size- and shape-dependent conformational changes of the transmembrane segments, alluding to an induced-fit for substrate binding (40). Taken together, some of these structural characteristics may explain the incredibly broad substrate specificity observed for the P-gp transporter.

P-gp transports a wide variety of structurally and functionally diverse compounds including: opioids, steroids, antibiotics, calcium-channel blockers, chemotherapeutics, immunosuppressants, anti-HIV drugs, linear and cyclic peptides, ionophores, bilirubin,

and many others (41) (Table 1.1). Many P-gp substrates are nonpolar, weakly amphipathic compounds and contain planar aromatic rings and positively charged tertiary nitrogens. However, there are no clearly defined recognition elements that are highly conserved among all P-gp substrates and modulators. It is worth noting though, that many of P-gp's substrates are also found to be substrates of the CYP3A4 enzyme, suggesting MDR1 and CYP3A4 have a synergistic protective role to reduce the intestinal absorption of xenobiotics (42-44; 5).

P-glycoprotein functions as a unidirectional lipid flipase (45). Substrate binding initiates ATP-binding, which causes dimerization of the nucleotide binding domains (NBD), which results in a large structural change of the transporter protein into its outward facing conformation. The substrate is then released into extracellular space as ATP is hydrolyzed. Simultaneously, the ATP hydrolysis disrupts the NBD dimerization, hence causing P-gp to revert back to its original inward facing conformation (46). In P-gp's active conformation, the internal cavity formed by the transmembrane helices, is oriented inward, open to both the cytoplasm and the inner membrane leaflet (47). Substrates in the outer membrane leaflet and the extracellular space do not have direct access to the pocket (36; 48) and P-gp extrudes its substrates directly from the inner leaflet; this is a common feature among transporters with a binding site located in a transmembrane domain of α -helices. Many P-gp substrates readily partition into the plasma membrane and require association with lipids for drug-stimulated ATPase activity (49).

1.2.2.3 Tissue expression and role in absorption, distribution and elimination

Cells that express P-gp extrude substrates directly from the membrane, thereby preventing substrate drugs and toxins from entering the cell. Immunohistochemical analysis has indicated that human P-gp is expressed typically at the apical membrane of polarized cells in several tissues with barrier functions (e.g. small intestine, blood-brain barrier, blood-testis barrier, blood-ovarian barrier and placenta) or secretory functions (e.g. liver, kidney and adrenal gland) (50; 51; 44; 52-54). The greatest MDR1 expression is found in the intestinal epithelia; again indicating an important role of P-gp in modulating intestinal absorption. Indeed, induction of intestinal P-gp by the antibiotic rifampin correlated with a significant decrease in the AUC of orally administered

digoxin, a P-gp substrate, in humans (55). Beyond this, P-gp is apically expressed in liver and kidney epithelia, and on the blood side of brain capillary endothelial cells. It plays a significant role in the biliary and urinary excretion of various drugs and is known to limit central nervous system (CNS) penetration, as part of the blood-brain barrier (26; 56).

Despite the broad activity of P-gp, the Collie dog breed and a substrain of the CF-1 mouse are viable and fertile even though they are both naturally devoid of any P-gp expression (57-59). From this it can be concluded, in dogs and mice at least, that P-gp does not carry an essential physiological function. However, no human null allele has ever been reported for P-glycoprotein to date. Also of note, collie dogs and CF-1 mice do show significantly heightened sensitivity to drug and xenobiotic exposure; this once again emphasizing the important protective role of P-gp in the body (58-60).

1.2.2.4 Gene regulation

For decades, it has been well appreciated that the body mounts an adaptive response when exposed to xenobiotics, which is meant to limit exposure to toxic compounds. Indeed, in 1963 Cucinell *et al.* first reported decreased concentrations of phenytoin and coumarin in humans treated with phenobarbital; likely in response to upregulation of drug metabolizing enzymes (61-63). This kind of ADME protein regulation occurs via ligand-activated nuclear receptor signaling. In the case of most nuclear receptors, the receptor binds its ligand in the cytoplasm and then translocates to the nucleus, where it forms a heterodimer with the 9-cis retinoic acid receptor (RXR). The formed heterodimer complex may bind in the regulatory region of a given ADME protein gene, thereby affecting the binding and recruitment of co-repressor and co-activator proteins, which suppress and stimulate gene transcription respectively (64).

The transcription of many drug metabolizing enzymes has been shown to be modulated in response to xenobiotic ligands that bind the nuclear receptors: Pregnane X Receptor (PXR) (65-69), Constitutive Androstane Receptor (CAR) (70-73), Vitamin D Receptor (VDR) (74; 75), Farnesoid X Receptor (FXR) (76-78) and others.

It is only in the past 2 decades or so that regulation of drug transporters by the same nuclear receptor mechanisms has gained attention as part of a coordinated response to

xenobiotic toxic exposure. The P-gp transporter was shown to be regulated by PXR, similar to CYP3A4 (43). Both PXR and CAR binding sites are located in an *ABCB1* regulatory region 8 kb upstream of the MDR1 gene transcription start site (80; 81). P-gp has also been shown to be regulated by Vitamin D. When testing for substances that can induce CYP3A4 expression in Caco-2 cells, Schmiedlin-ren *et al.* observed an increase in P-gp expression after treating cells with 0.05 μM – 1 μM 1,25(OH)₂D₃, and $\geq 0.5 \mu\text{M}$ and $\geq 2.5 \mu\text{M}$ 25-(OH)-D₃ (82). Thummel *et al.* later demonstrated similar vitamin D modulation of P-gp in Caco-2 cells and LS180 human colon carcinoma cells by 50-1000 nM 1,25(OH)₂D₃; with a lower limit of induction at 1 nM and an upper limit at 250 nM (83). Eventually the vitamin D response elements were identified in the human MDR1 promoter between -7880 and -7810 bp upstream of the *MDR1* gene, where the VDR/RXR α heterodimer binds to induce transcription (84). Fan *et al.* has since confirmed that vitamin D and associated analogues induce P-gp mRNA, protein, and transport activity in a human colorectal adenocarcinoma (Caco-2) cell monolayers (85).

1.2.2.5 Relevance of P-gp to clinical pharmacology

A large number of chemically diverse drugs have been demonstrated to interact with P-gp (Tables 1.1 and 1.2) and thus P-gp has the potential to contribute to a great many clinically significant drug-drug interactions. For example, in a study of healthy volunteers, Schwarz *et al.* showed respectively a 52% and 26% increase in the AUC and peak plasma concentration of a prototypical P-gp substrate, talinolol, in response to concomitant administration of the P-gp inhibitor erythromycin (86). This study notwithstanding though, much of the evidence for clinical drug interactions mediated by P-gp is derived indirectly from *in vitro* studies or from animal studies; and few clinically relevant DDIs have actually been attributed solely to P-gp. One significant reason for this is the extensive overlap in substrate selectivity, tissue localization, and gene modulation profile that is shared between MDR1 and CYP3A4 (87). It can be difficult to distinguish the *in vivo* contributions of metabolism and transport to DDIs; and metabolism is often assumed the major cause of DDI, particularly for substrates with fair or extensive metabolism. However, DDIs involving poorly metabolized P-gp substrates and potent and selective P-gp modulators have been linked more unambiguously to P-gp (88; 55;

Table 0.1. P-glycoprotein substrates.

Substrate	References
Anticancer agents	
Actinomycin D	Jette et al., 1995
Daunorubicin	Sharpiro and Ling, 1998
Docetaxel	Wils et al., 1994
Doxorubicin	Sharpiro and Ling, 1998
Etoposide	Sharpiro and Ling, 1998
Imatinib	Widmer et al., 2003
Irinotecan	Arimori et al., 2003
Mitomycin C	Relling, 1996
Mitoxantrone	Relling, 1996
Paclitaxel	Sparreboom et al., 1997
Teniposide	Relling, 1996
Topotecan	Relling, 1996
Vinblastine	Wils et al., 1994
Vincristine	Relling, 1996
Antihypertensive agents	
Celiprolol	Karlsson et al., 1993
Diltiazem	Saeki et al., 1993
Losartan	Soldner et al., 2000
Talinolol	Wetterich et al., 1996
Antiarrhythmics	
Digoxin	de Lannoy and Silverman, 1992
Quinidine	Kim et al., 1999
Verapamil	Kim, 2002
Antiplatelet agents	
Clopidogrel	Taubert et al., 2006
Ticagrelor	Teng et al., 2010
Glucocorticoids	
Aldosterone	Ueda et al., 1992
Cortisol	Ueda et al., 1992
Dexamethasone	Ueda et al., 1992
Methylprednisolone	Saitoh et al., 1998
Oral anticoagulants	
Warfarin	Schulman et al., 2010
Dabigatran	Walenga and Adiguzel, 2010
Rivaroxaban	Gnoth et al., 2011
Apixaban	Warson et al., 2011
Edoxaban	Mendell et al., 2011
Miscellaneous	
Atrovastatin	Wu et al., 2000
Colchicine	Kim, 2002
Fexofenadine	Cvetkovic et al., 1999
Ivermectin	Didier and Loof, 1995
Loperamide	Schinkel et al., 1996
Melfoquine	Pham et al., 2000
Rhodamine 123	Kim, 2002
Terfenadine	Kim et al., 1999
Vecuronium	Smit et al., 1998
Antiviral agents	
Ampranavir	Polli et al., 1999

Indinavir	Kim et al., 1998
Nelfinavir	Kim et al., 1998
Ritonavir	Kim et al., 1998
Saquinavir	Kim et al., 1998
Antibiotics	
Erythromycin	Schuetz et al., 1998
Levofloxacin	Ito et al., 1997
Rifampin	Schuetz et al., 1996
Sparfloxacin	Tamai et al., 2000
Tetracycline	Kavallaris et al., 1993
Antimycotics	
Intraconazole	Miyama et al., 1998
Immunosuppressants	
Cyclosporine	Schinkel et al., 1996
Sirolimus	Paine et al., 2002
Tacrolimus	Saeki et al., 1993
Valspodar	Tai, 2000
Antidepressants	
Amitriptyline	Uhr et al., 2000
Antiepileptics	
Phenobarbital	Potschka et al., 2002
Phenytoin	Schinkel et al., 1996
Antiacids	
Cimetidine	Collett et al., 1999
Ranitidine	Collett et al., 1999
Opioids	
Morphine	Callagan and Riordan, 1993
Antiemetics	
Domperidon	Schinkel et al., 1996
Ondansetron	Schinkel et al., 1996

Table 0.2. Drugs shown in clinical and/or *in vitro* study to affect the pharmacokinetics of a P-gp probe substrate by inhibition or induction of P-gp.

Interacting Drug	Inhibitor/Inducer	Substrate(s)	References
Antihypertensive agents			
Carvedilol	Inhibitor	vinblastine, paclitaxel, doxorubicin, daunorubicin	kakumoto <i>et al.</i> , 2003
Nicardipine	Inhibitor	daunorubicin, digoxin	Katoh <i>et al.</i> , 2000
Reserpine	Inhibitor	ATP hydrolysis assay	Wang <i>et al.</i> , 2001
Antiarrhythmics			
Amiodarone	Inhibitor	digoxin	Kakumoto <i>et al.</i> , 2002
Propafenone	Inhibitor	digoxin	Woodland <i>et al.</i> , 1997
Quinidine	Inhibitor	digoxin	Fromm <i>et al.</i> , 1999
Verapamil	Inhibitor	digoxin	Pauli-Magnus <i>et al.</i> , 2000
Glucocorticoids			
Dexamethasone	Inducer	indinavir	Lin <i>et al.</i> , 1999
Miscellaneous			
Atrovastatin	Inhibitor	digoxin	boyd <i>et al.</i> , 2000
Bromocriptine	Inhibitor	vincristine	Orlowski <i>et al.</i> , 1998
Dipyridamole	Inhibitor	digoxin	Verstuyft <i>et al.</i> , 2003
Emetine	Inhibitor	ATP hydrolysis assay	Wang <i>et al.</i> , 2001
Melfoquine	Inhibitor	vinblastine, fluo-3 acetomethoxy ester, rhodamine 123	Riffkin <i>et al.</i> , 1996
Progesterone	Inhibitor	vinblastine	Bernes <i>et al.</i> , 1996
Retinoic acid	Inducer	vinblastine, colchicine	Elhafny <i>et al.</i> , 1997
Spirolactone	Inhibitor	digoxin	Nakamura <i>et al.</i> , 2001
Antiviral agents			
Amprenavir	Inhibitor		
Indinavir	Inhibitor/Inducer		
Nelfinavir	Inhibitor/Inducer		
Ritonavir	Inhibitor	digoxin	Reinhard <i>et al.</i> , 2004; Schmitt <i>et al.</i> 2010
Saquinavir	Inhibitor	digoxin	Schmitt <i>et al.</i> 2010
Antibiotics			
Clarithromycin	Inhibitor	digoxin	Wakasugi <i>et al.</i> , 1998
Erythromycin	Inhibitor	digoxin	Kim <i>et al.</i> , 1999
Rifampin	Inducer	digoxin	Greiner <i>et al.</i> , 2002
Antimycotics			
Intraconazole	Inhibitor	vinblastine, daunorubicin, dauxorubicin	Takara <i>et al.</i> , 1999
Ketoconazole	Inhibitor	rhodamine 123	Takano <i>et al.</i> , 1998
Immunosuppressants			
Cyclosporine	Inhibitor	rhodamine 123	Yacyshyn <i>et al.</i> , 1996
Sirolimus	Inhibitor	digoxin	Minocha <i>et al.</i> , 2012
Tacrolimus	Inhibitor	vincristine	Kochi <i>et al.</i> , 1999
Valspodar	Inhibitor	N-methyl-quinidine	PSC 833
Antidepressants			
Fluoxetine	Inhibitor	digoxin	Parianteet <i>et al.</i> , 2009
Paroxetine	Inhibitor	calcein-AM	Weiss <i>et al.</i> , 2003
Sertraline	Inhibitor	calcein-AM	Weiss <i>et al.</i> , 2003

St John's wort	Inducer	digoxin	Durr <i>et al.</i> , 2000
Neuroleptics			
Chlorpromazine	Inhibitor	verapamil	Saitoh and Aungst, 1995
Flupenthixol	Inhibitor	iodoarylazidoprazosin	Maki <i>et al.</i> , 2003
Phenothiazine	Inducer	vincristine	Watanabe <i>et al.</i> , 1995
Opioids			
Methadone	Inhibitor	vinblastine	Callaghan and Riordan, 1993
Morphine	Inducer	expression	Aquilante <i>et al.</i> , 2000
Pentazocine	Inhibitor	vinblastine	Callaghan and Riordan, 1993

Table 0.3. Genetic polymorphisms in *MDR1* with clinically observed PK effects.

SNP	Drug	Parameter	Effect	Reference
C3435T (Exon 26)	Digoxin (oral, ss)	Drug level	Higher for TT	Hoffmeyer et al., 2000
	Digoxin (oral, sd)	AUC	Higher for TT	Verstuyft et al., 2003
	Digoxin (oral, sd)	AUC(0-4 h), C _{max}	No difference	Gerloff et al., 2002
	Digoxin (oral, sd)	AUC	Lower for TT	Sakaeda et al., 2001
	Digoxin (oral, sd)	AUC, t _{max}	Lower for TT	Horinouchi et al., 2002
	Fexofenadine	AUC	No difference	Drescher et al., 2002
	Fexofenadine	AUC	Lower for TT	Kim et al., 2001
	Nelfinavir	Drug level	Lower for TT	Fellay et al., 2002
	Cyclosporine	Trough level	No difference	von Ahnen et al., 2001
	Cyclosporine	AUC, C _{max} , t _{max}	No difference	Min and Ellingrod, 2002
	Cyclosporine	AUC, C _{max}	Lower for CT/TT	Yates et al., 2003
	Cyclosporine	AUC(0-4 h)	Higher for TT (trend)	Balram et al., 2003
	Tacrolimus	Drug level	Higher for TT	Macphee et al., 2002
	Tacrolimus	Drug level	Higher for TT/CT	Zheng et al., 2003
	Tacrolimus	Drug level	No difference	Anglicheau et al., 2003
	Tacrolimus	Drug level	No difference	Goto et al., 2002
	Tacrolimus	Tacrolimus induced neurotoxicity	No difference	Yamauchi et al., 2002
	Nortriptyline	Drug level	No difference	Roberts et al., 2002
	Talinolol	AUC	No difference	Siegmund et al., 2002
	Loperamide	C _{max} , AUC, CNS effects	No difference	Pauli-Magnus et al., 2003
Dicloxacillin	Drug level	No difference	Putnam et al., 2003	
Docetaxel	Clearance	No difference	Goh et al., 2002	
Phenytoin	Drug level	Higher for TT	Kerb et al., 2001	
G2677T/A (Exon 21)	Digoxin (oral, sd)	AUC	Higher for TT	Verstuyft et al., 2003
	Digoxin (oral, sd)	AUC(0-4h), C _{max}	No difference	Gerloff et al., 2002
	Digoxin (oral, sd)	AUC, t _{max}	Lower for TT	Horinouchi et al., 2002
	Digoxin (oral-iv, sd)	Bioavailability	Higher for TT	Kurata et al., 2002
	Fexofenadine	AUC	Lower for TT	Kim et al., 2001
	Tacrolimus	Drug level	Higher for TT/GT	Zheng et al., 2003
	Tacrolimus	Drug level	Higher for TT	Anglicheau et al., 2003
Tacrolimus	Drug level, dose ratio	No difference	Goto et al., 2002	

Tacrolimus	Tacrolimus induced neurotoxicity	Higher for TT (trend)	Yamauchi et al., 2002
Talinolol	AUC	Slightly higher for TA/TT	Siegmund et al. 2002

ss, steady state; sd, single dose

89).

In recent decades, DDIs with selective P-gp inhibitors have been exploited to boost the efficacy of anticancer drugs. The idea was first introduced in 1981 when Tsuruo *et al.* discovered that verapamil increased the sensitivity of multi-drug resistant leukemia cells to chemotherapeutic drugs *in vitro* (90). As a consequence of this study, additional work has been put into designing potent and selective P-gp inhibitors to be used as adjuncts to chemotherapy. In one Phase I clinical study, there was an 89% increase in AUC and 46% decrease in clearance of etoposide in response to intravenous infusion of the selective P-gp inhibitor PSC-833 (91). Today, P-gp inhibitors may also be applied to enhancing drug penetration through the blood-brain-, blood-cerebrospinal-, and maternal-fetal-barriers as well (92-94).

Beyond DDIs, different polymorphisms of the *MDR1* gene exist in the population with varied functional consequences (Table 1.3). Kioka *et al.* were the first to identify *MDR1* polymorphisms in 1989 from *in vitro* study of cancer cells; since that time over 2 dozen *MDR1* SNPs have been reported with different frequencies across ethnic populations (95-98). A cytosine to thymine SNP at position 3435 in exon 26 (C3435T) was the first polymorphism reported to affect P-gp protein expression, although this SNP does not alter the encoded amino acid – thus referred to as a synonymous SNP (99). Healthy Caucasian subjects with the variant T allele were shown to have a 2-fold reduction in duodenal P-gp expression as compared to subjects with the wild type C allele (99). These individuals also showed increased plasma concentration of the P-gp probe substrate digoxin following its oral administration; this suggesting enhanced oral absorption in individuals with diminished duodenal P-gp expression. Several different studies confirmed the impact of this polymorphism (100-102). But others have actually reported the variant allele (3435T) to yield decreased serum digoxin (103; 104), or to have no clinical effect at all (105). As with DDIs, the clinical impact of P-gp polymorphisms can be quite ambiguous and complex.

1.2.2.6 Relevance to drug development

Owing to improvements in CYP molecular biology, to readily available *in vitro* models, and to *in silico* approaches, high-throughput scanning of CYP enzymes has been increasingly embraced by industry and regulatory agencies for almost 2 decades (106-108). As the body of work in the area of drug transporters catches up with DMEs and the role of drug transport in clinical PK is further elucidated, pre-clinical assessment of transporter interactions has become an area of growing interest in drug discovery and development (109-111). An early understanding of P-gp in drug pharmacokinetics facilitates the recognition of important clinical DDIs and polymorphisms that may greatly impact the disposition, dosing regimens, therapeutic efficacy and safety of a great number of drugs and drug candidates (112; 12). Current FDA guidance describes experimental systems, experimental designs and decision criteria to assess new chemical entities (NCEs) and drug candidates for P-gp interactions (113). Compounds that demonstrate significant interaction with P-gp, based on up-to-date *in vitro* and/or *in vivo* testing, may be required to undergo additional studies to demonstrate safety and optimal use, or may even be withdrawn in extreme cases. Study of P-gp is an integral component of pre-market drug development and regulatory review (12; 114; 115) and P-gp testing is typically carried out, like other PK tests, in parallel to pharmacodynamic studies of drug response (116). P-gp tests are especially important for drugs that are intended for oral administration, or are targeted to the CNS. Furthermore, as part of post market drug monitoring, P-gp interaction studies have elucidated the mechanisms of several reported drug-drug interactions, population variations, or rare adverse drug events.

1.2.2.7 Animal models

Shortly after the physiological expression of P-glycoprotein in human tissues became apparent in the late 80s, P-gp was also found to be expressed in the isolated brain capillaries of mice, rats, pigs and cows (117-120). Various forms of P-gp have also been reported to express in numerous other species of insects, fish, amphibians, reptiles, birds, and mammals. Today, closely related homologues of *ABCB1* have been cloned and sequenced in human, mouse, Chinese hamster, dog and other species including, *Caenorhabditis elegans* and *Drosophila melanogaster* (121; 122). In higher mammals P-

gp forms a small gene family, with only one drug transporting isoform expressed in humans (*MDR1/ABCB1*), and two co-operative drug transporter isoforms expressed in rodents (*mdr1/ABCB1a* and *mdr3/ABCB1b*) (123-125).

Recent advancements in transgenic animal models and knock out animals allow us to study the *in vivo* role of specific ADME proteins in human PK and drug-drug interactions. For instance, single and double P-gp knockout mouse models, lacking *ABCB1a* and *ABCB1b*, have been bred for *in vivo* pharmacokinetic studies. While these mice do show increased sensitivity to drug and xenobiotic exposure, they are viable and fertile for study (126). Moreover, although compensatory upregulation of complimentary enzymes or transporters may somewhat disguise the absence of P-gp in the mice (127), P-gp-deficient animal models provide valuable information about whether a drug is a substrate or modulator of MDR1 (128-130). As well, these particular knockout models have proven very useful in assessment of the impact of P-gp on the CNS penetration of psycho-active drugs. For example, Schinkel *et al.* compared the disposition of the veterinary pesticide ivermectin in knockout mice against wild type mice (57; 131). They saw a 100-fold greater brain ivermectin AUC in *mdr1a* (-/-) mice as compared to wild type. The increased brain exposure in the knockout mice resulted in a much greater neurotoxicity and mortality in the knockout mice versus the wild type mice that had regular expression of blood-brain-barrier P-glycoprotein.

Of note, caution must be taken when extrapolating the pharmacokinetics in an animal model to the human situation. Scaling animal pharmacokinetics solely by weight (allometric scaling) is not always effective due to species differences in a variety of physiological and biochemical properties, including organ blood perfusion, pH, gastric emptying time and various other factors. Moreover, species differences in the expression, localization, regulation and substrate specificity of DMEs and drug transporters can yield significantly different pharmacokinetics for a drug in humans versus an animal model. Early studies looked at the resistance profiles of Chinese hamster ovary cells overexpressing human *MDR1* and murine *mdr1* and *mdr3* genes; the resistance conferred by MDR1 versus *mdr1/3* was significantly different for various MDR drugs, as was the effect of different P-gp modulators on vinblastine resistance (132). A variety of

subsequent studies further confirmed species differences for several different P-gp substrates and modulators (50; 133-135). Although transgenic animal models expressing humanized proteins are currently available to improve the accuracy of human extrapolation, most are created for human drug metabolizing enzymes.

1.3 *In vitro* to *in vivo* (IVIV) prediction of pharmacokinetics

1.3.1 General scheme

Various transporter and DME interactions and DDIs have led to prescribing restrictions, market withdrawals, new drug submission rejections and early development terminations, for many pharmaceutical agents (136). So, it's not surprising that regulatory bodies, including the FDA and the European Medicines Agency (EMA), as well as academics are increasingly concerned about the contributions of key DMEs and transporters to drug disposition. *In vitro* to *in vivo* extrapolation (IVIVE) allows us to characterize the activity of ADME proteins *in vitro*, so as to clarify and predict their roles in the *in vivo* kinetics of drugs and drug candidates. It helps us to explain and predict the bioavailability, clearance and tissue distributions of clinically important drugs. For example, a compound that is identified *in vitro* as a strong P-gp substrate will likely show a high level of P-gp efflux *in vivo*. One *in vivo* consequence of compounds with efficient efflux by P-gp would be a significant decrease in oral absorption of the compound, since P-gp is highly expressed in the intestinal lumen where it actively opposes the absorption of substrate compounds. Characterizing drug-transporter and drug-enzyme interactions through *in vitro* studies is an essential step in understanding drug PK or in anticipating whether or not a drug is likely to exhibit favourable clinical PK. Certainly, important early decisions in drug discovery and development (DDD) are based on the interpretation of preclinical *in vitro* studies and their implications to *in vivo* kinetics (116; 137; 136).

1.3.2 Quantitative IVIVE

For quantitative IVIVE, additional information is required about the ADME protein and about the *in vitro* and *in vivo* systems that are being compared (Figure 1.1).

The rate of metabolism for a given enzyme-substrate pair in any *in vitro* or *in vivo* system, is proportional both to the absolute intrinsic activity of that enzyme on its

substrate and to the total amount of that enzyme expressed in the given system. Likewise, the rate of carrier-mediated transport for a given transporter-substrate pair in a system, is proportional to the absolute intrinsic activity and amount of that transporter in the system (138). Absolute intrinsic activity describes the characteristic efficiency at which an individual enzyme or transporter turns over substrate. It is a system-independent, inherent biochemical property of each individual ADME protein and is thus consistent, for a given protein, across *in vitro* and *in vivo* systems. So, it follows that quantitative *in vitro* to *in vivo* extrapolation is accomplished by scaling the amount of enzyme and/or transporter between systems, with a constant absolute intrinsic activity. Absolute intrinsic activity can be determined from the *in vitro* intrinsic activity in a system of known enzyme/transporter amount. In order to quantify transporter/enzyme amount, functional units of a system, such as cell number or protein content, are often used as convenient surrogates for actual transporter/enzyme content.

More sophisticated IVIVE models include information about the *in vivo* relative abundances of interacting enzymes and transporters, along with physiological parameters that dictate enzyme or transporter access to unbound drug (e.g. tissue perfusion rates, solubility etc.). Physiologically-based pharmacokinetic (PBPK) models have been developed in the past decades to integrate quantitative description of various simultaneous and dynamic physiological and pharmacokinetic processes, arranged within a structural framework that represents the anatomical arrangement of the body. These models have enjoyed increasing popularity in recent years for their ability to compile and contextualize a wealth of available *in vitro* and *in vivo* data. PBPK models have proven most useful in the prediction of DDIs, population PK and toxin exposure (139-142).

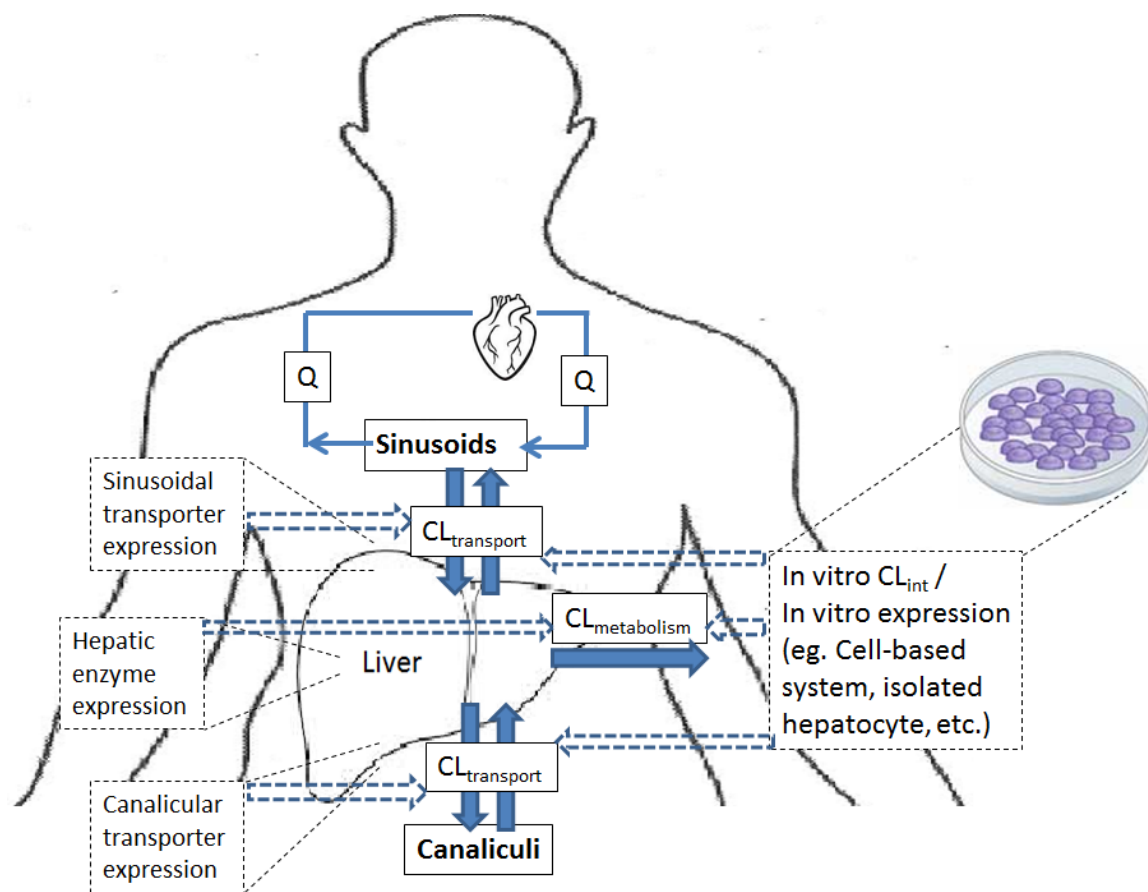


Figure 1.1. Simplified general scheme of quantitative IVIVE for hepatically eliminated drugs. Models are organized as tissue and extracellular compartments (eg. Liver, hepatic sinusoids, hepatic canaliculi) perfused by blood flow (Q). Movement of unbound drug into and out of compartments is defined by physiologically relevant, drug-specific clearance parameters ($CL_{\text{metabolism}}$; $CL_{\text{transport}}$) that relate to ADME protein activities. The clearance parameters are estimated from information about ADME protein expression in *in vivo* human tissues; and from information about *in vitro* ADME protein intrinsic clearance, normalized to *in vitro* protein expression. All clearance and flow parameters interplay dynamically with each other and have differing relative contribution to the overall PK of a given drug.

1.3.2.1 Intrinsic clearance in PK modeling

Intrinsic clearance (CL_{int}), a term first coined in 1975 by Wilkinson and Shand, describes the perfusion-rate-independent clearance of a drug from a system by the cumulative intrinsic activities of the contributing drug metabolizing enzymes and/or transporters. It is a cardinal PK parameter in quantitative IVIVE and PBPK modeling. Indeed, scaling of the intrinsic clearance of *in vitro* expressed liver enzymes and transporters has shown to be a robust method of predicting *in vivo* hepatic drug clearance (143-147). Intrinsic metabolic clearance (CL_{int} or $CL_{int(Metabolism)}$) was first described, for hepatic enzyme kinetics in an isolated hepatocyte *in vitro* system, as the initial metabolic activity (V_0) in the hepatocytes proportional to the concentration of free drug (C_u) available to the hepatocytes for metabolism,

$$CL_{int} = \frac{V_0}{C_u} \quad [1.5]$$

Substituting this into the Michaelis-Menten equation for enzyme kinetics (described in section 1.3.2.2),

$$v = \frac{V_{max}C_u}{K_m + C_u} \quad [1.6]$$

gives the following relationship:

$$CL_{int} = \frac{V_{max}}{K_m + C_u} \quad [1.7]$$

So, at low substrate concentration ($C_u \ll K_m$), intrinsic clearance is proportional to V_{max} , inversely proportional to K_m and independent of substrate concentration; expressed as,

$$CL_{int} = \frac{V_{max}}{K_m} \quad [1.8]$$

The situations in equations [1.5-1.8] can all be applied analogously to describe the intrinsic transporter-mediated clearance (CL_{int} or $CL_{int(Transport)}$) of any drug from a given compartment. This could be, for instance, applied to describe the *in vitro* carrier-mediated uptake of a drug into cultured cells in suspension, or applied to describe the *in vivo* secretion of a drug from the liver into the bile.

Along with $CL_{\text{int(Metabolism)}}$ and $CL_{\text{int(Transport)}}$, several other physiological parameters (e.g. blood flow, tissue perfusion) and drug-specific parameters relating to the free drug concentrations (e.g. plasma protein binding, tissue binding), chemical disposition, chemical dispersion, and availability for clearance, all factor into determination of the true *in vivo* clearance. The so-called “well-stirred” model description for hepatic metabolic clearance (148) provides a simple example:

$$CL_{\text{Total Liver}} = \frac{Q_L \times f_u \times CL_{\text{int}}}{Q_L + f_u \times CL_{\text{int}}} \quad [1.9]$$

where, Q_L is the physiological blood flow to the liver, f_u is the fraction of drug in the blood that is unbound and available for metabolism, and CL_{int} is the overall intrinsic metabolic clearance of the liver (scaled up from *in vitro* isolated hepatocytes). The CL_{int} rate in this model may define the intrinsic activity of one enzyme or, depending on the drug, it could incorporate the intrinsic activities of a collection of hepatic enzymes that all contribute to the elimination of a common substrate drug. Note though, that there is no term for intrinsic carrier-mediated clearance in equation [1.9]; this simplified case describes a metabolic clearance that is rate-limited by hepatic blood perfusion, in which unbound drug in the blood bathing the liver establishes instantaneous equilibrium with the hepatocytes by rapid passive diffusion, such that the intrahepatic and extrahepatic concentrations of free drug are viewed to be equal. Thus, as unbound drug perfuses the liver it is immediately available for metabolism at a rate, CL_{int} , that is intrinsic to the liver enzymes and any active transport is assumed to be negligible. In reality, for many drugs that display lower passive permeability, carrier-mediated transport into the liver (uptake) or into the bile (efflux) may rate-limit *in vivo* liver clearance (149; 150). Kinetic models that fail to account for important active uptake and/or efflux processes can result in an under- or over-estimation of system intrinsic clearance parameters (151).

Successful quantitative IVIVE of drug clearance requires proper integration of the multiple dynamic PK processes of different relative importances. A model of the *in vivo* hepatic clearance of enalapril in rats, by Sirianni and Pang (Figure 1.2) (152), demonstrates some of the interplay between transport and metabolism:

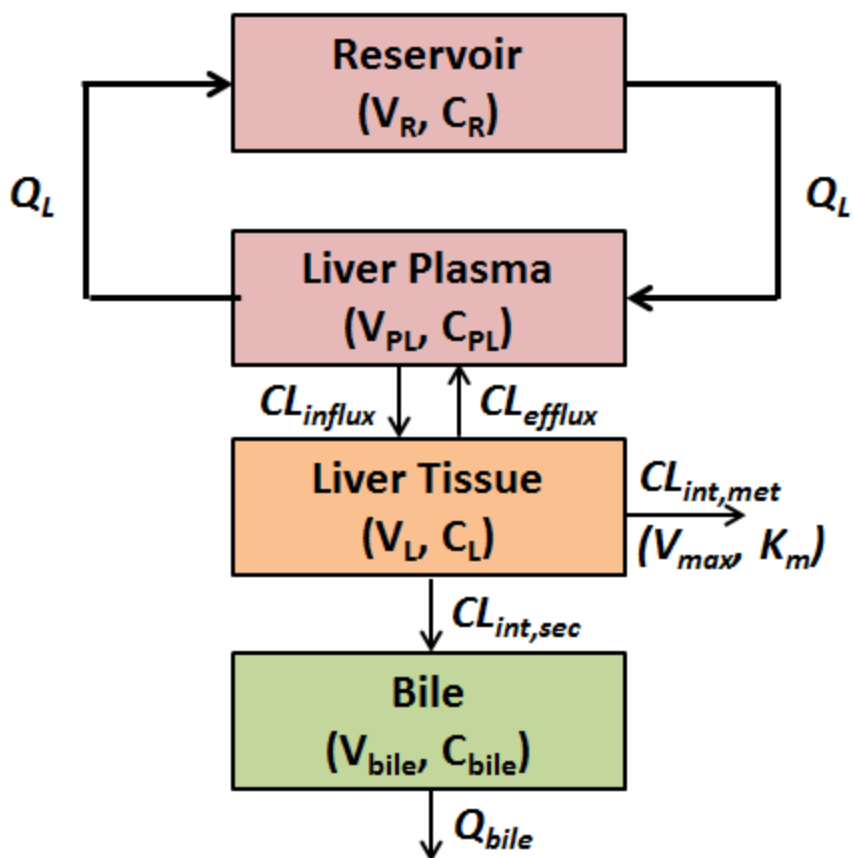


Figure 1.2. Schematic depiction of the physiological model for liver clearance. The liver is divided into three compartments: the reservoir (R , or systemic blood compartment), liver plasma (PL), and liver tissue (L). Q , C , and V represent flow, concentration, and volume, respectively. The transport clearances for drug from hepatic plasma to tissue and from tissue to hepatic plasma are characterized by influx (CL_{influx}) and efflux (CL_{efflux}) clearances, respectively. Drug metabolism within the liver tissue is characterized by the intrinsic clearance, $CL_{int,met}$. Biliary excretion of drug is characterized by the intrinsic clearance, $CL_{int,sec}$. Modified from Sirianni and Pang, 1997.

$$CL_{\text{Total Liver}} = \frac{Q_L \times f_u \times CL_{\text{influx}}(CL_{\text{int,met}} + CL_{\text{int,sec}})}{Q_L(CL_{\text{efflux}} + CL_{\text{int,met}} + CL_{\text{int,sec}}) + f_u CL_{\text{influx}}(CL_{\text{int,sec}} + CL_{\text{int,met}})} \quad [1.10]$$

where, Q_L is the blood flow to the liver, f_u is the fraction of drug in the blood that is unbound and available for metabolism, $CL_{\text{int,met}}$ is the intrinsic metabolic clearance, CL_{influx} and CL_{efflux} are respectively the intrinsic influx and intrinsic efflux at the sinusoidal membrane, and $CL_{\text{int,sec}}$ is the secretory intrinsic efflux at the canalicular membrane. $CL_{\text{Total Liver}}$ in the rat is solved for by writing mass balance equations for the reservoir, liver plasma, liver tissue, and bile compartments. In order to find agreement between model simulations and *in vivo* rat data sets, the *in vivo* relationships between many of the interacting parameters had to be defined. For example, since CL_{influx} and $CL_{\text{int,met}}$ simultaneously contribute to the tissue compartment drug level, Liu and Pang defined the $CL_{\text{influx}}/CL_{\text{int,met}}$ ratio as 6.56, based on the V_{max} and K_m kinetics observed for enalapril uptake and metabolism that were previously observed in homogenous isolated rat hepatocyte studies (152-154).

As a greater amount of kinetic information about transporter and enzyme intrinsic clearances, along with other physiological information, becomes available for different drugs, the precision of more detailed physiologically-based models can continually improve. Indeed, there has been continued development in dynamic models for intestinal absorption and BBB permeability in recent years as well (155-158).

1.3.2.2 Facilitated (Carrier-mediated) transport kinetics

Carrier-mediated transport of substrate across a membrane is characterized by saturability and it can be described analogously with the Michaelis-Menten equation for enzyme kinetics,

$$v = \frac{V_{\text{max}}C}{K_m + C} \quad [1.6]$$

where v is the rate of carrier-mediated transport; V_{max} is the maximum rate of carrier-mediated transport; C is the substrate concentration; and K_m , is the Michaelis constant, calculated as the substrate concentration at half of V_{max} . When C is much smaller than K_m , the rate of transport, v , shows a linear proportionality with substrate concentration. However, as C gets large compared to K_m the rate of transport no longer increases in

proportion to C , and v plateaus at a constant value (V_{\max}). At V_{\max} transport is saturated and v is limited by the rate at which transporters turn over substrate and by the density of transporters on the plasma membrane. To determine V_{\max} and K_m *in vitro*, transport is measured over a time course and over a range of drug concentrations. The Michaelis constant is a substrate-dependent parameter that relates to the affinity of a given transporter for a specific substrate.

The Michaelis-Menten equation was originally developed for soluble enzymes, which bind their substrates directly from the aqueous phase. Application of this equation to the kinetics of transport assumes that the equation parameters correlate reasonably well with the association and dissociation elementary rate constants of the substrate, transporter, and substrate-transporter complex (159). This is a reasonable approximation for drug transporters that bind their substrates directly from the aqueous phase and/or for the ATPase activity that occurs in the aqueous phase for ABC transporters (160). Thus, while the Michaelis-Menten parameters may not directly describe the discrete physical processes of drug transport, they still offer a useful estimate of transporter activity and good predictive value.

1.3.3 *In vitro* systems for estimating metabolism and transport

1.3.3.1 Hepatocytes, recombinant cells, and membrane vesicles

Drug metabolizing enzyme activity is estimated *in vitro*, often as an *in vitro* intrinsic metabolic clearance using equation [1.7], by incubating a drug substrate in an appropriate *in vitro* system and measuring metabolite formation or substrate disappearance over a range of concentrations. Currently, isolated human hepatocytes in suspension are the most practical *in vitro* system for metabolism studies to predict whole organ drug clearance (161; 138; 162). Microsomal fractions and recombinant enzyme systems may be used for more specific testing of particular enzymes of interest. Routine studies are recommended by the FDA to characterize the interactions of compounds with the following enzymes: CYP1A2, CYP2B6, CYP2C8, CYP2C9, CYP2C19, CYP2D6, and CYP3A (113).

Freshly isolated cryopreserved hepatocytes can also be used to study hepatic uptake transporters *in vitro* (162; 163). The common approach is to incubate substrate with a suspension of hepatocytes and measure drug accumulation in the cell after a period of time. Typically accumulation is measured over a range of concentrations to demonstrate saturable active transport kinetics. These active transport studies yield Michaelis-Menten kinetic parameters for carrier-mediated transport:

$$V = \left(\frac{V_{\max} \times C}{K_m + C} \right) + (P_{\text{diff}} \times C) \quad [1.11]$$

Where V is the rate of carrier-mediated transport, V_{\max} is the maximum rate of carrier-mediated uptake, K_m is the Michaelis constant, C is the drug concentration, and P_{diff} is the non-carrier-mediated passive clearance. Addition of the $P_{\text{diff}} \times C$ product to the usual Michaelis-Menten equation for active transport is necessary to account for the component of *in vitro* transport rate into the cell that is due to passive, non-carrier-mediated transport.

Application of Michaelis-Menten kinetics to *in vitro* carrier-mediated transport studies often operates under the assumption that only one type of transporter is responsible for transport in the system. Significant contribution by other transporters with overlapping substrate specificity can obscure the activity of the transporter of interest and interfere with the estimation of its kinetics. In the case of fresh hepatocytes, a variety of different transporter families are in fact expressed that may contribute to transport of various drug substrates. Also, cryopreserved hepatocytes cannot be used to study efflux transporters because the process of hepatocyte isolation causes canalicular efflux transporters to be internalized (164; 165). As well, none of the *in vitro* studies done in hepatocytes are appropriate for the study of transporters that are not expressed in the liver, including organic cation transporter 2 (OCT2) and organic anion transporter 1 and 3 (OAT1 and 3) proteins, which localize to the kidney. Recombinant cells can be used to better isolate the activity of any individual uptake transporter on a drug of interest.

An important distinction must be made before attempting to apply the models described above to the *in vitro* study of drug efflux transporters. Uptake transporters bind substrate

from the extracellular environment, where measurement and manipulation of drug concentrations is technically achieved very easily in a suspension or permeable-support system. Efflux transporters, on the other hand, extrude substrate from the intracellular space, which is largely inaccessible in these experimental systems. As such, more sophisticated *in vitro* strategies must be employed in determining the kinetics of efflux transport.

The ATPase, calcein-AM fluorescence, and rhodamine-123 fluorescence assays all circumvent the issue of intracellular inaccessibility by using indirect measures of substrate transport. The ATPase assay estimates the activity of ABC efflux transporters, by measuring the ATP hydrolysis that is coupled to their transport activity. Calcein-AM and rhodamine-123 fluorescence cell assays are designed specifically to evaluate *ABCB1* (P-gp) or *ABCC1* (Multidrug resistance-associated protein 1, MRP1) efflux transporter activity. Non-flourescent calcein-AM or non-flourescent rhodamine-123 diffuses into cells where it is hydrolyzed by intracellular esterases into a fluorescent compound, which accumulates intracellularly. Membrane P-gp and MRP1, however, opposes the inward diffusion of these non-flourescent compounds into the cells. Consequently, drugs that interact with P-gp or MRP1 can affect efflux transporter activity, resulting in a measureable change in the rate of accumulation of intracellular fluorescent compound. (166; 167) Each of these indirect assays offers a high throughput analysis of potential substrates that is readily automated. But, the ATPase, calcein-AM fluorescence, and rhodamine-123 fluorescence assays are not able to distinguish efflux transporter substrates from inhibitors (167-169).

Alternatively, other strategies allow direct measurement of efflux transporter activity; the inverted membrane vesicle assay is one such strategy. Transporter-expressing plasma membrane vesicles are inverted, such that the efflux transporters bind and actively pump substrate from the external environment into the closed vesicle. This orientation permits easy manipulation and measurement of the donor drug concentrations that is seen by the efflux transporters. In this orientation transporter kinetics can be evaluated just as they would be for an uptake transporter. However, compounds with moderate-to-high passive permeability leak back out of the vesicle after being pumped in and thus may be falsely

labeled as non-substrates by the inverted membrane vesicle assay. Moreover, the relative orientation of efflux transporters, they being inside-out or outside-in facing, will impact the effectiveness and interpretation of transport kinetics.

1.3.3.2 The cell monolayer permeability assay for efflux transport

The cell monolayer permeability assay is also designed to measure efflux transport activity in a direct fashion and it is the gold standard used in industry (Figure 1.4). The assay estimates efflux transporter activity by assessing permeability – comprised of both passive diffusion and active transport – across a monolayer composed of an immortalized cell line. The monolayer cells either have innate polarized efflux transporter expression, or are transfected to stably or transiently express polarized recombinant efflux transporter. A “transwell” set up is employed, where the monolayer is grown on a semipermeable insert, which is set into a well. This set up creates one accessible compartment on each side of the cell monolayer; commonly, as determined by cell polarization in culture, the top compartment is apical and the bottom is basolateral. Then, in order to estimate apical efflux transporter activity, which pumps drug away from the basolateral compartment and towards the apical compartment, drug is added to either side of the monolayer (the donor compartment) and its appearance on the opposing side (the receiver compartment) is measured. Efflux transporter activity is reflected in the degree of drug movement from donor to receiver compartments.

Like the inverted membrane vesicle assay, monolayer permeability assays may also fail to identify the efflux transport of some highly permeable drugs, but carrier-mediated efflux is unlikely to pose a significant barrier to the *in vivo* absorption of highly permeable drugs. Another limitation of this model is its inability to directly measure intracellular drug concentrations, which is the level that actually drives the rate of apical efflux transporters. For convenience, the intracellular concentration is often assumed to be in rapid equilibrium with the drug concentration measured in the basolateral compartment, which can be easily manipulated. In this way the system can be viewed as a single apical efflux barrier between two testable compartments: the basolateral/intracellular compartment and the apical compartment. In reality however, the intracellular concentration can vary significantly from the basolateral compartment

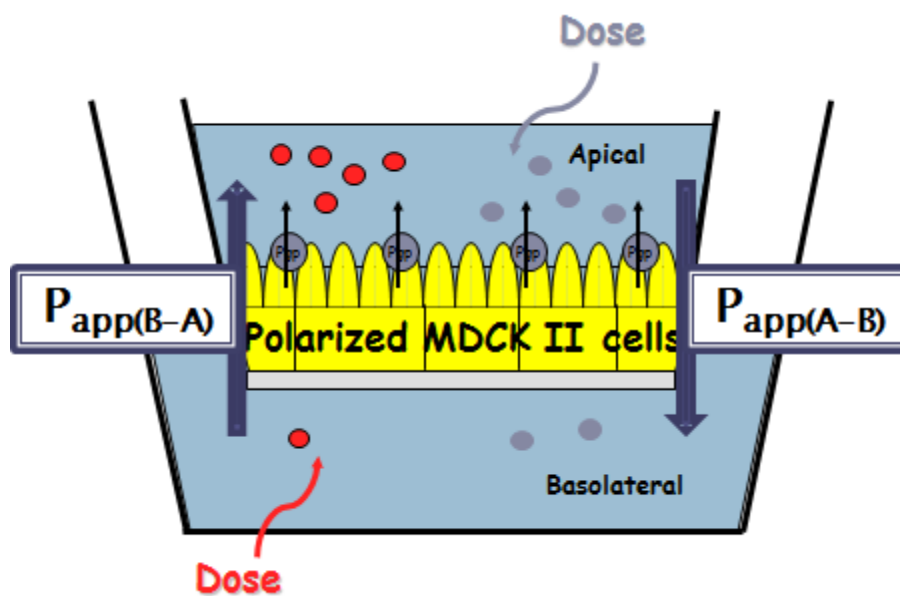


Figure 1.3. The cell monolayer permeability assay. A polarized monolayer of cells with apical P-gp expression. P_{app} is calculated in both directions from drug flux into the receiver compartment following apical or basolateral administration.

depending on the presence of unaccounted for basolateral uptake processes, which may differ between the monolayer cell lines used and/or between laboratory culture conditions (170-174). As previously mentioned, the presence of unaccounted for transporters can obscure accurate determination of the activity and kinetics of a transporter of interest.

1.3.4 *In vitro* estimation of drug efflux activity in the monolayer permeability assay

Various calculations have been proposed to estimate efflux transporter activity from a cell monolayer permeability assay.

1.3.4.1 Directional apparent permeability

Since the presence of P-gp or other unidirectional apical efflux transporters can both enhance basolateral to apical flux and attenuate apical to basolateral flux of a substrate drug, efflux transporter activity can be assessed from the permeability in either direction. Both increased basolateral to apical apparent permeability ($P_{app(B-A)}$) and decreased apical to basolateral apparent permeability ($P_{app(A-B)}$) are used to identify a compound as a substrate for efflux transport.

The apparent permeability (P_{app}) of a compound in one direction across the monolayer is estimated from the rate of appearance of drug in the receiver compartment measured during an incubation time. It is given by the following equation,

$$P_{app} = (dA_R/dt)/(S \times C_{D,0}) \quad [1.12]$$

Where P_{app} is the apparent permeability in distance per unit time, dA_R/dt is the cumulative amount of compound appearing in the receiver compartment with respect to incubation time, S is the surface area across which transport occurs, and $C_{D,0}$ is the initial concentration administered to the donor compartment. For $P_{app(B-A)}$, dA_R/dt specifies the rate at which drug appears in the apical compartment and $C_{D,0}$ is the initial concentration added in the basolateral compartment. Oppositely, for $P_{app(A-B)}$, dA_R/dt specifies the rate at which drug appears in the basolateral compartment and $C_{D,0}$ is the donor concentration added in the apical compartment.

1.3.4.2 Efflux ratio

Efflux ratio (EfR), the ratio of $P_{app(B-A)}$ to $P_{app(A-B)}$, is also used to evaluate efflux transporter activity. It relates the relative permeabilities in both directions across the monolayer, demonstrated by the relationship in Equation 1.13,

$$EfR = P_{app(B-A)} / P_{app(A-B)} \quad [1.13]$$

Where EfR is the efflux ratio, $P_{app(B-A)}$ is the basolateral to apical permeability of the drug across the cell monolayer and $P_{app(A-B)}$ is the apical to basolateral permeability. A drug that does not experience any active efflux would have an EfR equal to 1. Conversely, a substrate for apical efflux transport would show increased EfR (value > 1), demonstrating asymmetric basolateral to apical permeability.

1.3.4.3 Modeled intrinsic transport clearance

Efflux transporter activity can also be estimated from a cell monolayer permeability assay as a modeled intrinsic transporter clearance ($CL_{int(Transport)}$). Cellular kinetic models of varying complexity have been designed to describe drug movement between compartments of a transwell system, with respect to time (171; 172; 176-178). The drug concentrations, which are experimentally measured from the donor and receiver compartments throughout the drug incubation period, can be used as inputs for mathematical models to derive parameter values for the dynamic kinetic processes of the transwell. The intrinsic efflux clearance ($CL_{int(Efflux)}$ or CL_{int}), as it is defined in any given model, provides a direct quantitative estimate of the activity of efflux transporters on an *in vitro* test drug. This is different than P_{app} and EfR, which only qualitatively estimate efflux transporter kinetics. Also unlike P_{app} and EfR, this modeled approach isolates and quantifies the activity of the efflux transporter of interest. Take for example, the compartmental model applied by Tam *et al.* (Figure 1.4); this model was able to examine specifically the effect of P-gp efflux transport on drug metabolism in cytochrome P450 expressing Caco-2 cell intestinal models (173).

Since the modeled clearance approach isolates the activity of a given transporter, it should also be more easily relatable across the various cell lines that are commonly used

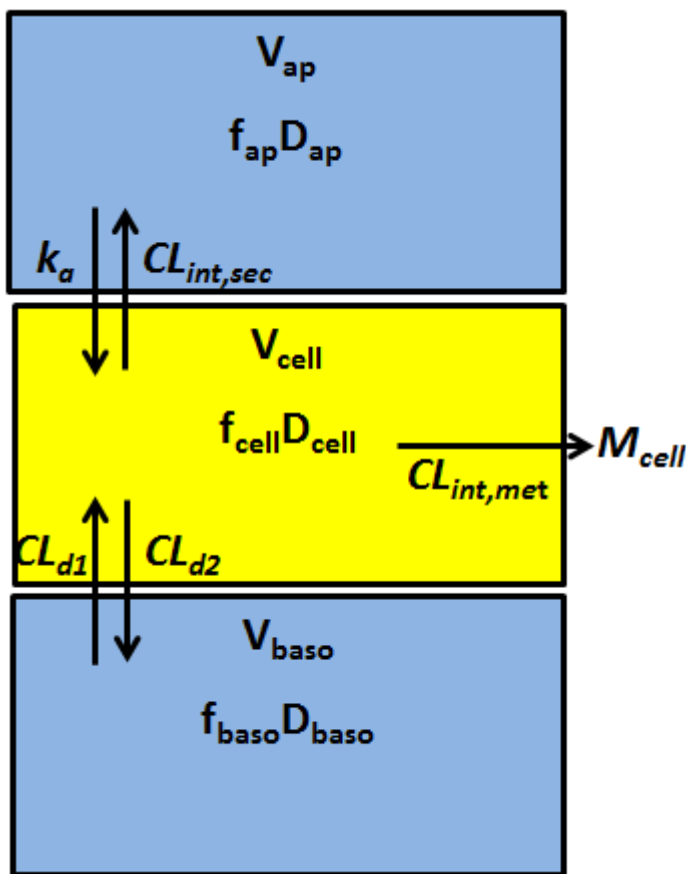


Figure 1.4. Compartment model for drug transport in a Transwell experimental system. Permeation of drug (D) from the apical compartment into the cell compartment, whether mediated by uptake transporters or passive diffusion, is associated with the absorption rate constant, k_a ; secretion (efflux) from the cell back into the apical compartment occurs with the intrinsic clearance, $CL_{int,sec}$. Drug partitioning between the cell and the basolateral compartment is mediated by influx and efflux clearances, CL_{d1} and CL_{d2} , respectively, as shown. Drug binding to proteins present in the apical compartment due to sloughed off mucosal cells (unbound fraction f_{ap}), within the cell (unbound fraction f_{cell}), and in the basolateral compartment (unbound fraction f_{baso}) affects the transfer and metabolic rates based on unbound drug concentrations. The rate of total metabolite formed, under first-order conditions, is given by $f_{cell}D_{cell}CL_{int,met}/V_{cell}$, where D_{cell} is the amount of drug within the cellular compartment of volume, V_{cell} . Modified from Tam et al., 2003.

for monolayer permeability assays. Modeled clearance can account for uptake transport parameters as well as other passive and active transport processes that may be specific to different cell lines or culture conditions. In this way, modeled CL_{int} should be transfereable between systems, whereas P_{app} and EfR values derived from different systems may not relate well. CL_{int} is thus likely more useful for extrapolating the efflux transport activity of a particular transporter in question.

1.3.5 Current recommendations for *in vitro* assessment of efflux transporter activity

Some of the most important considerations for constructing a successful *in vitro* study with good *in vivo* predictive value are: the selected test system, analysis of experimental data, and the chosen test drug.

Of the available *in vitro* techniques, monolayer permeability assays are recommended for *in vitro* assessment of efflux transporter activity (17; 179-183). More specifically, colorectal adenocarcinoma (Caco-2) cells have been commonly used in industry and academia for study of P-gp efflux transporter interaction and used as a general *in vitro* model of intestinal absorption (184-187). Caco-2 cells are a continuous cell of heterogeneous human epithelial colorectal adenocarcinoma cells, which shows high level of endogenous P-gp expression on the apical membrane. In culture they take on morphological and biochemical characteristics very similar to those of the human intestinal epithelium, forming a confluent monolayer with tight junctions and a brush border membrane. Data from Caco-2 cell assays has been shown to correlate well with the *in vivo* absorption of orally administered drugs in man (188).

Notably, Caco-2 cells also show polarized expression of a variety of uptake and efflux transporters. Many of these transporters share overlapping substrate specificities with P-gp and have the potential to contribute to the transport kinetics of P-gp substrates. In addition to P-glycoprotein, Caco-2 cells express significant levels of breast cancer resistance protein (BCRP) and multidrug resistance-associated protein 2 (MRP2) efflux transporters (189; 190) and fair levels of other transporters as well (Figure 1.5) (191-195).

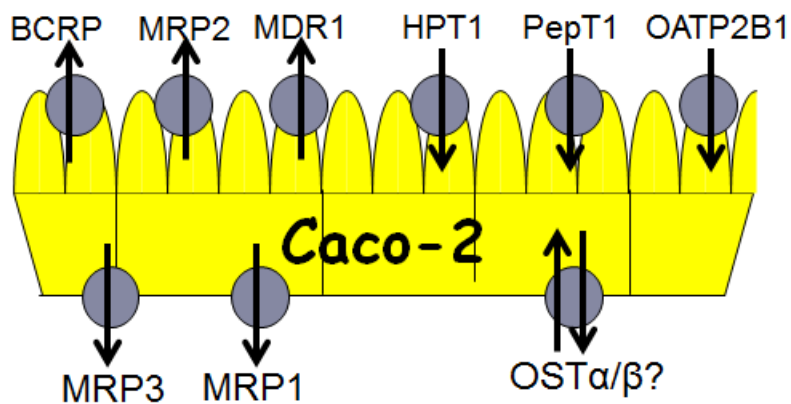


Figure 1.5. Some of the putative transporter proteins expressed in cultured Caco-2 cells, including: apical BCRP, MRP2, MDR1, HPT1 (human peptide transporter 1), PepT1 (peptide transporter 1), and OATP2B1 (organic anion-transporting polypeptide 2B1), and basolateral MRP3, MRP1, and OST- α/β (organic solute transporter- α/β).

Madin-Darby canine kidney (MDCK) cells and porcine kidney (LLCPK) cells can be transfected with *MDR1* and so are often used to form a polarized confluent monolayer *in vitro* as an alternative to Caco-2 cells. The MDCK-MDR1 (MDCK cells stably transfected with *MDR1*) and LMDR1 (LLCPK cells stably transfected with *MDR1*) cells boast a shorter culture period and greater inter-passage homogeneity (182; 98). Also, when transfected with *MDR1* these cell lines typically overexpress P-gp at levels greater than endogenous Caco-2 cell expression. Nonetheless, LLC PK and MDCK cells have also been reported to show some native expression of other transporters and enzymes, including fairly prominent canine P-gp expression in MDCK cells (196).

In terms of data analysis, some monolayer permeability studies report using unidirectional apparent permeability for the evaluation of efflux transporter activity and classification of P-gp substrates and modulators (197). However, efflux ratio is commonly used in many other studies (179). Digoxin is also viewed as the ideal substrate for the investigation of P-gp DDIs (113), and it will be discussed in detail in Section 1.4.

1.4 Digoxin

1.4.1 Historical perspectives

The cardiac glycosides are a group of chemically similar compounds that are often referred to as digitalis or digitalis glycosides because most are derived from the digitalis (foxglove) plant. The plant is native to western and south-western Europe, north-western Africa, western and central Asia and Australasia. In 1785 physician William Withering provided the first English language report of the use of cardiac glycoside-containing digitalis extract in the treatment of heart conditions. Cardiac glycosides are now known to inhibit the Na^+/K^+ -ATPase pump in myocardial and smooth muscle cells. This creates an increased intracellular sodium concentration, which induces elevated intracellular calcium by means of the $\text{Na}^+/\text{Ca}^{2+}$ exchanger. The end result is increased contractility of the heart through a positive inotropic effect. Typical cardiac glycosides function by the same mechanism of action, but vary in their potency and pharmacokinetics.

The first digoxin product was brought to the American market in 1934 by Wellcome Chemical Works (now GlaxoSmithKline) at a time when the FDA had limited power to

regulate pharmaceuticals. As federal legislation evolved the FDA was empowered to impose more stringent safety and efficacy tests on all pharmaceuticals, including those already on the market. This resulted in several recalls of digoxin and eventually its resubmission as a new drug. The secondary glycoside digoxin (Lanoxin) was ultimately approved by the FDA in 1998 for heart failure, on the basis of the Digitalis Investigators Group (DIG), Randomized Assessment of Digoxin on Inhibitors of the Angiotensin Converting Enzyme (RADIANCE), and Prospective Randomized Study of Ventricular Function and Efficacy of Digoxin (PROVED) clinical trials (198; 199; 200). Today digoxin is the cardiac glycoside most commonly used in North America.

1.4.2 Indications and use in Canada

Current Heart Failure Society of America (AHA)/American College of Cardiology (ACC) joint guidelines and Heart Failure Society of America (HSFA) guidelines recommend digoxin use for the treatment of symptomatic chronic heart failure with reduced or preserved systolic function and for ventricular rate control in atrial fibrillation (201; 202). At present, digoxin is the only effective oral inotropic agent available for treatment of chronic severe left systolic dysfunction (198; 203). Judicious use may also be warranted in cases of renal hypokalemia, renal impairment, hypomagnesemia, and hypothyroidism. When necessary, digoxin may also be carefully used in patients who suffer acute myocardial infarction with ongoing ischemia or electrical cardioversion.

The therapeutic concentration of digoxin for most heart failure patients is between 0.5 and 1.0 ng/mL from a daily dose of 0.125 to 0.25 mg/day. Close drug monitoring is especially imperative for digoxin because it has a very narrow therapeutic window, which means that the concentration at which toxic effects appear (≥ 2 ng/mL) is not substantially greater than therapeutic concentration. Early signs of digoxin toxicity are central nervous systems effects including dizziness, visual disturbance and nausea. Major digoxin toxicity is in large part a consequence of intracellular potassium depletion.

Digoxin is an affordable drug that, if properly monitored, can be used safely and effectively in conjunction with other heart failure drugs. Importantly though, co-administration of digoxin with intravenous calcium can precipitate potentially fatal

arrhythmias. Digoxin should also be avoided in patients with sinus node disease, second- or third-degree atrioventricular block, accessory atrioventricular pathways, hypertrophic cardiomyopathy, and cardiac amyloidosis. As well, physicians must be aware of the potential for drug-drug interactions, particularly those mediated by P-glycoprotein.

1.4.3 Clinical pharmacology

Drug-drug interactions are a real concern because of their potential to push serum digoxin concentrations outside of the narrow therapeutic window. Several clinically significant DDIs involving digoxin have been previously reported (181). One of the most studied is between digoxin and quinidine; first reported in 1968. Several prospective studies independently confirmed the interaction, reporting 2- to 3-fold increase in digoxin concentrations following concomitant quinidine administration (204; 205). This was demonstrated to be a result of increased oral bioavailability by quinidine inhibition of intestinal P-gp (206) and reduced renal clearance by inhibition of renal P-gp (207). Likewise, concomitant administrations of cyclosporine, quinidine, amiodarone, dronedarone, and valsopodar with digoxin have all been reported to increase digoxin plasma concentrations by competing for P-gp transport or protein binding (208-212). Foods and other natural products have been shown to significantly affect digoxin pharmacokinetics as well. For instance, several studies with St John's Wort have demonstrated decreased digoxin AUC resulting from induction of P-gp activity (213-216).

1.4.4 Discovery as a P-gp substrate

Evidently, many digoxin DDIs are mediated by P-glycoprotein. The first *in vitro* evidence for digoxin as a P-gp substrate came in 1992 from a study by de Lannoy and Silverman in Canada and from a study in the same year by Tanigawara *et al.* in Japan. Tanigawara's group showed greater basolateral to apical transport of digoxin across an epithelial monolayer of polarized LMDR1 cells. The directionality was diminished significantly by the addition of the P-gp inhibitors vinblastine, quinidine, or verapamil. Tanigawara's group further demonstrated that while digoxin transport directionality is reduced by cyclosporin inhibition of P-gp, digoxin did not reduce cyclosporin transport.

In other words, digoxin is a substrate of P-gp, but not a modulator (218). Similar studies conducted in different P-gp-expressing cells, including Caco-2 cells, and MDCK-MDR1 cells also identified digoxin as a P-gp substrate (219; 220; 98).

Additional *in vivo* work was done in knockout animal models. For example, Schinkel *et al.* assessed digoxin disposition in *mdr1a* (-/-) mice (131). Following intravenous injection they saw 35-fold greater digoxin accumulation in the brain of knockout mice compared to wild type, demonstrating the efflux activity of blood-brain-barrier P-gp in wild type mice. They also found that *mdr1a* (-/-) mice had 2-fold greater digoxin exposure in the plasma and tissues overall, reflecting slower digoxin elimination in the absence of active excretion by renal P-gp. *In vitro* work by Tsuruoka *et al.* further supported the activity of mouse renal P-gp on digoxin (221). Finally, a study in IV-dosed *mdr1a* (-/-) mice by Kawahara *et al.* also reported significant increase in digoxin AUC and mean residence time, as well as reduced renal and biliary clearance in P-gp-knockout mice (222).

At the turn of the century, human studies were underway to establish digoxin as a clinical P-gp substrate. In 8 healthy volunteers, co-administration of rifampin significantly reduced the AUC of orally dosed digoxin and, to a lesser extent, IV dosed digoxin (55). This was attributed to rifampin induction of P-gp, which was directly measured from duodenal biopsies. Decisive, in depth mechanistic clinical studies performed using segmental intestinal perfusions demonstrated definitively that digoxin is indeed secreted by the P-gp transporter (223; 224). A variety of similar studies with P-gp induction and inhibition all confirmed convincingly that digoxin is a substrate of the human P-gp transporter and that P-gp has a significant impact on digoxin disposition (225-229).

1.4.5 Digoxin pharmacokinetics

Digoxin is commonly administered as a commercially available tablet (Lanoxin), which is taken orally. Peak serum concentrations (C_{\max}) are rapidly achieved 1 to 3 hours following oral administration (230). The C_{\max} is somewhat delayed when taken with food, but the total amount absorbed is generally unchanged, except in the case of a high fiber meal. By the Biopharmaceutics Classification System (BCS), digoxin is a class II

compound, with high permeability and low aqueous solubility (231). The bioavailability of the oral dose is between 60 percent and 80 percent (232). However, patients with malabsorption syndromes or with certain populations of colonic bacteria may see a reduced digoxin oral bioavailability. Importantly, digoxin is also a substrate of the P-gp efflux transporter, which can limit oral absorption at the apical membrane of enterocytes (233).

The distribution phase of digoxin is between 6 and 8 hours, with a distribution half-life of 0.35 hours (234). The steady-state serum concentrations achieved after distribution are in equilibrium with the digoxin concentrations in the tissues and thus these are the most relevant serum concentrations for evaluating therapeutic and toxic effects. Digoxin has a large V_d , showing substantial distribution into tissues (233). Very little digoxin moves into adipose tissue however, and thus dosing should be based on lean body mass rather than total body mass. Not surprisingly then, loss of muscle mass in elderly patients results in a diminished V_d . Renal disease and hypothyroidism can also contribute to V_d reduction. Digoxin has been shown to cross both the blood-brain-barrier and the blood-placenta-barrier and is 25% serum protein bound (233).

Digoxin shows very little metabolism, only 13 percent. The primary metabolites are dihydrodigoxin, digoxigenin and bisdigitoxoside and they are produced by non-CYP enzymes. Renal excretion is the major route of digoxin elimination and between 50 and 70 percent of the parent compound is excreted unchanged in the urine (235). Given the importance of the kidney in the elimination of digoxin, its half-life is prolonged in patients suffering from renal failure. The typical half-life in patients with healthy renal function though, is between 1.5 and 2 days (233).

1.4.6 Digoxin as a model P-gp substrate

Digoxin's pharmacokinetics makes it an ideal *in vitro* probe substrate for the P-gp drug transporter. According to the FDA 2006 draft guidance for drug interaction studies, an *in vitro* P-gp probe substrate should be: selective to the P-gp transporter, have low passive membrane permeability, show minimal metabolism, be commercially available, and be safe for *in vivo* studies (17). Additional requirements applicable to human studies

should include a drug that is: safe and well tolerated by healthy subjects, approved for human administration, rapidly absorbed with a short half-life to avoid long clinical studies, minimally plasma protein bound, and quantifiable from plasma and/or urine and/or fecal samples using validated analytical methods (236). Digoxin is a P-gp substrate drug that is commercially available, both as cold- and radiolabelled- drug and it adequately fulfills the aforementioned probe substrate criteria. It remains the recommended probe drug for P-gp interaction studies according to the FDA and is viewed as the gold standard for industry testing (17; 181; 183; 237; 238).

Though used less frequently than digoxin, fexofenadine – a histamine H₁-receptor antagonist used for the treatment of seasonal allergic rhinitis – is also an effective P-gp probe drug. It is a demonstrated P-gp substrate: showing directional transport in Caco-2 cells that is suppressed by P-gp inhibitors, as well as significantly increased plasma and tissue levels in *MDR1* knockout mice (239-241). It shows minimal metabolism, with 95% of a dose excreted unchanged in the urine and feces (242). Moreover, the 60 mg single oral dose that is commonly used for *in vivo* studies is safe and tolerable and results in accurate and detectable plasma concentrations (243; 244). Notably though, while fexofenadine is commercially available, it is not available as an intravenous formulation. As a result, fexofenadine has limited *in vivo* usefulness in distinguishing the activity of intestinal versus renal P-gp. As well, commercially available fexofenadine is a racemic mixture, which may introduce chiral-associated differences in the drug's pharmacokinetics that are independent of P-gp (245). Moreover, fexofenadine is reported to be a substrate for several other transporters, many of which are expressed in cells commonly used for permeability assay, including organic anion-transporting polypeptide 2B1 (OATP2B1) and multidrug resistance-associated protein 2 and 3 (MRP2 and MRP3). These competing transporters can complicate interpretation of P-gp transport kinetics (246).

1.5 Rationale

It is well appreciated that the activity of membrane transporter proteins plays an important role in drug disposition, a critical determinant of the pharmacological and toxicological profile of all drugs (247; 12). Like drug metabolizing enzymes, drug

transporters are known to mediate significant drug-drug interactions as well as contribute to population variation in pharmacokinetics. P-glycoprotein (P-gp) is a key clinically important and well-characterized efflux transporter, which affects drug absorption, distribution and elimination (112; 12; 114; 115). A great number of clinically relevant, pharmacologically and structurally unrelated drugs are substrates for P-gp. Consequently, the efflux transport activity of P-gp on various drugs and drug candidates is routinely tested using the gold standard *in vitro* permeability assay across a monolayer of polarized, P-gp expressing Caco-2, LMDR1, or MDCK-MDR1 cells. Different metrics – namely apparent permeability P_{app} and efflux ratio EfR – are employed to evaluate P-gp transporter activity in this assay, in order to identify P-gp substrates or modulators and to extrapolate to *in vivo* and clinical pharmacokinetics. However, comparative assessment of how well these metrics can specifically characterize the efflux transport activity of P-gp is limited in the literature. In one study investigating the sources of inter-lab variability in Caco-2 cell intestinal model predictions, Hayeshi *et al.* reported on the correlation between varied P-gp mRNA expression levels in Caco-2 monolayers and the corresponding P-gp activity estimates calculated by P_{app} and by EfR (248). Taipalensuu *et al.* also reported on the correlation between efflux ratio and P-gp protein expression in Caco-2 monolayers (249). But, there are no studies that evaluate the efficacy of P_{app} or EfR to estimate P-gp activity across the various commonly used monolayer cell types. Our study compares traditional metrics of P-gp activity in Caco-2, LLCPK and LMDR1 monolayer permeability assays, against a mechanistically-based compartmental modeling approach, which generates a clearance CL_{P-gp} to quantitatively describe the intrinsic efflux activity of the P-gp transporter. We believe that a modeled clearance approach is a superior metric for the permeability assay because it does not rely on the potentially erroneous assumption that intracellular concentration is equal to basolateral concentration. Rather, the modeled approach specifically and quantitatively estimates P-gp activity from a fitted intracellular concentration. At the same time, it accounts for uptake transport parameters as well as other passive and active transport processes that may be specific to the different cell lines that are used for monolayer permeability assays. In this way, modeled CL_{P-gp} should be transferable between different monolayer cell types (e.g. Caco-2, LLCPK, and LMDR1) and *in vivo*, whereas P_{app} and EfR values

derived from different systems may not interrelate well. Compared to the qualitative P-gp transporter activity assessments offered by P_{app} and EfR, modeled CL_{P-gp} is likely more useful for the precise quantitative evaluation of the activity of the P-gp transporter in cell monolayer permeability assays and ultimately more useful for quantitative *in vitro* to *in vivo* extrapolation. To compare the merit of our model against the standard metrics, we conducted monolayer permeability assays across Caco-2, LLCPK, and LMDR1 cell monolayers that had a range of P-gp expression level and we employed unidirectional permeability, efflux ratio, and modeled clearance metrics to estimate P-gp activity in each assay. We then performed a statistical analysis to compare all metrics for overall validity and sensitivity across cell systems.

1.6 Objectives

1. To establish multiple cell monolayer permeability *in vitro* systems with different levels of P-gp expression/activity.
2. To evaluate P-gp efflux activity in the different cell systems using the traditional metrics and a modeled intrinsic P-gp clearance.
3. To compare the validity and sensitivity of the different metrics of efflux transporter activity across cell systems.

1.7 Hypothesis

We hypothesize that modeled clearance ($CL_{int(Transport)}$) is a more valid and sensitive measure of P-gp activity in the *in vitro* cell monolayer permeability assay than P_{app} and EfR.

1.8 References

1. Shimada T, Yamazaki H, Mimura M, Inui Y, Guengerich FP (1994) Interindividual variations in human liver cytochrome P-450 enzymes involved in the oxidation of drugs, carcinogens and toxic chemicals: studies with liver microsomes of 30 Japanese and 30 Caucasians. *Journal of Pharmacology and Experimental Therapeutics* 270: 414–423
2. Rendic S, Di Carlo FJ (1997) Human cytochrome P450 enzymes: a status report summarizing their reactions, substrates, inducers, and inhibitors. *Drug Metabolism Reviews* (1-2): 413-580
3. Ma Q and Lu AYH (2011) Pharmacogenetics, Pharmacogenomics, and Individualized Medicine. *Pharmacological Reviews* 63(2): 437–459
4. Sim MS, Hatim A, Reynolds GP, Mohamed Z (2013) Association of a functional FAAH polymorphism with methamphetamine-induced symptoms and dependence in a Malaysian population. *Pharmacogenetics* 14: 505-514
5. Cascorbi I (2006) Role of pharmacogenetics of ATP-binding cassette transporters in the pharmacokinetics of drugs. *Pharmacology and Therapeutics* 112(2): 457–473
6. Bruhn O and Cascorbi I (2014). Polymorphisms of the drug ABCC2 and ABCC3 and their impact on drug bioavailability and clinical relevance. *Expert opinion on drug metabolism & toxicology* 10(10): 1337-1354
7. Christensen LK, Hansen JM, Kristensen M (1963) Sulfaphenazole-induced hypoglycemic attacks in tolbutamide-treated diabetics *Lancet* ii:1298–1301
8. Surveillance BCD (1972) Adverse drug interactions. *The Journal of the American Medical Association* 220: 1238–1239
9. Dean M (2005) The genetics of ATP-binding cassette transporters. *Methods in Enzymology* 400: 409-29
10. Borst P and Elferink RO (2007) Mammalian ABC transporters in health and disease. *Annual Review of Biochemistry* 71: 537–592
11. He L, Vasiliou K, Nebert DW (2009) Analysis and update of the human solute carrier (SLC) gene superfamily. *Human Genomics* 3(2): 195-206
12. International Transporter Consortium, Giacomini KM, Huang SM, Tweedie DJ, Benet LZ, Brouwer KL, Chu X, Dahlin A, Evers R, Fischer V, Hillgren KM, Hoffmaster KA, Ishikawa T, Keppler D, Kim RB, Lee CA, Niemi M, Polli JW, Sugiyama Y, Swaan PW, Ware JA, Wright SH, Yee SW, Zamek- Gliszczynski MJ, Zhang L (2010). Membrane transporters in drug development. *Nature Reviews Drug Discovery* 9(3): 215–236

13. Giacomini KM and Sugiyama Y (2005) Membrane transporters and drug response. In: Brunton, L.L., Lazo, J.S., Parker, K.L. (Eds.), *Goodman & Gilman's The Pharmacological Basis of Therapeutics*, 11th ed. McGraw-Hill Professional, New York, pp. 41–70
14. Cui Y, Konig J, Keppler D (2001) Vectorial transport by double-transfected cells expressing the human uptake transporter SLC21A8 and the apical export pump ABCB2. *Molecular Pharmacology* 60: 934–943
15. Horio M, Pastan I, Gottesman MM, Handler, J.S (1990) Transepithelial transport of vinblastine by kidney-derived cell lines: Application of a new kinetic model to estimate in situ K_m of the pump. *Biochimica et Biophysica Acta* 1027: 116–122
16. Ayrton A and Morgan P (2001). Role of transport proteins in drug absorption. *Xenobiotica* 31(8): 469–497
17. FDA Guidance for Industry (2006) *Drug Interaction Studies — Study Design, Data Analysis, and Implications for Dosing and Labeling*
18. Zhang L1, Zhang YD, Zhao P, Huang SM (2009) Predicting drug-drug interactions: an FDA perspective. *AAPS Journal* 11(2): 300-6
19. Goldstein MN, Slotnick IJ, Journey LJ (1960) *In vitro* studies with HeLa cell line sensitive and resistant to actinomycin D. *Annals of the New York Academy of Sciences* 89: 474-83
20. Biedler JL, Riehm H (1970) Cellular resistance to actinomycin D in Chinese hamster cells *in vitro*: Cross-resistance, radioautographic, and cytogenetic studies. *Cancer Research* 30: 1174–1184
21. Dano K (1973) Active outward transport of daunomycin in resistant Ehrlich ascites tumor cells. *Biochimica et Biophysica Acta* 323: 466-83
22. Juliano RL, Ling V (1976) A surface glycoprotein modulating drug permeability in Chinese hamster ovary cell mutants. *Biochimica et Biophysica Acta* 455(1): 152-62
23. Riordan JR, Deuchars K, Kartner N, Alon N, Trent J, Ling V (1985) Amplification of P-glycoprotein genes in multidrug-resistant mammalian cell lines. *Nature* 316(6031): 817-9
24. Fojo AT, Ukda K, Slamon DJ, Poplack DC, Gottesman MM, Pastan I (1987) Expression of a multidrug-resistance gene in tumor and tissues. *Proceedings of the National Academy of Sciences of the United States of America* 84: 265-269

25. Saito T, Zhang ZJ, Shibamori Y, Ohtsubo T, Noda I, Yamamoto T, Saito H (1997) P-glycoprotein expression in capillary endothelial cells of the 7th and 8th nerves of guinea pig in relation to blood-nerve barrier sites. *Neuroscience Letters* 232: 41–44
26. Thiebaut F, Tsuruo T, Hamada H, Gottesman MM, Pastan I, Willingham MC (1987) Cellular localization of the multidrug-resistance gene product P-glycoprotein in normal human tissues. *Proceedings of the National Academy of Sciences of the United States of America* 84: 7735-8
27. Thiebaut F, Tsuruo T, Hamada H, Gottesman MM, Pastan I, Willingham MC (1989) Immunohisto- chemical localization in normal tissues of different epitopes in the multidrug transport protein P170: evidence for localization in brain capillaries and crossreactivity of one antibody with a muscle pro- tein. *Journal of Histochemistry & Cytochemistry* 37: 159-64
28. Cordon-Cardo C, O'Brien JP, Casals D, Rittman-Grauer L, Biedler JL, Melamed MR, Bertino JR (1989) Multidrug-resistance gene (P-glycoprotein) is expressed by endothelial cells at blood-brain barrier sites. *Proceedings of the National Academy of Sciences of the United States of America* 86: 695-8
29. Sugawara I (1990) Expression and functions of P-glycoprotein (mdr1 gene product) in normal and malignant tissues. *Acta pathologica japonica* 40: 545-53
30. Tsuji A, Terasaki T, Takabatake Y, Tenda Y, Tamai I, Yamashita T, Moritani S, Tsuruo T, Yamashita J (1992) P-glycoprotein as the drug efflux pump in primary cultured bovine brain capillary endothelial cells. *Life Sciences* 51: 1427-37
31. Tanaka Y, Abe Y, Tsugu A, Takamiya Y, Akatsuka A, Tsuruo T, Yamazaki H, Ueyama Y, Sato O, Tamaoki N, Nakamura M (1994) Ultrastructural localization of P-glycoprotein on capillary endothelial cells in human gliomas. *Virchows Arch* 425: 133-8
32. Shirai A, Naito M, Tatsuta T, Dong J, Hanaoka K, Mikami K, Oh-hara T, Tsuruo T (1994) Transport of cyclosporin A across the brain capillary endothelial cell monolayer by P-glycoprotein. *Biochimica et Biophysica Acta* 1222: 400-4
33. Biegel D, Spencer DD, Pachter JS (1995) Isolation and culture of human brain microvessel endothelial cells for the study of blood-brain barrier properties *in vitro*. *Brain Research* 692: 183-9
34. Beaulieu E, Demeule M, Ghitescu L, Beliveau R (1997) P-glycoprotein is strongly expressed in the luminal membranes of the endothelium of blood vessels in the brain. *Biochemical Journal* 326 (Pt 2): 539- 44
35. Sharom FJ (1997) The P-glycoprotein efflux pump: how does it transport drugs? *The Journal of Membrane Biology* 160: 161-75

36. Aller SG, Yu J, Ward A, Weng Y, Chittaboina S, Zhuo R, Harrell PM, Trinh YT, Zhang Q, Urbatsch IL, Chang G (2009) Structure of P-glycoprotein reveals a molecular basis for poly-specific drug binding. *Science* 323(5922): 1718–1722
37. Jones PM and George AM (2000) Symmetry and structure in P-glycoprotein and ABC transporters what goes around comes around. *European Journal of Biochemistry* 267: 5298-305
38. Loo TW and Clarke DM (1995) P-glycoprotein Associations Between Domains and Between Domains and Molecular Chaperones. *Journal of Biological Chemistry* 270: 21839-21844
39. Kast C, Canfield V, Levenson R, Gros P (1996) Transmembrane organization of mouse P-glycoprotein determined by epitope insertion and immunofluorescence. *Journal of Biological Chemistry* 271(16): 9240-8
40. Loo TW, Bartlett MC, Clarke DM (2003) Substrate-induced conformational changes in the transmembrane segments of human P-glycoprotein. Direct evidence for the substrate-induced fit mechanism for drug binding. *Journal of Biological Chemistry* 278: 13603-6
41. Chen Y and Simon SM (2000) In situ biochemical demonstration that P-glycoprotein is a drug efflux pump with broad specificity. *Journal of Cell Biology* 148: 863-70
42. Wachter VJ, Wu CY, Benet LZ (1995) Overlapping substrate specificities and tissue distribution of cytochrome P450 3A and p-glycoprotein: implications for drug delivery and activity in cancer chemotherapy. *Molecular Carcinogenesis* 13: 129–134
43. Schuetz EG, Beck WT, Schuetz JD (1996) Modulators and substrates of p-glycoprotein and cytochrome P4503A coordinately up-regulate these proteins in human colon carcinoma cells. *Molecular Pharmacology* 49: 311–318
44. Zhang Y and Benet LZ (2001) The gut as a barrier to drug absorption: combined role of cytochrome P450 3A and p-glycoprotein. *Clinical Pharmacokinetics* 40: 159–168
45. Sharom FJ (2008) ABC multidrug transporters: Structure, function and role in chemoresistance. *Pharmacogenomics* 9(1): 105–127
46. Tomblin G, Urbatsch IL, Virk N, Muharemagic A, White LB, Senior AE (2006) Expression, purification, and characterization of cysteine-free mouse P-glycoprotein. *Archives of Biochemistry and Biophysics* 445(1): 124-8
47. Rosenberg MF, Callaghan R, Ford RC, Higgins CF (1997) Structure of the multidrug resistance P- glycoprotein to 2.5 nm resolution determined by electron

- microscopy and image analysis. *Journal of Biological Chemistry* 272: 10685-94
48. Lugo MR and Sharom FJ (2005) Interaction of LDS-751 with P-glycoprotein and mapping of the location of the R drug binding site. *Biochemistry* 44: 643–655
 49. Callaghan R, Berridge G, Ferry DR, Higgins CF (1997) The functional purification of P-glycoprotein is dependent on maintenance of a lipid-protein interface. *Biochimica et Biophysica Acta* 1328(2): 109-24
 50. Schinkel AH, Wagenaar E, Mol CA, van Deemter L (1996) P-glycoprotein in the blood-brain barrier of mice influences the brain penetration and pharmacological activity of many drugs. *Journal of Clinical Investigation* 97: 2517–2524
 51. Terao T, Hisanaga E, Sai Y, Tamai I, Tsuji A (1996) Active secretion of drugs from the small intestinal epithelium in rats by P- glycoprotein functioning as an absorption barrier. *Journal of Pharmacology & Pharmacotherapeutics* 48: 1083–1089
 52. Varma MV, Ashokraj Y, Dey CS, Panchagnula R (2003) P-glycoprotein inhibitors and their screening: a perspective from bioavailability enhancement. *Pharmacological Research* 48(4): 347-59
 53. Thörn M, Finnström N, Lundgren S, Rane A, Löf L (2005) Cytochromes P450 and MDR1 mRNA expression along the human gastrointestinal tract. *British Journal of Clinical Pharmacology* 60(1): 54-60
 54. Canaparo R, Finstrom N, Serpe L, Nordmark A (2007) Expression of CYP3A Isoforms and P- glycoprotein in human stomach, jejunum and ileum. *Clinical and Experimental Pharmacology and Physiology* 34: 1138–1144
 55. Greiner B, Eichelbaum M, Fritz P, Kreichgauer HP, von Richter O, Zundler J, Kroemer HK (1999) The role of intestinal p-glycoprotein in the interaction of digoxin and rifampin. *Journal of Clinical Investigation* 104: 147–153
 56. Ernest S, Rajaraman S, Megyesi J, Bello-Reuss EN (1997) Expression of MDR1 (multidrug resistance) gene and its protein in normal human kidney Nephron 77(3): 284-9
 57. Schinkel AH, Smit JJ, van Tellingen O (1994) Disruption of the mouse *mdr1a* P-glycoprotein gene leads to a deficiency in the blood–brain barrier and to increased sensitivity to drugs. *Cell* 77: 491–502
 58. Lankas GR, Cartwright ME, Umbenhauer D (1997) P-glycoprotein deficiency in a subpopulation of CF-1 mice enhances avermectin-induced neurotoxicity. *Toxicology and Applied Pharmacology* 143(2): 357-65

59. Roulet A, Puel O, Gesta S, Lepage JF, Drag M, Soll M, Alvinerie M, Pineau T (2003) MDR1-deficient genotype in Collie dogs hypersensitive to the P-glycoprotein substrate ivermectin. *European Journal of Pharmacology* 460(2-3): 85-91
60. Lankas G and Gordon L (1989) *Toxicology* Campbell WC. Ivermectin and abamectin. New York (NY): Springer-Verlag
61. Cucinell SA, Koster R, Conney AH, Burns JJ (1963) Stimulatory effect of phenobarbital on the metabolism of diphenylhydantoin. *Journal of Pharmacology and Experimental Therapeutics* 141: 157–160
62. Remmer H, Schoene B, Fleischmann RA (1973) Induction of the unspecific microsomal hydroxy- lase in the human liver. *Drug Metabolism and Disposition* 1: 224–230
63. Schoene B, Fleischmann RA, Remmer H, von Oldershausen HF (1972) Determination of drug metabolizing enzymes in needle biopsies of human liver. *European Journal of Clinical Pharmacology* 4: 65–73
64. Shulman AI, Larson C, Mangelsdorf DJ, Ranganathan R (2004) Structural determinants of allosteric ligand activation in RXR heterodimers. *Cell* 116: 417–429
65. Goodwin B, Hodgson E, Liddle C (1999) The orphan human pregnane X receptor mediates the transcriptional activation of CYP3A4 by rifampicin through a distal enhancer module. *Molecular Pharmacology* 56: 1329–1339
66. Kliewer SA, Moore JT, Wade L, Staudinger JL, Watson MA, Jones SA, McKee DD, Oliver BB, Willson TM, Zetterström RH, Perlmann T, Lehmann JM (1998) An orphan nuclear receptor activated by pregnanes defines a novel steroid signaling pathway. *Cell* 92: 73–82
67. Bertilsson G, Heidrich J, Svensson K, Asman M, Jendeberg L, Sydow-Bäckman M, Ohlsson R, Postlind H, Blomquist P, Berkenstam A (1998) Identification of a human nuclear receptor defines a new signaling pathway for CYP3A induction. *Proceedings of the National Academy of Sciences of the United States of America* 95: 12208–12213
68. Blumberg B, Sabbagh W Jr, Juguilon H, Bolado J Jr, van Meter CM, Ong ES, Evans RM (1998) SXR, a novel steroid and xenobiotic-sensing nuclear receptor. *Genes and Development* 12: 3195–3205
69. Lehmann JM, McKee DD, Watson MA, Willson TM, Moore JT, Kliewer SA (1998) The human orphan nuclear receptor PXR is activated by compounds that regulate CYP3A4 gene expression and cause drug interactions. *Journal of Clinical Investigation* 102: 1016–1023

70. Sueyoshi T, Kawamoto T, Zelko I, Honkakoski P, Negishi M (1999) The repressed nuclear receptor CAR responds to phenobarbital in activating the human CYP2B6 gene. *Journal of Biological Chemistry* 274: 6043–6046
71. Honkakoski P, Zelko I, Sueyoshi T, Negishi M (1998) The nuclear orphan receptor CAR-retinoid X receptor heterodimer activates the phenobarbital-responsive enhancer module of the CYP2B gene. *Molecular and Cell Biology* 18: 5652–5658
72. Forman BM, Tzamelis I, Choi HS, Chen J, Simha D, Seol W, Evans RM, Moore DD (1998) Androstane metabolites bind to and deactivate the nuclear receptor CAR-beta. *Nature* 395: 612–615
73. Baes M, Gulick T, Choi HS, Martinoli MG, Simha D, Moore DD (1994) A new orphan member of the nuclear hormone receptor superfamily that interacts with a subset of retinoic acid response elements. *Molecular Cell Biology* 14: 1544–1551
74. Baker AR, McDonnell DP, Hughes M, Crisp TM, Mangelsdorf DJ, Haussler MR, Pike JW, Shine J, O'Malley BW (1988) Cloning and expression of full-length cDNA encoding human vitamin D receptor. *Proceedings of the National Academy of Sciences* 85: 3294–3298
75. Makishima M, Lu TT, Xie W, Whitfield GK, Domoto H, Evans RM, Haussler MR, Mangelsdorf DJ. (2002) Vitamin D receptor as an intestinal bile acid sensor. *Science* 296: 1313–1316
76. Wang H, Chen J, Hollister K, Sowers LC, Forman BM (1999) Endogenous bile acids are ligands for the nuclear receptor FXR/BAR. *Molecular Cell* 3: 543–553
77. Parks DJ, Blanchard SG, Bledsoe RK, Chandra G, Consler TG, Kliewer SA, Stimmel JB, Willson TM, Zavacki AM, Moore DD, Lehmann JM (1999) Bile acids: natural ligands for an orphan nuclear receptor. *Science* 284: 1365–1368
78. Makishima M, Okamoto AY, Repa JJ, Tu H, Learned RM, Luk A, Hull MV, Lustig KD, Mangelsdorf DJ, Shan B (1999) Identification of a nuclear receptor for bile acids. *Science* 284: 1362–1365
79. Cerveny L, Svecova L, Anzenbacherova E, Vrzal R, Staud F, Dvorak Z, Ulrichova J, Anzenbacher P, Pavek P (2007) Valproic acid induces CYP3A4 and MDR1 gene expression by activation of constitutive androstane receptor and pregnane X receptor pathways. *Drug Metabolism and Disposition* 35(7): 1032-41
80. Geick A, Eichelbaum M, Burk O (2001) Nuclear receptor response elements mediate induction of intestinal MDR1 by rifampin. *Journal of Biological Chemistry* 276: 14581-7

81. Burk O, Arnold KA, Nussler AK, Schaeffeler E, Efimova E, Avery BA, Avery MA, Fromm MF, Eichelbaum M (2005) Antimalarial artemisinin drugs induce cytochrome P450 and MDR1 expression by activation of xenosensors pregnane X receptor and constitutive androstane receptor. *Molecular Pharmacology* 67: 1954–1965
82. Schmiedlin-Ren P, Thummel KE, Fisher JM, Paine MF, Lown KS, Watkins PB (1997) Expression of enzymatically active CYP3A4 by Caco-2 cells grown on extracellular matrix-coated permeable supports in the presence of 1 α , 25-dihydroxyvitamin D₃. *Molecular Pharmacology* 51: 741–754
83. Thummel KE, Brimer C, Yasuda K, Thottassery J, Senn T, Lin Y, Ishizuka H, Kharasch E, Schuetz J, Schuetz E (2001) Transcriptional control of intestinal cytochrome P-4503A by 1 α , 25-dihydroxy vitamin D₃. *Molecular Pharmacology* 60: 1399–1406
84. Saeki M, Kurose K, Tohkin M, Hasegawa R (2008) Identification of the functional vitamin D response elements in the human MDR1 gene. *Biochemical Pharmacology* 76: 531–542
85. Fan J., Liu S, Du Y, Morrison J, Shipman R, Pang KS (2009) Up-regulation of transporters and enzymes by the vitamin D receptor ligands, 1 α ,25-dihydroxyvitamin D₃ and vitamin D analogs, in the Caco-2 cell monolayer. *Journal of Pharmacology and Experimental Therapeutics* 330: 389–402
86. Schwarz UI, Gramatte T, Krappweis J, Oertel R, Kirch W (2000) P-glycoprotein inhibitor erythromycin increases oral bioavailability of talinolol in humans. *International Journal of Clinical Pharmacology and Therapeutics* 38: 161–167
87. Cummins CL, Jacobsen W, Benet LZ (2002) Unmasking the dynamic interplay between intestinal P-glycoprotein and CYP3A4. *Journal of Pharmacology and Experimental Therapy* 300: 1036–1045
88. Verschraagen M, Koks CHW, Schellens JHM, Beijnen JH (1999) P-glycoprotein system as a determinant of drug interactions: the case of digoxin-verapamil. *Pharmacological Research* 40: 301-306
89. Gramatté T and Oertel R (1999) Intestinal secretion of intravenous talinolol is inhibited by luminal R-verapamil. *Clinical Pharmacology and Therapeutics* 66(3): 239-45
90. Tsuruo T, Iida H, Tsukagoshi S, Sakurai Y (1981) Overcoming of vincristine resistance in P388 leukemia *in vivo* and *in vitro* through enhanced cytotoxicity of vincristine and vinblastine by verapamil. *Cancer Research* 41: 1967-72
91. Boote DJ, Dennis IF, Twentyman PR, Osborne RJ, Laburte C, Hensel S, Smyth JF, Brampton MH, Bleehen NM (1996) Phase I study of etoposide with SDZ PSC

- 833 as a modulator of multidrug resistance in patients with cancer. *Journal of Clinical Oncology* 14(2): 610-8
92. Kemper EM, van Zandbergen AE, Cleypool C, Mos HA, Boogerd W, Beijnen JH, van Tellingen O (2003) Increased penetration of paclitaxel into the brain by inhibition of P-Glycoprotein. *Clinical Cancer Research* 9: 2849-55
 93. Sadeque AJ, Wandel C, He H (2000) Increased drug delivery to the brain by P-glycoprotein inhibition. *Clinical Pharmacology and Therapeutics* 68: 231–237
 94. Breedveld P, Beijnen JH, Schellens JH (2006) Use of P-glycoprotein and BCRP inhibitors to improve oral bioavailability and CNS penetration of anticancer drugs. *Trends in Pharmacological Sciences* 27(1): 17-24
 95. Cascorbi I, Gerloff T, Johne A, Meisel C, Hoffmeyer S, Schwab M, Schaeffeler E, Eichelbaum M, Brinkmann U, Roots I (2001) Frequency of single nucleotide polymorphisms in the P-glycoprotein drug transporter MDR1 gene in white subjects. *Clinical Pharmacology and Therapy* 69: 169–174
 96. Kim RB, Leake BF, Choo EF, Dresser GK, Kubba SV, Schwarz UI, Taylor A, Xie HG, McKinsey J, Zhou S, Lan LB, Schuetz JD, Schuetz EG, Wilkinson GR (2001) Identification of functionally variant MDR1 alleles among European Americans and African Americans. *Clinical Pharmacology and Therapy* 70: 189–199
 97. Ito S, Ieiri I, Tanabe M, Suzuki A, Higuchi S, Otsubo K (2001) Polymorphism of the ABC transporter genes, MDR1, MRP1 and MRP2/cMOAT, in healthy Japanese subjects. *Pharmacogenetics* 11(2): 175-84
 98. Tang K, Ngoi SM, Gwee PC, Chua JM, Lee EJ, Chong SS, Lee CG (2002) Distinct haplotype profiles and strong linkage disequilibrium at the MDR1 multidrug transporter gene locus in three ethnic Asian populations. *Pharmacogenetics* 12(6): 437-50
 99. Hoffmeyer S, Burk O, von Richter O, Arnold HP, Brockmüller J, Johne A, Cascorbi I, Gerloff T, Roots I, Eichelbaum M, Brinkmann U (2000) Functional polymorphisms of the human multidrug-resistance gene: multiple sequence variations and correlation of one allele with P-glycoprotein expression and activity *in vivo*. *Proceedings of the National Academy of Sciences of the United States of America* 97: 3473–3478
 100. Johne A, Köpke K, Gerloff T, Mai I, Rietbrock S, Meisel C, Hoffmeyer S, Kerb R, Fromm MF, Brinkmann U, Eichelbaum M, Brockmüller J, Cascorbi I, Roots I (2002) Modulation of steady-state kinetics of digoxin by haplotypes of the P-glycoprotein MDR1 gene. *Clinical Pharmacology and Therapeutics* 72: 584–594

101. Verstuyft C, Schwab M, Schaeffeler E, Kerb R, Brinkmann U, Jaillon P, Funck-Brentano C, Becquemont L (2003) Digoxin pharmacokinetics and MDR1 genetic polymorphisms. *European Journal of Clinical Pharmacology* 58: 809–812
102. Kurata Y, Ieiri I, Kimura M, Morita T, Irie S, Urae A, Ohdo S, Ohtani H, Sawada Y, Higuchi S, Otsubo K (2002) Role of human MDR1 gene polymorphism in bioavailability and interaction of digoxin, a substrate of P-glycoprotein. *Clinical Pharmacology and Therapeutics* 72: 209–219
103. Sakaeda T, Nakamura T, Horinouchi M, Kakumoto M, Ohmoto N, Sakai T, Morita Y, Tamura T, Aoyama N, Hirai M, Kasuga M, Okumura K (2001) MDR1 genotype-related pharmacokinetics of digoxin after single oral administration in healthy Japanese subjects. *Pharmaceutical Research* 18: 1400–1404
104. Horinouchi M, Sakaeda T, Nakamura T, Morita Y, Tamura T, Aoyama N, Kasuga M, Okumura K (2002) Significant genetic linkage of MDR1 polymorphisms at positions 3435 and 2677: functional relevance to pharmacokinetics of digoxin. *Pharmaceutical Research* 19: 1581–1585
105. Gerloff T, Schaefer M, Johne A, Oselin K, Meisel C, Cascorbi I, Roots I (2002) MDR1 genotypes do not influence the absorption of a single oral dose of 1 mg digoxin in healthy white males. *British Journal of Clinical Pharmacology* 54(6): 610-6
106. Lin JH and Lu AY (1998) Inhibition and induction of cytochrome P450 and the clinical implications. *Clinical Pharmacokinetics* 35: 361–390
107. White RE (2000) High-throughput screening in drug metabolism and pharmacokinetic support of drug discovery. *Annual Review of Pharmacology and Toxicology* 40: 133–157
108. Riley RJ (2001) The potential pharmacological and toxicological impact of P450 screening. *Current Opinion in Drug Discovery and Development* 4: 45–54
109. Hsiao P, Bui T, Ho RJ, Unadkat JD (2007) *In vitro* to *in vivo* prediction of p-glycoprotein based drug interactions at the human and rodent blood-brain barrier. *Drug Metabolism and Disposition* 34: 786–792
110. Miners JO, Smith PA, SorichMJ, McKinnon RA, Mackenzie PI (2004) Predicting human drug glucuronidation parameters: application of *in vitro* and *in silico* modeling approaches. *Annual Review of Pharmacology and Toxicology* 44: 1–25
111. Hidalgo I (2001) Assessing the absorption of new pharmaceuticals. *Current Topics in Medicinal Chemistry* 1: 385–401

112. Marchetti S, Mazzanti R, Beijnen JH, Schellens JH (2007) Concise review: Clinical relevance of drug drug and herb drug interactions mediated by the ABC transporter ABCB1 (MDR1, P-glycoprotein). *Oncologist* 12: 927–941
113. FDA Guidance for Industry (2012) Drug Interaction Studies — Study Design, Data Analysis, and Implications for Dosing and Labeling
114. Huang C, Zheng M, Yang Z, Rodrigues AD, Marathe P (2008) Projection of exposure and efficacious dose prior to first-in-human studies: how successful have we been?. *Pharmacology Research* 25: 713–726
115. Zhang L, Reynolds KS, Zhao P, Huang SM (2010) Drug interactions evaluation: an integrated part of risk assessment of therapeutics. *Toxicology and Applied Pharmacology* 243: 134–145
116. Yengi LG, Leung L, Kao J (2007) The evolving role of drug metabolism in drug discovery and development. *Pharmaceutical Research* 24(5): 842-58
117. Jette L and Beliveau R (1993) P-glycoprotein is strongly expressed in brain capillaries. *Advances in Experimental Medicine and Biology* 331: 121-5
118. Jette L, Tetu B, Beliveau R (1993) High levels of P-glycoprotein detected in isolated brain capillaries. *Biochimica et Biophysica Acta* 1150: 147-54
119. Nobmann S, Bauer B, Fricker G (2001) Ivermectin excretion by isolated functionally intact brain endothelial capillaries. *British Journal of Pharmacology* 132: 722-8
120. Tsai CE, Daood MJ, Lane RH, Hansen TW, Gruetzmacher EM, Watchko JF (2002) P-glycoprotein expression in mouse brain increases with maturation. *Biology of the Neonate* 81: 58-64
121. Croop JM (1993) P-glycoprotein structure and evolutionary homologies. *Cytotechnology* 12(1-3): 1-32
122. Lincke CR, Broeks A, The I, Plasterk RH, Borst P (1993) The expression of two P-glycoprotein (pgp) genes in transgenic *Caenorhabditis elegans* is confined to intestinal cells. *EMBO Journal* 12(4): 1615-20
123. del Amo EM, Heikkinen AT, Mönkkönen J (2009) *In vitro-in vivo* correlation in P-glycoprotein mediated transport in intestinal absorption. *European Journal of Pharmaceutical Sciences* 36(2-3): 200-11
124. Linnet K, Ejlsing T (2008) A review on the impact of P-glycoprotein on the penetration of drugs into the brain. Focus on psychotropic drugs. *European Neuropsychopharmacology* 18: 157-169

125. Yamazaki M, Neway WE, Ohe T, Chen I, Rowe JF, Hochman JH, Chiba M, Lin JH (2001) *In vitro* substrate identification studies for p-glycoprotein-mediated transport: species difference and predictability of *in vivo* results. *Journal of Pharmacology and Experimental Therapeutics* 296: 723–35
126. Schinkel AH, Mayer U, Wagenaar E, Mol CA, van Deemter L, Smit JJ, van der Valk MA, Voordouw AC, Spits H, van Tellingen O, Zijlmans JM, Fibbe WE, Borst P (1997) Normal viability and altered pharmacokinetics in mice lacking *mdr1*-type (drug-transporting) P-glycoproteins. *Proceedings of the National Academy of Sciences of the United States of America* 94: 4028–4033
127. Lee SD, Thornton SJ, Sachs-Barrable K, Kim JH, Wasan KM (2013) Evaluation of the contribution of the ATP binding cassette transporter, P-glycoprotein, to *in vivo* cholesterol homeostasis. *Molecular Pharmaceutics* 10(8): 3203-12
128. Batrakova EV, Miller DW, Li S, Alakhov VY, Kabanov AV, Elmquist WF (2001) Pluronic P85 enhances the delivery of digoxin to the brain: *in vitro* and *in vivo* studies. *Journal of Pharmacology Experimental Therapeutics* 296(2): 551-7
129. Chu C, Abbara C, Noël-Hudson MS, Thomas-Bourgneuf L, Gonin P, Farinotti R, Bonhomme-Faivre L (2009) Disposition of everolimus in *mdr1a*-/*1b*- mice and after a pre-treatment of lapatinib in Swiss mice. *Biochemical Pharmacology* 77(10): 1629-34
130. Milane A, Fernandez C, Vautier S, Bensimon G, Meininger V, Farinotti R (2007) Minocycline and riluzole brain disposition: interactions with p-glycoprotein at the blood-brain barrier. *Journal of Neurochemistry* 103(1): 164-73
131. Schinkel AH, Wagenaar E, van Deemter L, Mol CA, Borst P (1995) Absence of the *mdr1a* P-glycoprotein in mice affects tissue distribution and pharmacokinetics of dexamethasone, digoxin, and cyclosporin A. *Journal of Clinical Investigation* 96: 1698–1705
132. Tang-Wai DF, Kajiji S, DiCapua F, de Graaf D, Roninson IB, Gros P (1995) Human (MDR1) and mouse (*mdr1*, *mdr3*) P-glycoproteins can be distinguished by their respective drug resistance profiles and sensitivity to modulators *Biochemistry* 34(1): 32-9
133. Yamazaki M, Neway WE, Ohe T, Chen IW, Rowe JF, Hochman JH, Chiba M, Lin JH (2001) *In vitro* substrate identification studies for P-glycoprotein-mediated transport: species difference and predictability of *in vivo* results. *Journal of Pharmacology and Experimental Therapeutics* 296: 723–735
134. Katoh M, Suzuyama N, Takeuchi T, Yoshitomi S, Asahi S, Yokoi T (2006) Kinetic analyses for species differences in P-glycoprotein-mediated drug transport. *Journal of Pharmaceutical Sciences* 95: 2673–2683

135. Baltes S, Gastens AM, Fedrowitz M, Potschka H, Kaever V, Löscher W (2007) Differences in the transport of the antiepileptic drugs phenytoin, levetiracetam and carbamazepine by human and mouse P-glycoprotein. *Neuropharmacology* 52(2): 333-46
136. Bjornsson TD, Callaghan JT, Einolf HJ, Fischer V, Gan L, Grimm S, Kao J, King SP, Miwa G, Ni L, Kumar G, McLeod J, Obach RS, Roberts S, Roe A, Shah A, Snikeris F, Sullivan JT, Tweedie D, Vega JM, Walsh J, Wrighton SA (2003) The conduct of *in vitro* and *in vivo* drug- drug interaction studies: a Pharmaceutical Research and Manufacturers of America (PhRMA) perspective. *Drug Metabolism and Disposition* 31: 815-832
137. Xia CQ, Liu N, Miwa GT, Gan LS (2007) Interactions of cyclosporin A with breast cancer resistance protein. *Drug Metabolism and Disposition* 35: 576-582
138. Kedderis GL. (2007). *In vitro* to *in vivo* extrapolation of metabolic rate constants for physiologically based pharmacokinetic models. In: Lipscomb, JC, Ohanian EV. (eds.) *Toxicokinetics and risk assessment*. New York: Informa healthcare
139. Huang SM, Rowland M (2012) The role of physiologically based pharmacokinetic modeling in regulatory review. *Clinical Pharmacology Therapeutics* 91: 542-549
140. Huang SM (2012) PBPK as a tool in regulatory review. *Biopharmaceutics and Drug Disposition* 33(2): 51-2
141. Zhao P, Rowland M, Huang SM (2012) Best practice in the use of physiologically based pharmacokinetic modeling and simulation to address clinical pharmacology regulatory questions. *Clinical Pharmacology and Therapeutics* 92(1): 17-20
142. Zhao W, Fakhoury M, Baudouin V, Storme T, Maisin A, Deschênes G, Jacqz-Aigrain E (2013) Population pharmacokinetics and pharmacogenetics of once daily prolonged-release formulation of tacrolimus in pediatric and adolescent kidney transplant recipients. *European Journal of Clinical Pharmacology* 69(2): 189-95
143. Nakajima M, Nakamura S, Tokudome S, Shimada N, Yamazaki H, Yokoi T (1999) Azelastine N-demethylation by cytochrome P-450 (CYP)3A4, CYP2D6, and CYP1A2 in human liver microsomes: evaluation of approach to predict the contribution of multiple CYPs. *Drug Metabolism and Disposition* 27(12): 1381-91
144. McGinnity DF, Parker AJ, Soars M, Riley RJ (2000) Automated definition of the enzymology of drug oxidation by the major human drug metabolizing cytochrome P450s. *Drug Metabolism and Disposition* 28(11): 1327-34

145. McGinnity DF, Riley RJ (2001) Predicting drug pharmacokinetics in humans from *in vitro* metabolism studies. *Biochemical Society Transactions* 29(Pt 2): 135-9
146. Proctor NJ, Tucker GT, Rostami-Hodjegan A (2004) Predicting drug clearance from recombinantly expressed CYPs: intersystem extrapolation factors. *Xenobiotica* 34(2): 151-78
147. Watanabe T, Kusuhara H, Maeda K, Shitara Y, Sugiyama Y (2009) Physiologically based pharmacokinetic modeling to predict transporter-mediated clearance and distribution of pravastatin in humans. *Journal of Pharmacology and Experimental Therapeutics* 328: 652–662
148. Pang KS and Rowland M (1977) Hepatic clearance of drugs. I. Theoretical considerations of a "well-stirred" model and a "parallel tube" model. Influence of hepatic blood flow, plasma and blood cell binding, and the hepatocellular enzymatic activity on hepatic drug clearance. *Journal of Pharmacokinetics and Biopharmaceutics* 5: 625–653
149. Obach RS (1999) Prediction of human clearance of twenty-nine drugs from hepatic microsomal intrinsic clearance data: an examination of *in vitro* half-life approach and nonspecific binding to microsomes. *Drug Metabolism and Disposition* 27: 1350–1359
150. Huang L, Berry L, Ganga S, Janosky B, Chen A, Roberts J, Colletti AE, Lin MH (2010) Relationship between passive permeability, efflux, and predictability of clearance from *in vitro* metabolic intrinsic clearance. *Drug Metabolism and Disposition* 38(2): 223-31
151. Chiba M, Ishii Y, Sugiyama Y (2009) Prediction of hepatic clearance in human from *in vitro* data for successful drug development. *AAPS Journal* 11(2): 262-76
152. Liu L and Pang KS (2005) The roles of transporters and enzymes in hepatic drug processing. *Drug Metabolism and Disposition* 33(1): 1-9
153. Abu-Zahra TN, Wolkoff AW, Kim RB, Pang KS (2000) Uptake of enalapril and expression of organic anion transporting polypeptide 1 in zonal, isolated rat hepatocytes. *Drug Metabolism and Disposition* 28: 801–806
154. Abu-Zahra TN and Pang KS (2000) Effect of zonal transport and metabolism on hepatic removal: enalapril hydrolysis in zonal, isolated rat hepatocytes *in vitro* and correlation with perfusion data. *Drug Metabolism and Disposition* 28: 807–813
155. Badhan RK, Chenel M, Penny JI (2014) Development of a physiologically-based pharmacokinetic model of the rat central nervous system. *Pharmaceutics* 6(1): 97-136

156. Ball K, Bouzom F, Scherrmann JM, Walther B, Declèves X (2013) Physiologically based pharmacokinetic modelling of drug penetration across the blood-brain barrier--towards a mechanistic IVIVE-based approach. *AAPS Journal* 15(4): 913-32
157. Neuhoff S, Yeo KR, Barter Z, Jamei M, Turner DB, Rostami-Hodjegan A (2013) Application of permeability-limited physiologically-based pharmacokinetic models: part I-digoxin pharmacokinetics incorporating P-glycoprotein-mediated efflux. *Journal of Pharmaceutical Sciences* 102(9): 3145-60
158. Pang KS, Chow EC (2012) Commentary: theoretical predictions of flow effects on intestinal and systemic availability in physiologically based pharmacokinetic intestine models: the traditional model, segregated flow model, and QGut model. *Drug Metabolism and Disposition* 40(10): 1869-77
159. Meyer-Almes FJ, Auer M (2000) Enzyme inhibition assays using fluorescence correlation spectroscopy: a new algorithm for the derivation of k_{cat}/K_m and K_i values at substrate concentrations much lower than the Michaelis constant. *Biochemistry* 39(43): 13261-8
160. Stein, WD (1997) Kinetics of the multidrug transporter (P-glycoprotein) and its reversal. *Physiological Reviews* 77: 545–590
161. Gómez-Lechón MJ, Donato MT, Castell JV, Jover R (2003) Human hepatocytes as a tool for studying toxicity and drug metabolism. *Current Drug Metabolism* 4(4): 292-312
162. Hewitt NJ, Lecluyse EL, Ferguson SS (2007) Induction of hepatic cytochrome P450 enzymes: methods, mechanisms, recommendations, and *in vitro-in vivo* correlations. *Xenobiotica* 37: 1196–1224
163. Shitara Y, Itoh T, Sato H, Li AP, Sugiyama Y (2003) Inhibition of transporter-mediated hepatic uptake as a mechanism for drug-drug interaction between cer- ivastatin and cyclosporin A. *Journal of Pharmacology and Experimental Therapeutics* 304: 610–616
164. Roelofsen H, Bakker CT, Schoemaker B, Heijn M, Jansen PL, Elferink RP (1995) Redistribution of canalicular organic anion transport activity in isolated and cultured rat hepatocytes. *Hepatology* 21(6): 1649-57
165. Ghibellini G, Leslie EM, Brouwer KL (2006) Methods to evaluate biliary excretion of drugs in humans: an updated review. *Molecular Pharmaceutics* 3(3): 198-211
166. Liminga G, Nygren P, Larsson R (1994) Microfluorometric evaluation of calcein acetoxymethyl ester as a probe for P-glycoprotein-mediated resistance: effects of cyclosporin A and its nonimmunosuppressive analogue SDZ PSC 833. *Experimental Cell Research* 212: 291–296

167. Tiberghien F and Loo R (1996) Ranking of P-glycoprotein substrates and inhibitors by calcein-AM fluorometry screening assay. *Anticancer Drugs* 7: 568–578
168. Scarborough GA (1995) Drug-stimulated ATPase activity of the human P-glycoprotein. *Journal of Bioenergetics and Biomembranes* 27: 37–41
169. Litman T, Zeuthen T, Skovsgaard T, Stein WD (1997) Structure-activity relationships of P-glycoprotein interacting drugs: kinetic characterization of their effects on ATPase activity. *Biochimica et Biophysica Acta* 1361: 159–168
170. Sun H and Pang KS (2008) Permeability, transport, and metabolism of solutes in Caco-2 cell monolayers: a theoretical study. *Drug Metabolism and Disposition* 36: 102–123
171. Ito K, Kusuhara H, Sugiyama Y (1999) Effects of intestinal CYP3A4 and P-glycoprotein on oral drug absorption—theoretical approach. *Pharmaceutical Research (NY)* 16: 225–231
172. González-Alvarez I, Fernández-Teruel C, Garrigues TM, Casabo VG, Ruiz-García A, Bermejo M (2005) Kinetic modelling of passive transport and active efflux of a fluoroquinolone across Caco-2 cells using a compartmental approach in NONMEM. *Xenobiotica* 35(12): 1067–88
173. Tam D, Sun H, Pang KS (2003) Influence of P-glycoprotein, transfer clearances, and drug binding on intestinal metabolism in Caco-2 cell monolayers or membrane preparations: a theoretical analysis. *Drug Metabolism Disposition* 31: 1214–1226
174. Irie M, Terada T, Okuda M, Inui K-I (2004) Efflux properties of basolateral peptide transporter in human intestinal cell line Caco-2. *Pflügers Archiv European Journal of Physiology* 449: 186–194
175. Abu-Zahra TN and Pang KS (2000) Effect of zonal transport and metabolism on hepatic removal: enalapril hydrolysis in zonal, isolated rat hepatocytes *in vitro* and correlation with perfusion data. *Drug Metabolism and Disposition* 28: 807–813
176. Bourdet DL, Pollack GM, Thakker DR (2006) Intestinal absorptive transport of the hydrophilic cation ranitidine: a kinetic modeling approach to elucidate the role of uptake and efflux transporters and paracellular vs. transcellular transport in Caco-2 cells. *Pharmaceutical Research* 23: 1178–1187
177. Ho NFH, Raub TJ, Burton PS, Barsuhn CL, Adson A, Audus KL, Borchardt RT (2000) Quantitative approaches to delineate passive transport mechanisms in cell culture monolayers, in *Transport Processes in Pharmaceutical Systems* (Amidon GL, Lee PI, and Topp EM eds) pp 219–317, Marcel Dekker, New York

178. Tran TT, Mittal A, Aldinger T, Polli JW, Ayrton A, Ellens H, Bentz J (2005) The elementary mass action rate constants of P-gp transport for a confluent monolayer of MDCKII-hMDR1 cells. *Biophysical Journal* 88: 715–738
179. Zhang L, Strong JM, Qiu W, Lesko LJ, Huang SM (2006) Scientific perspectives on drug transporters and their role in drug interactions. *Molecular Pharmaceutics* 3: 62–69
180. Balimane PV, Han YH, Chong S (2006) Current industrial practices of assessing permeability and P-glycoprotein interaction. *AAPS Journal* 8: E1–E13
181. Keogh JP, Kunta JR (2006) Development, validation and utility of an *in vitro* technique for assessment of potential clinical drug-drug interactions involving P-glycoprotein. *European Journal of Pharmaceutical Sciences* 27: 543–554
182. Polli JW, Wring SA, Humphreys JE, Huang L, Morgan JB, Webster LO, Serabjit-Singh CS (2001) Rational use of *in vitro* P-glycoprotein assays in drug discovery. *Journal of Pharmacology and Experimental Therapeutics* 299: 620–628
183. Rautio J, Humphreys JE, Webster LO, Balakrishnan A, Keogh JP, Kunta JR, Serabjit-Singh CJ, Polli JW (2006) *In vitro* p-glycoprotein inhibition assays for assessment of clinical drug interaction potential of new drug candidates: a recommendation for probe substrates. *Drug Metabolism and Disposition* 34: 786–792
184. Hidalgo IJ, Raub TJ, Borchardt RT (1989) Characterization of the human colon carcinoma cell line (Caco-2) as a model system for intestinal epithelial permeability. *Gastroenterology* 96: 736–749
185. Burton PS, Conradi RA, Hilgers AR, Ho NF (1993) Evidence for a polarized efflux system for peptides in the apical membrane of Caco-2 cells. *Biochemical and Biophysical Research Communications* 190: 760–766
186. Anderle P, Niederer E, Rubas W, Hilgendorf C, Spahn-Langguth H, Wunderli-Allenspach H, Merkle HP, Langguth P (1998) P-Glycoprotein (P-gp) mediated efflux in Caco-2 cell monolayers: the influence of culturing conditions and drug exposure on P-gp expression levels. *Journal Pharmaceutical Sciences* 87: 757–762
187. Gao J, Murase O, Schowen RL, Aubé J, Borchardt RT (2001) A functional assay for quantitation of the apparent affinities of ligands of P-glycoprotein in Caco-2 cells. *Pharmaceutical Research* 18: 171–176
188. Artursson P and Karlsson J (1991) Correlation between oral drug absorption in humans and apparent drug permeability coefficients in human intestinal epithelial (Caco-2) cells. *Biochemical and Biophysical Research Communications* 175(3): 880–885

189. Taipalensuu J, Tornblom H, Lindberg G, Einarsson C, Sjoqvist F, Melhus H, Garberg P, Sjoström B, Lundgren B, Artursson P (2001) Correlation of gene expression of ten drug efflux proteins of the ATP-binding cassette transporter family in normal human jejunum and in human intestinal epithelial Caco-2 cell monolayers. *Journal of Pharmacology and Experimental Therapeutics* 299: 164–170
190. Prime-Chapman HM, Fearn RA, Cooper AE, Moore V, Hirst BH (2004) Differential multidrug resistance-associated protein 1 through 6 isoform expression and function in human intestinal epithelial Caco-2 cells. *Journal of Pharmacology and Experimental Therapeutics* 311: 476–484
191. Hidalgo IJ and Borchardt RT (1990) Transport of bile acids in a human intestinal epithelial cell line, Caco-2. *Biochimica et Biophysica Acta* 1035: 97–103
192. Riley SA, Warhurst G, Crowe PT, Turnberg LA (1991) Active hexose transport across cultured human Caco-2 cells: characterisation and influence of culture conditions. *Biochimica et Biophysica Acta* 1066: 175–182
193. Hu M and Borchardt RT (1992) Transport of a large neutral amino acid in a human intestinal epithelial cell line (Caco-2): uptake and efflux of phenylalanine. *Biochimica et Biophysica Acta* 1135: 233–244
194. Ma TY, Dyer DL, Said HM (1994) Human intestinal cell line Caco-2: a useful model for studying cellular and molecular regulation of biotin uptake. *Biochimica et Biophysica Acta* 1189: 81–88
195. Mesonero J, Matosin M, Cambier D, Rodriguez-Yoldi MJ, Brot-Laroche E (1995) Sugar-dependent expression of the fructose transporter GLUT5 in Caco-2 cells. *Biochemical Journal* 312: 757–762
196. Goh LB, Spears KJ, Yao D, Ayrton A, Morgan P, Wolf CR, Friedberg T (2002) Endogenous drug transporters in *in vitro* and *in vivo* models for the prediction of drug disposition in man. *Biochem Pharmacol* 64: 1569–1578
197. Pauli-Magnus C, von Richter O, Burk O, Ziegler A, Mettang T, Eichelbaum M, Fromm MF (2000) Characterization of the major metabolites of verapamil as substrates and inhibitors of P-glycoprotein. *Journal of Pharmacology and Experimental Therapeutics* 293: 376–382
198. The Digitalis Investigation Group (1997) The Effect of Digoxin on Mortality and Morbidity in Patients with Heart Failure. *New England Journal of Medicine* 336: 525–533
199. Packer M, Gheorghide M, Young JB, Costantini PJ, Adams KF, Cody RJ, Smith LK, Van Voorhees L, Gourley LA, Jolly MK (1993) Withdrawal of digoxin from patients with chronic heart failure treated with angiotensin-converting-

enzyme inhibitors. RADIANCE Study. *New England Journal of Medicine* 329(1): 1-7

200. Uretsky BF, Young JB, Shahidi FE, Yellen LG, Harrison MC, Jolly MK (1993) Randomized study assessing the effect of digoxin withdrawal in patients with mild to moderate chronic congestive heart failure: results of the PROVED trial. PROVED Investigative Group. *Journal of the American College of Cardiology* (4): 955-62
201. Hunt SA, Abraham WT, Chin MH, Feldman AM, Francis GS, Ganiats TG, Jessup M, Konstam MA, Mancini DM, Michl K, Oates JA, Rahko PS, Silver MA, Stevenson LW, Yancy CW, Antman EM, Smith SC Jr, Adams CD, Anderson JL, Faxon DP, Fuster V, Halperin JL, Hiratzka LF, Jacobs AK, Nishimura R, Ornato JP, Page RL, Riegel B; American College of Cardiology, American Heart Association Task Force on Practice Guidelines, American College of Chest Physicians, International Society for Heart and Lung Transplantation, and Heart Rhythm Society (2005) ACC/AHA 2005 Guideline Update for the Diagnosis and Management of Chronic Heart Failure in the Adult: a report of the American College of Cardiology/American Heart Association Task Force on Practice Guidelines (Writing Committee to Update the 2001 Guidelines for the Evaluation and Management of Heart Failure): developed in collaboration with the American College of Chest Physicians and the International Society for Heart and Lung Transplantation: endorsed by the Heart Rhythm Society. *Circulation* 112: e154 –235
202. Adams JF, Lindenfield JA, Arnold JM, Baker D, Barnard DH, Baughman KL, Boehmer JP, Deedwania P, Dumbar SB, Elkayam U, Gheorghide M, Howlett JG, Konstam MA, Kronenberg MW, Massie BM, Mehra M, Miller AB, Moser DK, Patterson JK, Rodeheffer RJ, Sackner-Bernstein J, Silver MA, Starling RC, Stevenson LW, Wagoner LE. Heart Failure Society of America (HFSA) (2006) Comprehensive heart failure practice guidelines. *Journal of Cardiac Failure* 12: 10–36
203. Wyse DG, Waldo AL, DiMarco JP, Domanski MJ, Rosenberg Y, Schron EB, Kellen JC, Greene HL, Mickel MC, and Dalquist JE, Corley SD; Atrial Fibrillation Follow-up Investigation of Rhythm Management (AFFIRM) Investigators (2002) A comparison of rate control and rhythm control in patients with atrial fibrillation. *New England Journal of Medicine* 347: 1825–1833
204. Ejvinsson G (1978) Effect of quinidine on plasma concentrations of digoxin. *British Medical Journal* 1(6108): 279-80
205. Leahey EB Jr, Reiffel JA, Drusin RE, Heissenbuttel RH, Lovejoy WP, Bigger JT Jr (1978) Interaction between quinidine and digoxin. *JAMA* 240(6): 533-4
206. Su SF, Huang JD (1996) Inhibition of the intestinal digoxin absorption and exsorption by quinidine. *Drug Metabolism and Disposition* 24: 142–147

207. Hori R, Tomita Y, Katsura T, Yasuhara M, Inui K, Takano M (1993) Transport of bestatin in rat renal brush-border membrane vesicles. *Biochemical Pharmacology* 45: 1763–1768
208. Kovarik JM, Rigaudy L, Guerret M, Gerbeau C, Rost KL (1999) Longitudinal assessment of a P-glycoprotein-mediated drug interaction of valsopodar on digoxin. *Clinical Pharmacology and Therapeutics* 66: 391–400
209. MULTAQ (dronedarone) (2009) Package insert. Sanofi-Aventis
210. Rameis H (1985) Quinidine-digoxin interaction: are the pharmacokinetics of both drugs altered? *International Journal of Clinical Pharmacology* 23: 145–153
211. Robinson K, Johnston A, Walker S, Mulrow JP, McKenna WJ, Holt DW (1989) The digoxin- amiodarone interaction. *Cardiovascular Drugs and Therapy* 3: 25–28
212. Dorian P, Strauss M, Cardella C, David T, East S, Ogilvie R (1988) Digoxin-cyclosporine interaction: severe digitalis toxicity after cyclosporine treatment. *Clinical and investigative medicine* 11: 108–112
213. Johne A, Brockmoller J, Bauer S, Maurer A, Langheinrich M, Roots I (1999) Pharmacokinetic interaction of digoxin with an herbal extract from St John's wort (*Hypericum perforatum*). *Clinical Pharmacology and Therapeutics* 66: 338–345
214. Mueller SC, Uehleke B, Woehling H, Petzsch M, Majcher-Peszynska J, Hehl EM, Sievers H, Frank B, Riethling AK, Drewelow B (2004) Effect of St John's wort dose and preparations on the pharmacokinetics of digoxin. *Clinical Pharmacology and Therapeutics* 75(6): 546-57
215. Becquemont L, Verstuyft C, Kerb R, Brinkmann U, Lebot M, Jaillon P, Funck-Brentano C (2001) Effect of grapefruit juice on digoxin pharmacokinetics in humans. *Clinical Pharmacology and Therapeutics* 70(4): 311-6
216. Parker RB, Yates CR, Soberman JE, Laizure SC (2003) Effects of grapefruit juice on intestinal P-glycoprotein: evaluation using digoxin in humans. *Pharmacotherapy* 23(8): 979-87
217. Fromm MF, Kim RB, Stein CM, Wilkinson GR, Roden DM (1999) Inhibition of P-glycoprotein-mediated drug transport: A unifying mechanism to explain the interaction between digoxin and quinidine. *Circulation* 99: 552–557
218. Tanigawara Y, Okamura N, Hirai M, Yasuhara M, Ueda K, Kioka N, Komano T, Hori R (1992) Transport of digoxin by human P-glycoprotein expressed in a porcine kidney epithelial cell line (LLCPK). *Journal of Pharmacology and Experimental Therapeutics* 263(2): 840-5

219. Cavet ME, West M, Simmons NL (1996) Transport and epithelial secretion of the cardiac glycoside, digoxin, by human intestinal epithelial (Caco-2) cells. *British Journal of Pharmacology* 118: 1389–1396
220. Jalava KM, Partanen J, Neuvonen PJ (1997) Itraconazole decreases renal clearance of digoxin. *Therapeutic Drug Monitoring* 19: 609–613
221. Tsuruoka S, Sugimoto KI, Fujimura A, Imai M, Asano Y, Muto S (2001) P-glycoprotein-mediated drug secretion in mouse proximal tubule perfused *in vitro*. *Journal of the American Society of Nephrology* 12(1): 177-81
222. Kawahara M, Sakata A, Miyashita T, Tamai I, Tsuji A (1999) Physiologically based pharmacokinetics of digoxin in *mdr1a* knockout mice. *Journal of Pharmaceutical Sciences* 88: 1281–1287
223. Drescher S, Glaeser H, Mürdter T, Hitzl M, Eichelbaum M, Fromm MF (2003) P-glycoprotein-mediated intestinal and biliary digoxin transport in humans. *Clinical Pharmacology and Therapeutics* 73: 223-231
224. Igel S, Drescher S, Mürdter T, Hofmann U, Heinkele G, Tegude H, Glaeser H, Brenner SS, Somogyi AA, Omari T, Schafer C, Eichelbaum M, Fromm MF (2007) Increased absorption of digoxin from the human jejunum due to inhibition of intestinal transporter-mediated efflux. *Clinical Pharmacokinetics* 46: 777–785
225. Hughes J, Crowe A (2010) Inhibition of P-glycoprotein-mediated efflux of digoxin and its metabolites by macrolide antibiotics. *Journal of Pharmacological Sciences* 113(4): 315-24
226. Eberl S, Renner B, Neubert A, Reisig M, Bachmakov I, König J, Dörje F, Mürdter TE, Ackermann A, Dormann H, Gassmann KG, Hahn EG, Zierhut S, Brune K, Fromm MF (2007) Role of p-glycoprotein inhibition for drug interactions: evidence from *in vitro* and pharmacoepidemiological studies. *Clinical Pharmacokinetics* 46(12): 1039-49
227. Pauli-Magnus C, Mürdter T, Godel A, Mettang T, Eichelbaum M, Klotz U, Fromm MF (2001) P-Glycoprotein-mediated transport of digitoxin, alpha-methyldigoxin and beta-acetyldigoxin. *Naunyn-Schmiedeberg's Archives of Pharmacology* 363: 337–343
228. Haslam IS, Jones K, Coleman T, Simmons NL (2008) Rifampin and digoxin induction of MDR1 expression and function in human intestinal (T84) epithelial cells. *British Journal of Pharmacology* 154(1): 246-55
229. Tian Q, Zhang J, Chan E, Duan W, Zhou SF (2005) Multidrug resistance proteins (MRPs) and implication in drug development. *Drug Development and Research* 51: 1–18

230. Iisalo E (1997) Clinical pharmacokinetics of digoxin. *Clinical Pharmacokinetics* 2: 1-16
231. Wu CY and Benet LZ (2005) Predicting drug disposition via application of BCS: transport/absorption/elimination interplay and development of a biopharmaceutics drug disposition classification system. *Pharmaceutical Research* 22: 11–23
232. Gheorghide M, Adams KF Jr, Colucci WS (2004) Digoxin in the management of cardiovascular disorders. *Circulation* 109(24): 2959-64
233. Iisalo E (1997) Clinical pharmacokinetics of digoxin. *Clinical Pharmacokinetics* 2: 1-16
234. Ochs HR, Greenblatt DJ, Bodem G, Harmatz JS (1978) Dose-independent pharmacokinetics of digoxin in humans. *American Heart Journal* 96(4): 507-11
235. Rengelshausen J, Goggelmann C, Burhenne J, Riedel KD, Ludwig J, Weiss J, Mikus G, Walter-Sack I, Haefeli WE (2003) Contribution of increased oral bioavailability and reduced nonglomerular renal clearance of digoxin to the digoxin-clarithromycin interaction. *British Journal of Clinical Pharmacology* 56: 32–38
236. Ma JD, Tsunoda SM, Bertino JS Jr, Trivedi M, Beale KK, Nafziger AN (2010) Evaluation of *in vivo* P-glycoprotein phenotyping probes: a need for validation. *Clinical Pharmacokinetics* 49(4): 223-37
237. Cook JA, Feng B, Fenner KS, Kempshall S, Liu R, Rotter C, Smith DA, Troutman MD, Ullah M, Lee CA (2010) Refining the *in vitro* and *in vivo* critical parameters for P-glycoprotein, [I]/IC₅₀ and [I₂]/IC₅₀, that allow for the exclusion of drug candidates from clinical digoxin interaction studies. *Molecular Pharmaceutics* 7: 398–411
238. Fenner KS, Troutman MD, Kempshall S, Cook JA, Ware JA, Smith DA, Lee CA (2009) Drug-drug interactions mediated through P-glycoprotein: clinical relevance and *in vitro-in vivo* correlation using digoxin as a probe drug. *Clinical Pharmacology and Therapeutics* 85: 173–181
239. Perloff MD, von Moltke LL, Greenblatt DJ (2002) Fexofenadine transport in Caco-2 cells: inhibition with verapamil and ritonavir. *Journal of Clinical Pharmacology* 42(11): 1269-74
240. Petri N, Tannergren C, Rungstad D, Lennernäs H (2004) Transport characteristics of fexofenadine in the Caco-2 cell model. *Pharmaceutical Research* 21(8): 1398-404
241. Tahara H, Kusuhara H, Fuse E, Sugiyama Y (2005) P-glycoprotein plays a major role in the efflux of fexofenadine in the small intestine and blood-brain barrier,

but only a limited role in its biliary excretion. *Drug Metabolism and Disposition* 33(7): 963-8

242. Simpson K and Jarvis B (2000) Fexofenadine: a review of its use in the management of seasonal allergic rhinitis and chronic idiopathic urticaria. *Drugs* 59(2): 301-21
243. Pratt CM, Mason J, Russell T, Reynolds R, Ahlbrandt R (1999) Cardiovascular safety of fexofenadine HCl. *The American Journal of Cardiology* 83(10): 1451-4
244. Hamman MA, Bruce MA, Haehner-Daniels BD, Hall SD (2001) The effect of rifampin administration on the disposition of fexofenadine. *Clinical Pharmacology and Therapeutics* 69: 114–121
245. Tateishi T, Miura M, Suzuki T, Uno T (2008) The different effects of itraconazole on the pharmacokinetics of fexofenadine enantiomers. *British Journal of Clinical Pharmacology* (5): 693-700
246. Ming X, Knight BM, Thakker DR (2011) Vectorial Transport of Fexofenadine across Caco-2 Cells: Involvement of Apical Uptake and Basolateral Efflux Transporters. *Molecular Pharmaceutics* 8(5): 1677–1686
247. Shitara Y, Horie T, Sugiyama Y (2006) Transporters as a determinant of drug clearance and tissue distribution. *European Journal of Pharmaceutical Sciences* 27(5): 425-46
248. Hayeshi R, Hilgendorf C, Artursson P, Augustijns P, Brodin B, Dehertogh P, Fisher K, Fossati L, Hovenkamp E, Korjamo T, Masungi C, Maubon N, Mols R, Müllertz A, Mönkkönen J, O'Driscoll C, Oppers-Tiemissen HM, Ragnarsson EG, Rooseboom M, Ungell AL (2008) Comparison of drug transporter gene expression and functionality in Caco-2 cells from 10 different laboratories. *European Journal of Pharmaceutical Sciences* 35: 383–396
249. Taipalensuu J, Tavelin S, Lazorova L, Svensson AC, Artursson P (2004) Exploring the quantitative relationship between the level of MDR1 transcript, protein and function using digoxin as a marker of MDR1-dependent drug efflux activity. *European Journal of Pharmaceutical Sciences* 21(1): 69–75

Chapter 2

QUANTITATIVE ESTIMATION OF P-GLYCOPROTEIN-MEDIATED DRUG TRANSPORT IN THE MONOLAYER PERMEABILITY ASSAY BY MECHANISTICALLY MODELED INTRINSIC CLEARANCE

2.1 Introduction

Interindividual differences in drug response and toxicity continue to be a challenge to optimal drug therapy (1). It is well appreciated that differences in drug action among patients relate to variability in the levels of drug in the blood. Cell membrane-bound transporter proteins play an important role in drug absorption, distribution, and excretion pharmacokinetic processes, which are critical determinants of drug levels and hence the pharmacological and/or toxicological profile of all drugs and xenobiotics (2; 3). Many common polymorphisms in drug transporters have been linked to altered drug pharmacokinetics and transporters are also the basis of many clinically relevant drug-drug interactions (DDIs) (3). Whole cell and expression system *in vitro* assays of drug metabolizing enzyme activities yield kinetic information that is essential for *in vitro* to *in vivo* extrapolation (IVIVE) of drug levels and for mechanistic understanding and prediction of DDIs and pharmacokinetics in the clinical setting (4; 5). Interestingly though, such biochemical characterization of drug transporter activity today remains inadequate, despite the important role of transporters in drug pharmacokinetics (5).

P-glycoprotein (P-gp), encoded by the Multidrug Resistance 1 (*MDR1*, *ABCB1*) gene, is the most clinically important and well-characterized efflux transporter, responsible for pumping drugs from inside cells to the outside milieu. P-gp is widely expressed on the apical membrane in tissues such as liver, kidney, intestines, and at the blood-brain-barrier, indicating its important role in drug disposition. A large number of pharmacologically and structurally unrelated drugs are substrates for P-gp, including: anti-cancer agents, steroid hormones, antimicrobial agents, opioids, immunosuppressants, antiarrhythmics, antihistamines, cholesterol-lowering statins, and HIV protease inhibitors, to name a few (6).

Given the clinical relevance of P-gp, an initial *in vitro* assay of P-gp transporter activity is typically performed for a drug in order to predict P-gp-drug interaction and guide further *in vivo* studies. Convention has been to measure drug flux across a tight monolayer of apical-basolateral polarized cells that have apical P-gp expression (7; 8). The apparent permeability (P_{app}) of a drug across the monolayer is estimated from the appearance of drug in the receiver compartment over time [Equation 1.12]. Due to polarized expression of P-gp efflux transporter on the apical membrane, a P-gp substrate drug would be expected to show increased P_{app} in the basolateral-apical direction ($P_{app(B-A)}$) and decreased P_{app} in the apical-basolateral direction ($P_{app(A-B)}$). The ratio of $P_{app(B-A)}/P_{app(A-B)}$, known as the efflux ratio (EfR) [Equation 1.13], is then said to estimate P-gp transport activity on a substrate drug; the assumption being that EfR and $P_{app(B-A)}$ are proportional to P-gp activity and $P_{app(A-B)}$ is inversely proportional to P-gp activity (8).

$$P_{app} = (dA_R/dt)/(S \times C_{D,0}) \quad [1.12]$$

$$EfR = P_{app(B-A)} / P_{app(A-B)} \quad [1.13]$$

While EfR, $P_{app(B-A)}$, and $P_{app(A-B)}$ can effectively identify most P-gp substrates, specific estimation of P-gp activity may be limited. Apparent permeabilities and efflux ratios, which are measured directly from flux across the monolayer, view the system as a single barrier with drug actively transported directly from the donor compartment to the receiver compartment. In reality it is the intracellular drug concentration, not the donor compartment concentration that interacts with P-gp on the apical membrane. Therefore, EfR, $P_{app(B-A)}$, and $P_{app(A-B)}$ do not account for the potentially rate limiting active uptake processes on the basolateral or apical membranes that move drug from the donor compartment into the intracellular compartment, where drug-P-gp interaction occurs. Consequently, EfR, $P_{app(B-A)}$, and $P_{app(A-B)}$ metrics fail to specifically characterize P-gp transport and thus may not show direct proportionality with P-gp transporter activity and expression (9; 10).

We propose utilizing a mathematical model that incorporates all potentially rate limiting active and passive transport processes occurring at both the apical and basolateral membranes (Figure 2.1). By fitting flux data to this model, we can estimate the kinetics

of P-gp transport from the intracellular space. The output parameter from this exercise CL_{P-gp} , P-gp intrinsic clearance, is then a mechanistically-based quantitative estimate of P-gp transporter activity. In order to compare this modeled approach for P-gp activity estimation with the typical metrics, we conducted several monolayer permeability assays with a range of P-gp expression and appraised the correlation of P_{app} , EfR, and CL_{P-gp} with P-gp expression in each assay. In theory, the level of P-gp expression on the apical membrane of polarized cells should be directly proportional to measured P-gp transport activity when the transporter is not saturated. We hypothesize that the modeled clearance (CL_{P-gp}) is a superior metric of P-gp activity compared to P_{app} or EfR.

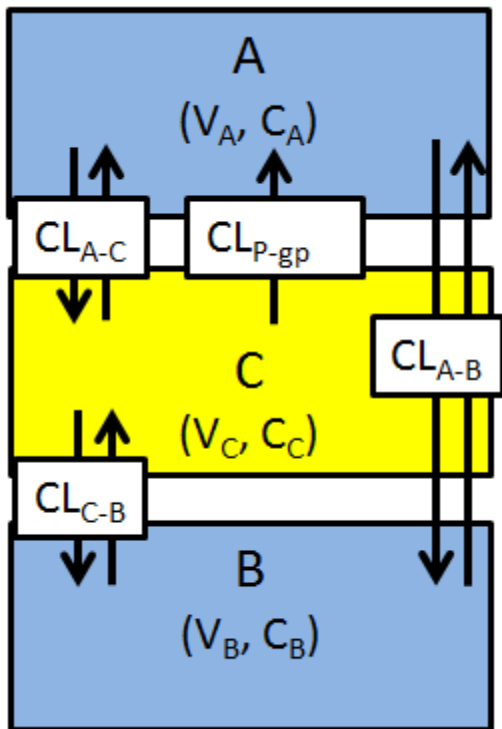


Figure 2.1. Schematic presentation of the compartmental model, with apical (A), basolateral (B), and cell (C) compartments represented. CL parameters define the transit efficiencies between compartments of volume V and drug concentration C .

2.2 Materials and Methods

2.2.1 Materials

Human colorectal adenocarcinoma [Caco-2] and porcine kidney epithelial [LLCPK] cells were obtained from American Type Culture Collection ATCC (Manassas, VA). LLC PK cells overexpressing MDR1 [LMDR1] were a generous gift from Dr. A.H. Schinkel (The Netherlands Cancer Institute, Amsterdam, Holland) and Dr. E. Schuetz (St. Jude Children's Research Hospital, Memphis, TN). Dulbecco's modified Eagle's medium (DMEM), fetal bovine serum (FBS), penicillin-streptomycin, nonessential amino acids (NEAA) and 0.05% trypsin-EDTA were all purchased from Life Technologies (Grand Island, NY). Vincristine sulfate with a purity exceeding 97.5 [HPLC], $1\alpha,25$ -dihydroxyvitamin D₃ with purity exceeding 99% [HPLC], thiazolyl blue tetrazolium bromide (MTT) with purity exceeding 98% [HPLC], digoxin with purity exceeding 96.4% [HPLC], and protease inhibitor were all sourced from Sigma-Aldrich (St. Louis, MO). Transwell cell culture inserts (12-well, 0.4 μ m) were purchased from VWR-International (Mississauga, ON). [³H]-Digoxin (specific activity, 21.8 Ci/mmol), was obtained from PerkinElmer Life & Analytical Sciences (Boston, MA). [¹⁴C]-Inulin (specific activity, 8.5mCi/mmol), with purity exceeding 95% [HPLC] was from Moravek Biochemicals (Brea, CA). Ultima Gold scintillation cocktail was purchased from PerkinElmer (Waltham, MA). Thermo Scientific Pierce IP lysis buffer and Thermo Scientific Restore Western Blot Stripping Buffer were obtained from Fischer Scientific (Ottawa, ON). Western Blocking Reagent was purchased from Roche (Indianapolis, IN). C219 monoclonal p-glycoprotein antibody was purchased from Covance (Dedham, MA). Polyclonal goat anti-actin antibody (C-11) was obtained from Santa Cruz Biotechnology, Inc. (Santa Cruz, CA). Goat anti-mouse IgG (H + L)-HRP conjugate was purchased from BioRad Canada (Mississauga, ON). Amersham ECL select western blotting detection reagent was purchased from GE Healthcare UK (Little Chalfont, Buckinghamshire).

2.2.2 Cell Culture

Caco-2 (passage no. 20-35), LLC PK (passage no. 5-15), and LMDR1 (passage no. 5-15) cells were cultured in DMEM supplemented with 50 μ g/ml streptomycin, 50 U/mL penicillin and 10% fetal bovine serum. LMDR1 culture media was also supplemented

with 10% NEAA and 640 nM vincristine to maintain P-glycoprotein expression. Cells were incubated at 37°C in 5% CO₂ in a humidified environment.

2.2.3 MTT Assay

MTT assay was performed on Caco-2 cells in 96-well plates with approximately 1.2×10^4 cells per well. Cells were treated in triplicate with 0 nM to 1500 nM $1\alpha,25(\text{OH})_2\text{D}_3$ every other day for 14 days. On day 15 cells were washed with phosphate-buffered saline (PBS) and 25 μL of 5 mg/mL MTT in PBS was added to each well. The plates were incubated for 4 h at 37 °C and the formazan formed was dissolved in 50 μL of dimethyl sulfoxide (DMSO). The background absorbance at 670 nm was subtracted from the absorbance at 569 nm to obtain the raw absorbance data (Thermo Multiskan spectrophotometer).

2.2.4 Digoxin Flux Studies

Cells were seeded in 12-well plates at a density of 90,000 cells per 0.4- μm cell culture insert and grown for 14 days with media changes every 2 days. Each time the media was changed, Caco-2 cells were treated with 0 nM (Caco-2 (0nM)), 10 nM (Caco-2 (10 nM)), or 100 nM (Caco-2 (100 nM)) of the P-gp inducer $1\alpha,25(\text{OH})_2\text{D}_3$ dissolved in DMSO. Approximately 1 h before the start of a transport experiment, the media was removed from each compartment (apical and basal) and washed and replaced with pH 7.4 Krebs-Henseleit Bicarbonate Buffer (KHB). Transport was initiated by removing the KHB and replacing it with 700 μL of KHB with or without 5 μM digoxin (3.5 μmol of digoxin) + 5.7 nM [³H]-digoxin to the appropriate compartment in triplicate. [¹⁴C]-Inulin was included in each plate in triplicate as a marker of paracellular flux. The cells were incubated at 37°C with 5% CO₂ in a humidified environment, and 25- μL aliquots were removed hourly from each compartment over 4 h. Each aliquot was mixed with 5 mL of Ultima Gold scintillation cocktail and counted using a PerkinElmer TriCarb2900 TR liquid scintillation counter.

2.2.5 Estimation of P-gp Activity

2.2.5.1 Conventional Estimates: $P_{app(A-B)}$, $P_{app(B-A)}$, and EfR

Apparent permeability (P_{app}) in both directions was determined as follows:

$$P_{app} = (dA_R/dt)/(S \times C_{D,0}) \text{ [cm/s]} \quad [1.12]$$

where dA_R/dt is the rate of drug ($[^3\text{H}]$ -digoxin or $[^{14}\text{C}]$ -inulin) appearance in the receiver compartment, S is the surface area of the cell culture insert, and $C_{D,0}$ is the initial concentration added to the donor compartment. This model is derived from Fick's first law of diffusion, assuming a constant linear concentration gradient across a single barrier and a sink condition. Efflux ratio (EfR) was determined as follows:

$$\text{EfR} = P_{app(B-A)}/P_{app(A-B)} \quad [1.13]$$

where $P_{app(B-A)}$ is the apparent permeability in the basolateral to apical direction and $P_{app(A-B)}$ is the apparent permeability in the apical to basolateral direction.

2.2.5.2 Mathematical Modeling of Transport Intrinsic clearance: CL_{P-gp}

The three-compartment kinetic model (Figure 2.1) uses a set of mass balance differential equations [Equations 2.1-2.3] to describe digoxin flux in a transwell as a one-dimensional process between an apical, a cellular, and a basolateral kinetic compartment. The volumes used for the apical, cell, and basolateral compartments were fixed at 700 μL , 2.76 μL and 700 μL respectively, and drug dispersion within the compartments was viewed as rapid and even. The cell volume was estimated using a previously reported geometric approach of multiplying cell heights by the surface area of cell culture inserts (9). CL_{P-gp} describes the efflux clearance at the apical membrane that is mediated by P-gp. CL_{A-C} and CL_{C-B} describe the net clearance due to all other transcellular transport processes (excluding P-glycoprotein-mediated clearance) across the apical membrane and the basolateral membrane respectively; we assumed symmetrical transcellular clearance at both membranes. Rate equations describing the model (Figure 2.1) were solved numerically using the Episode (Adams) integrator (Scientist, Micromath, Salt Lake City, Utah). The P-gp clearance parameter (CL_{P-gp}) and both net basolateral and apical clearance parameters (CL_{A-C} and CL_{C-B}) were estimated by simultaneous least

squares fitting of [³H]-digoxin flux data for drug administration in both directions to the model. Fitting of the paracellular clearance parameter (CL_{A-B}) was done separately using simultaneous fitting of bidirectional [¹⁴C]-inulin flux data, with all other clearance parameters set to zero. All fitted parameters were constrained to be positive numbers. The differential equations that describe the model are as follows:

In the apical compartment

$$V_A dC_A/dt = -C_A CL_{A-C} + C_C CL_{A-C} - C_A CL_{A-B} + C_B CL_{A-B} + C_C CL_{P-gp} \quad [2.1]$$

In the cellular compartment

$$V_C dC_C/dt = -C_C CL_{A-C} + C_A CL_{A-C} - C_C CL_{C-B} + C_B CL_{C-B} - C_C CL_{P-gp} \quad [2.2]$$

In the basolateral compartment

$$V_B dC_B/dt = -C_B CL_{C-B} + C_C CL_{C-B} - C_B CL_{A-B} + C_A CL_{A-B} \quad [2.3]$$

Where dC_A/dt , dC_C/dt and dC_B/dt is the rate of change of drug concentration in the apical, cell and basolateral compartments respectively; V_A , V_C and V_B are the volumes in each compartment; and C_A , C_C and C_B are the drug concentrations. Where CL_{A-B} represents the paracellular clearance; CL_{A-C} and CL_{C-B} represent the non-P-gp transcellular clearance across the apical and basolateral membranes respectively; and CL_{P-gp} represents the P-glycoprotein-mediated apical efflux clearance.

2.2.6 Immunoblotting and P-gp Quantitation

At the end of each transport experiment, the cells were collected from cell culture insert membranes, washed with ice cold PBS and then lysed in lysis buffer containing protease inhibitor by the Thermo Scientific IP lysis buffer protocol. The whole-cell lysates were then stored at -80 °C for future analysis by western blot. Control Caco-2 cells were grown in a 10 cm plate, lysed with the Thermo Scientific IP lysis buffer protocol and the whole cell lysate was loaded on every western blot. Protein concentrations of all lysates were determined by Pierce BCA protein assay (Fisher Scientific, Whitby, ON). Forty µg of control Caco-2, 20 µg of LLCPK, Caco-2 (0 nM), Caco-2 (10 nM), and Caco-2 (100

nM) and 5 μ g of LMDR1 whole cell lysate protein was separated on a NuPAGE 4-12% Bis-Tris gel (Invitrogen, Carlsbad, CA). Detection of P-glycoprotein expression was performed by overnight incubation with anti-P-glycoprotein antibody (C219), diluted 1:500 in PBS with 0.1% Tween 20 and 10% western blocking reagent. To confirm equal loading of lysates, the blot was stripped and incubated with a polyclonal goat anti-actin antibody, at a dilution of 1:20,000 (C-11; Santa Cruz Biotechnology, Inc., Santa Cruz, CA). Actin expression could not be assumed to be constant between LLCPK and Caco-2 cell types, thus normalizing to actin was not performed. Horseradish peroxidase-linked anti-mouse or anti-goat antibodies (Biorad) were used as the secondary antibodies. Blots were visualized using Amersham ECL Western blotting system (GE) and a Kodak ImageStation 4000 MM (Eastman Kodak Company, Rochester, New York). Protein expression was quantified by densitometry with ImageJ. All samples were quantified relative to the control Caco-2 whole cell lysate loaded on each blot. All quantified densitometry values were multiplied by a loading correction factor, to account for the different amounts of protein loaded between cell types.

2.2.7 Comparison of P-gp Transport Activity Metrics

For each transwell experiment, the derived CL_{P-gp} value was plot against the measured P-gp expression. CL_{P-gp} values vs. protein expression data set generated from the 5 different transwell experiment types (Caco-2 (0 nM), Caco-2 (10 nM), Caco-2 (100 nM), LLCPK, and LMDR1) was then fit by linear regression using Prism 5.0 (GraphPad Software Inc, San Diego, CA). The same process was repeated for $P_{app(A-B)}$, $P_{app(B-A)}$ and EfR estimates of P-gp activity respectively. The lines of best fit were then compared for goodness of fit (r^2) and slope.

2.2.8 Statistical Analysis

Statistical differences between group parameters were determined by 1-way ANOVA or 2-way ANOVA, using Bonferroni's multiple comparison test as appropriate (GraphPad Software Inc, San Diego, CA). A *P* value of <0.05 was considered statistically significant.

2.3 Results

2.3.1 Cell Monolayer Viability

The [^{14}C]-inulin permeability values for the cell monolayers used in the transport experiments are displayed in Table 2.1. Evidently, Vitamin D treatment (10 nM or 100 nM) did not significantly alter [^{14}C]-inulin permeability across Caco-2 cell monolayers. All Caco-2 cell conditions showed significantly higher [^{14}C]-inulin permeability than LLCPK and LMDR1 monolayers. But, all five monolayer conditions demonstrated acceptable membrane integrity, with inulin permeabilities $\leq 5 \times 10^{-6}$ cm/s.

Viability of Caco-2 cells treated with various concentrations of $1,25(\text{OH})_2\text{D}_3$ for 14 days was assessed by MTT assay (Figure 2.2). Concentrations as high as 500 nM $1,25(\text{OH})_2\text{D}_3$ were tolerable by Caco-2 cells, with only a 15% rate of cytotoxicity. This concentration was fivefold higher than the concentration used in our high vitamin D treatment condition.

2.3.2 Transport Experiments

[^3H]-Digoxin transport across the LLCPK and LMDR1 cell monolayers is shown in Figure 2.3. For [^3H]-digoxin movement out of the donor compartment (Figure 2.3A) there was a trend towards greater flux in the basolateral to apical (B-A) direction in the LMDR1 cells as compared to LLCPK. As well, flux in the apical to basolateral (A-B) direction was significantly smaller in the LMDR1 cells. In the receiver compartment (Figure 2.3B) flux in both directions was significantly different between the two cell types. The LMDR1 cells had comparatively greater B-A flux and less A-B flux than the LLCPK cells. Overall, the disparity in B-A versus A-B flux was significantly greater in the LMDR1 cells.

[^3H]-Digoxin transport across Caco-2 cells treated with 0 nM, 10 nM and 100 nM $1,25(\text{OH})_2\text{D}_3$ is shown in Figure 2.4. From the donor compartment (Figure 2.4A) A-B flux in the Caco-2 cells treated with 100 nM $1,25(\text{OH})_2\text{D}_3$ was significantly decreased compared to the Caco-2 cells not treated with $1,25(\text{OH})_2\text{D}_3$. Basolateral to apical flux however, did not significantly differ between the treatment groups. In the receiver

Table 0.1. Apparent permeability coefficients and net efflux ratio of bidirectional [^{14}C]-inulin transport over a 4 hour time course, across the various cell monolayers.

Monolayer Cell Type	$P_{\text{app(A-B)}} (\times 10^{-6} \text{ cm/s})$	$P_{\text{app(B-A)}} (\times 10^{-6} \text{ cm/s})$	EfR
LLCPK	3.122 ± 0.134	$2.989 \pm 0.153^{\text{a}}$	0.948 ± 0.014
LMDR1	3.886 ± 0.585	$2.481 \pm 0.175^{\text{a}}$	0.867 ± 0.079
Caco-2 (0 nM)	4.557 ± 0.277	$4.430 \pm 0.359^{\text{b}}$	0.953 ± 0.034
Caco-2 (10 nM)	4.142 ± 0.291	$4.067 \pm 0.285^{\text{b}}$	0.982 ± 0.002
Caco-2 (100 nM)	4.056 ± 0.299	$4.121 \pm 0.275^{\text{b}}$	1.026 ± 0.024

^{a,b} $p < 0.05$ compared between monolayer cell types

Caco-2 cells were treated every other day with culture media only (Caco-2 (0 nM)), or with culture media + 10 nM (Caco-2 (10 nM)) or + 100 nM (Caco-2 (100 nM))

1,23(OH) $_2$ D $_3$ for 2 weeks. Data are presented as mean \pm S.E. (n=6).

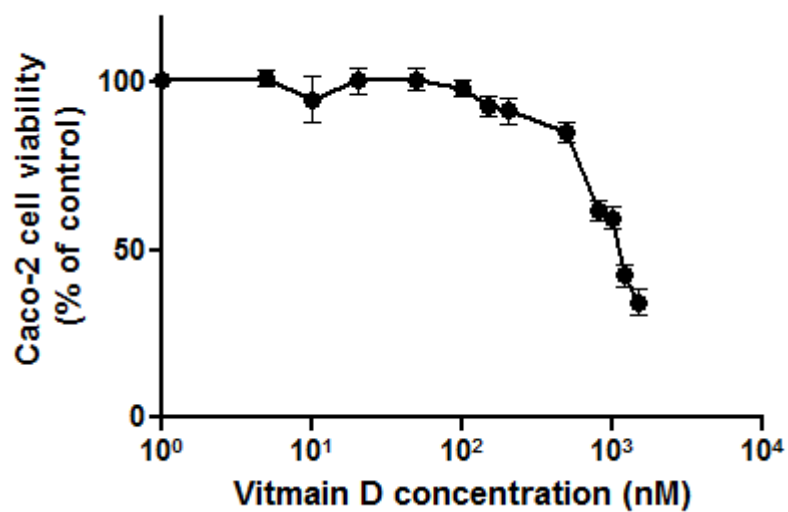


Figure 2.2. The cytotoxic effect of vitamin D ($1,25(\text{OH})_2\text{D}_3$) on cultured Caco-2 cells. Caco-2 cells (passage 15-35) were treated with various concentrations of vitamin D every other day for 14 days and cell survival was assessed by MTT assay. Data are expressed as the percentage of viability compared to control non-treated cells performed in the same experiment. Data are presented as mean \pm S.D. (n = 1 experiment, 3 technical replicates).

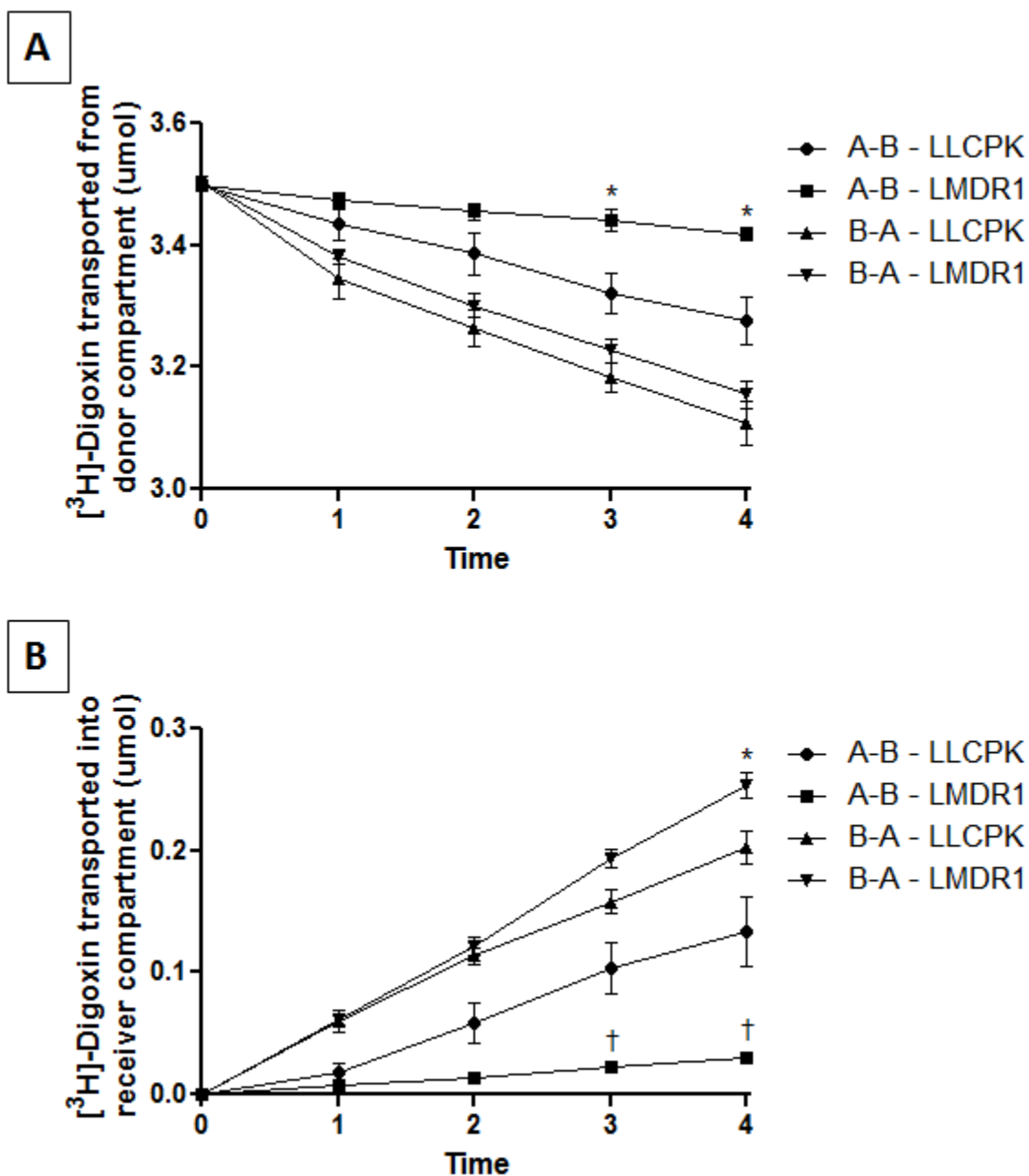


Figure 2.3. Cumulative amounts of [^3H]-digoxin transported from the donor compartment (**A**) and into the receiver compartment (**B**) of the LLCPK and LMDR1 cell monolayer, for the A-B and B-A direction, over a 4 hour time course. The transport study was performed on day 15. Data are presented as mean \pm S.E. (n=4-6).

*, $p < 0.05$ between A-B - LLCPK and A-B - LMDR1; †, $p < 0.001$ between B-A - LLCPK and B-A - LMDR1.

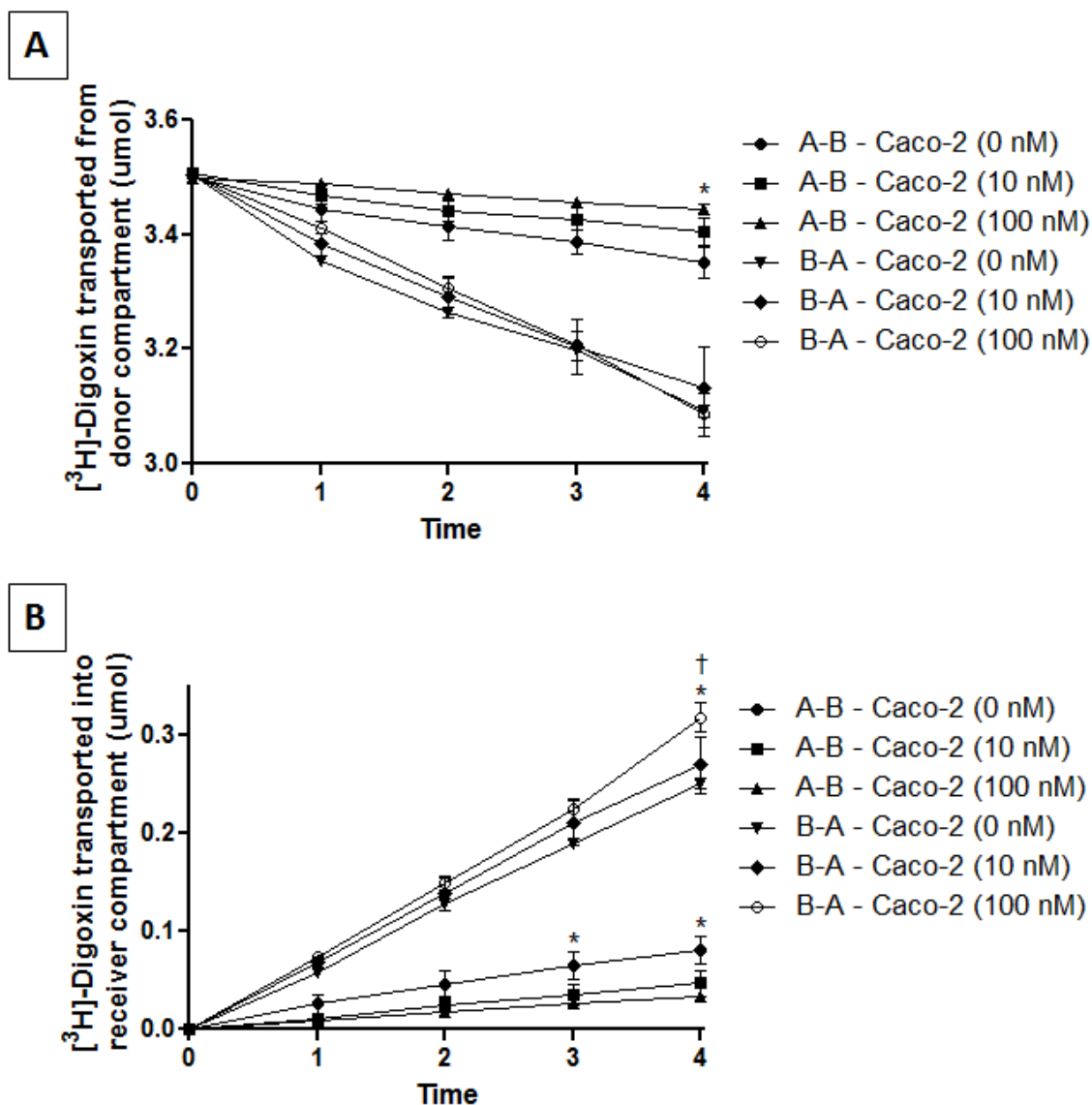


Figure 2.4. Cumulative amounts of ^{3}H -digoxin transported from the donor compartment (**A**) and into the receiver compartment (**B**) of the Caco-2 cell monolayer, for the A-B and B-A direction, over a 4 hour time course. Prior to transport, Caco-2 cells were treated every other day with culture media only (●/▼), or with culture media + 10 nM (■/◆) or + 100 nM (▲/○) $1,25(\text{OH})_2\text{D}_3$ for 2 weeks. The transport study was performed on day 15. Data are presented as mean \pm S.E. ($n \geq 4$).

*, $p < 0.05$ between A-B - Caco-2 (0 nM) and A-B - Caco-2 (100 nM); †, $p < 0.05$ B-A - Caco-2 (10 nM) and B-A - Caco-2 (100 nM).

compartment (Figure 2.4B) A-B flux was significantly lower and B-A flux was significantly higher in the Caco-2 (100 nM) cells as compared to the Caco-2 (0 nM) cells. B-A flux was also significantly smaller in the Caco-2 (10 nM) cells as compared to the Caco-2 (100 nM) cells. Evidently, the disparity in B-A versus A-B flux was significantly larger in Caco-2 cells treated with 100 nM 1,25(OH)₂D₃ versus Caco-2 cells treated 0 nM or 10 nM 1,25(OH)₂D₃.

2.3.3 P-gp Protein Expression

Figure 2.5 shows C219 antibody western blots of the whole cell lysates collected from the various transwell cell monolayers after each transport experiment; the 170 kDa P-gp protein was expressed in all cell types in a range increasing from LLCPK < Caco-2 (0 nM) < Caco-2 (10 nM) < Caco-2 (100 nM) < LMDR1. Table 2.2 shows the densitometry quantification of the P-gp western blots, corrected for the different sample amounts loaded. P-gp expression was generally consistent across experiment days; the standard deviation for P-gp expression within a cell type was between 5 and 10 percent. On average LLCPK cells showed 25 fold less P-gp expression than the LMDR1 cells stably transfected with the *MDR1* gene. Caco-2 cells showed about two fold more expression than LLCPK cells, but treatment with 10 nM and 100 nM 1,25(OH)₂D₃ induced approximately a 2-fold and 3-fold increase in Caco-2 cell P-gp expression, respectively.

2.3.4 Permeability and Efflux Ratios

We generated the apparent permeability values of digoxin across the different monolayers from flux data (Figure 2.6). Comparing bidirectional permeability between the LLCPK and the LMDR1 cell monolayers (Figure 2.6A), B-A permeability was significantly higher than A-B permeability in both cell types, but A-B permeability was significantly depressed, by 12 fold, in the LMDR1 cells versus the LLCPK cells. P-gp expression in the LMDR1 cells did not produce a significant increase in the B-A permeability of digoxin above that seen in the LLCPK cells. In examination of bidirectional permeability in the Caco-2 cells that were treated with various concentrations of 1,25(OH)₂D₃ (Figure 2.6B), B-A permeability was again significantly higher than A-B permeability in all cell monolayers. Caco-2 cells treated with 10 nM and

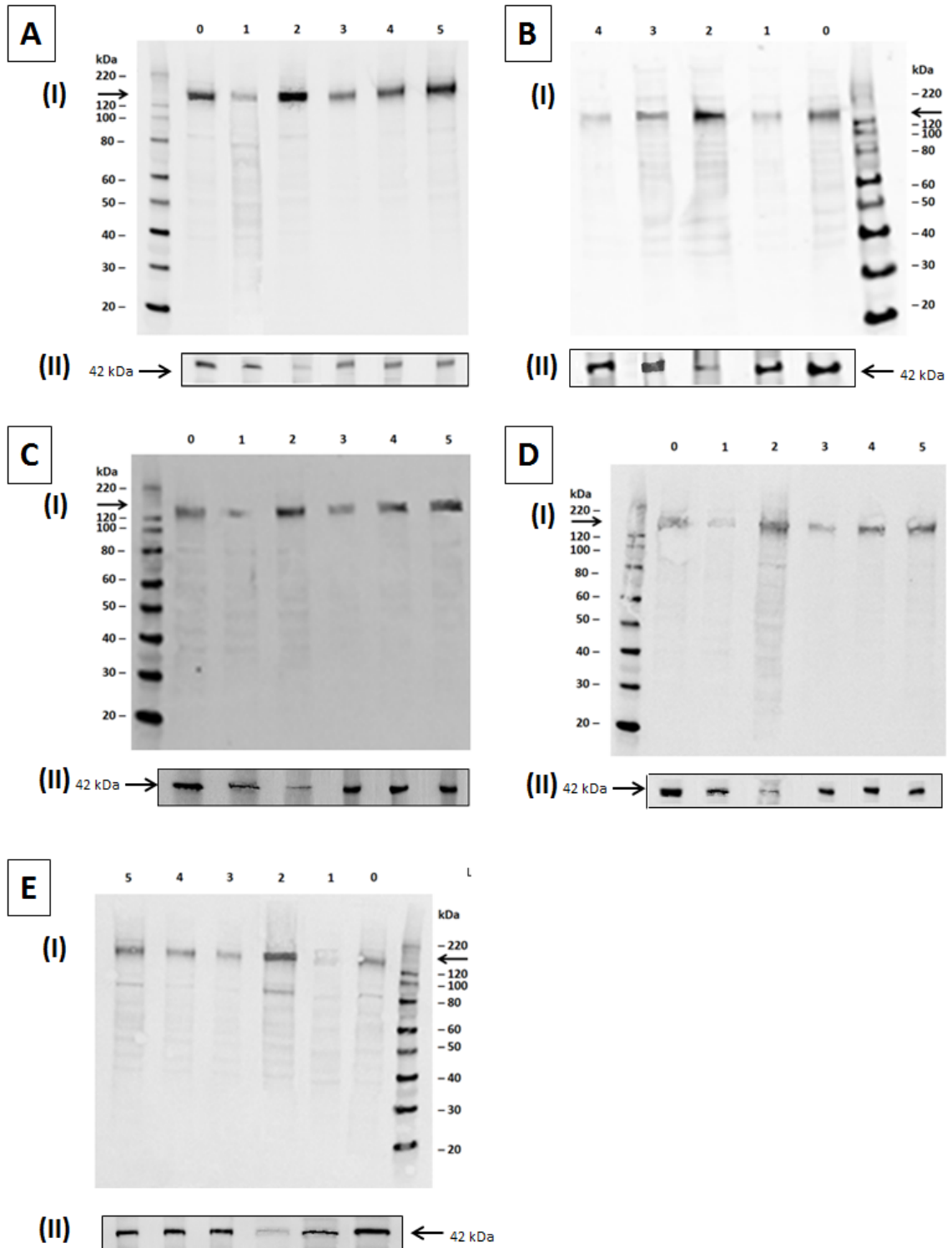


Figure 2.5. Western blots, using a mouse monoclonal anti-P-gp antibody (C219) (I) and a polyclonal goat anti-actin antibody (C-11) (II), of transwell monolayer cell lysates from experiment Day 1 (A), Day 2 and 3 (B), Day 4 (C), Day 5 (D), and Day 6 (E). , The

monolayer lysates in (A), (C), (D), and (E) were loaded as LLCPK [Lane 1], LMDR1 [Lane 2], Caco-2 (0 nM) [Lane 3], Caco-2 (10 nM) [Lane 4] and Caco-2 (100 nM) [Lane 5]; in (B) they were loaded as LLCPK (Day 2) [Lane 1], LMDR1 (Day 2) [Lane 2], Caco-2 (0 nM) (Day 2) [Lane 3], and LLCPK (Day 3) [Lane 4]. The same control Caco-2 cell lysate was loaded for densitometry comparison on every blot [Lane 0]. 40 μg of protein was loaded for all Caco-2 control lysates; 5 μg of protein was loaded for all LMDR1 monolayer lysates; 20 μg was loaded for all other monolayer lysates.

Table 0.2. Relative P-gp and Actin protein expression in transwell monolayer cells collected from each experiment day, as compared to the control Caco-2 cell lysate.

Day		LLCPK	LMDR1	Caco-2 (0nM)	Caco-2 (10nM)	Caco-2 (100nM)
1	<i>P-gp</i>	0.533	13.174	1.182	2.239	3.431
	<i>Actin</i>	1.028	1.082	1.024	1.040	1.014
2	<i>P-gp</i>	0.545	11.610	1.057	–	–
	<i>Actin</i>	0.997	0.999	0.973	–	–
3	<i>P-gp</i>	0.525	–	–	–	–
	<i>Actin</i>	1.038	–	–	–	–
4	<i>P-gp</i>	0.585	12.601	1.159	2.308	3.301
	<i>Actin</i>	1.053	1.050	0.979	1.048	0.965
5	<i>P-gp</i>	0.448	13.928	0.985	2.144	3.041
	<i>Actin</i>	1.094	1.014	0.998	1.019	0.972
6	<i>P-gp</i>	0.621	16.563	0.975	2.090	3.471
	<i>Actin</i>	1.054	1.088	0.991	0.975	1.008
<i>Avg</i>	<i>P-gp</i>	0.543	13.575	1.072	2.195	3.311
<i>SD</i>		0.059	1.873	0.096	0.097	0.194

*Cells from transwell experiments with leaky monolayers ($[^{14}\text{C}]$ -inulin permeability $> 5 \times 10^{-6}$ cm/s) were excluded from the study

100 nM $1,25(\text{OH})_2\text{D}_3$ showed respectively 2 fold and 2.7 fold less A-B permeability than untreated Caco-2 cells, but did not show significantly different A-B permeability compared to each other. Conversely, in the B-A direction Caco-2 cells treated with 10 nM $1,25(\text{OH})_2\text{D}_3$ did show significantly less permeability than 100 nM treated cells, by 1.3 fold, but 10 nM treated cells did not show significantly different B-A permeability compared to untreated Caco-2 cells. Comparing all cell monolayers in the A-B direction (Figure 2.6C), digoxin permeability was significantly higher in LLCPK cells than all other cell conditions. A-B permeability was significantly diminished by 2.8 fold in LMDR1 cells compared to untreated Caco-2 cells, but not significantly so when compared to Caco-2 cells treated with $1,25(\text{OH})_2\text{D}_3$. For all monolayers in the B-A direction (Figure 2.6D), 100 nM $1,25(\text{OH})_2\text{D}_3$ treated Caco-2 cells showed significantly higher B-A permeability, but a significant difference was not seen between the B-A permeabilities of any of the other conditions. There was a slight trend though towards decreased B-A permeability in the LLCPK cells.

Efflux ratios generated from the flux data are presented in Figure 2.7. LLCPK monolayer showed an EfR close to 1, which was significantly smaller than the LMDR1 monolayer by 5.4 fold and smaller than the three Caco-2 monolayer conditions by 2 fold, 3.7 fold, and 6.9 fold respectively. There was a significant trend towards increasing EfR values in response to increasing $1,25(\text{OH})_2\text{D}_3$ concentration. Untreated Caco-2 cells had the lowest EfR, Caco-2 cells treated with 10 nM $1,25(\text{OH})_2\text{D}_3$ were 1.7 fold higher than untreated. The EfR of Caco-2 (100 nM) cells was 2.6 fold higher than untreated Caco-2 cells and was not significantly different from the LMDR1 cell monolayer EfR.

2.3.5 Modeled Clearance

Generation of the $\text{CL}_{\text{P-gp}}$ values required fitting of the transport data to our kinetic compartmental model [Equations 2.1-2.3], which encompasses parameters for paracellular clearance between an apical and basolateral compartment, as well as parameters for clearance at separate apical and basolateral barriers. An average digoxin

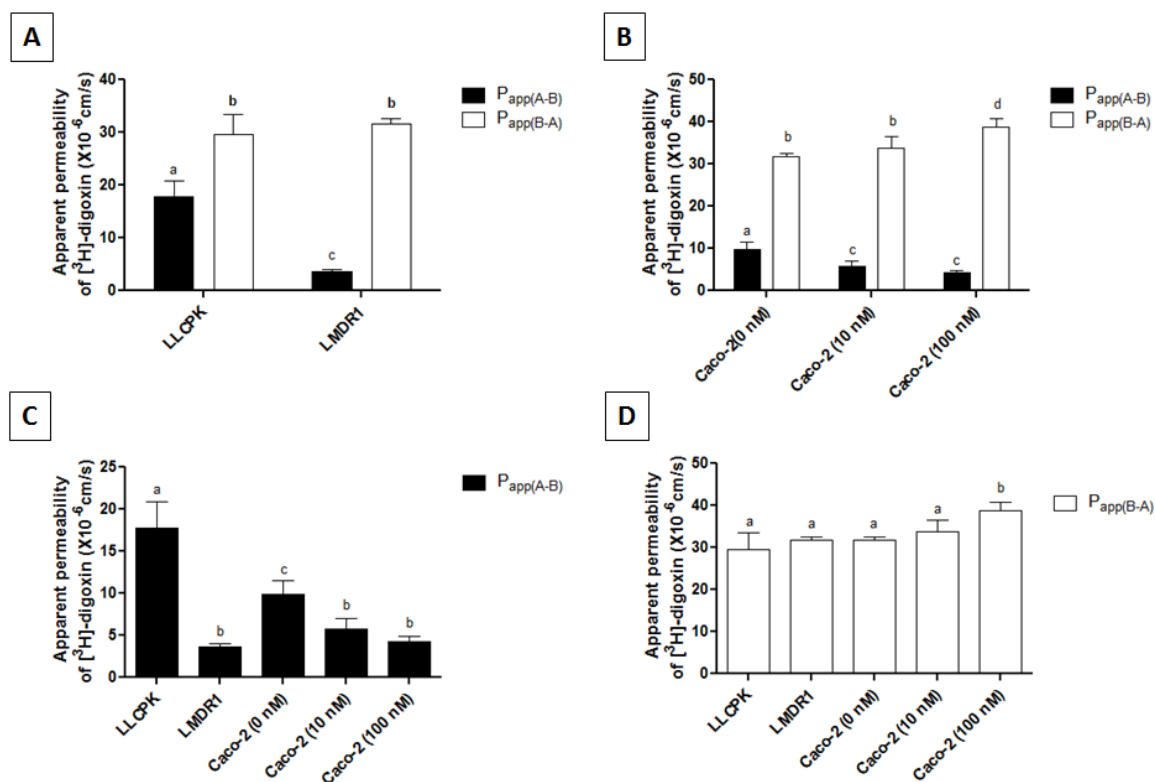


Figure 2.6. Apparent permeability coefficients for the transport of [3 H]-digoxin, over a 4 hour time course, in the A-B and B-A direction across LLCPK and LMDR1 cell monolayers (**A**), in the A-B and B-A direction across Caco-2 (0 nM), Caco-2 (10 nM) and Caco-2 (100 nM) cell monolayers (**B**), in the A-B direction across LLCPK, LMDR1, Caco-2 (0 nM), Caco-2 (10 nM) and Caco-2 (100 nM) cell monolayers (**C**), and in the B-A direction across LLCPK, LMDR1, Caco-2 (0 nM), Caco-2 (10 nM) and Caco-2 (100 nM) cell monolayers (**D**). Caco-2 cells were treated every other day with culture media only [Caco-2 (0 nM)], or with culture media + 10 nM [Caco-2 (10 nM)] or + 100 nM [Caco-2 (100 nM)] 1,25(OH) $_2$ D $_3$ for 2 weeks. Data are presented as mean \pm S.E. (n=4-6). Permeabilities with a different superscript letter (a, b, c, or d) are significantly different; $p < 0.05$.

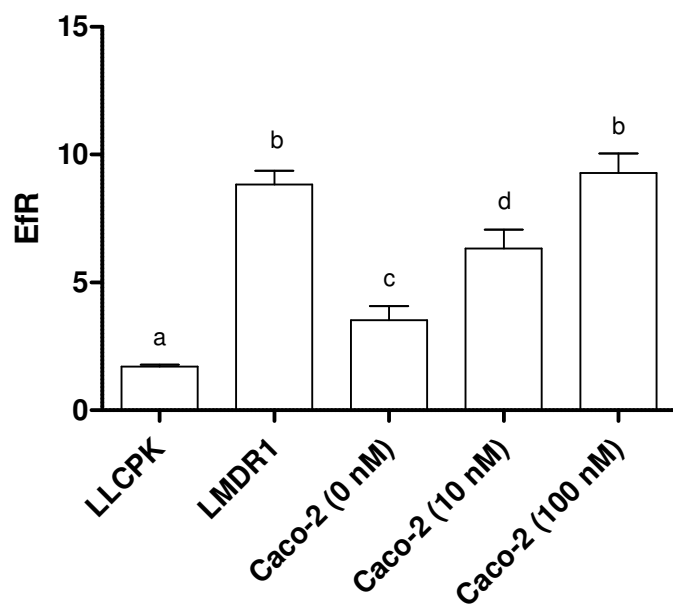


Figure 2.7. Efflux ratio of bidirectional [^3H]-digoxin transport for 4 hours across the different cell monolayers. Data are presented as mean \pm S.E. ($n \geq 4$). EfRs with a different superscript (a, b, c, or d) are significantly different; $p < 0.05$.

paracellular clearance parameter, CL_{A-B} , was estimated for each transwell cell type from fit of average [^{14}C]-inulin transwell flux data to the same compartmental model. Using these fitted CL_{A-B} values, the model was able to simulate the average [^{14}C]-inulin transport data very well for all cell types (Figure 2.8). Fixing these CL_{A-B} values as the paracellular clearance parameters in our digoxin compartmental model, we then fit the models to the average digoxin transport data for each cell type in order to generate average transcellular clearance parameters CL_{A-C} , CL_{C-B} , and CL_{P-gp} . Model simulation using these fitted CL_{A-C} , CL_{C-B} , and CL_{P-gp} parameter values also matched the average digoxin transport data quite well for all cell types (Figures 2.9 and 2.10).

As was seen with Efr, modeled P-gp clearance (CL_{P-gp}) values increased from LLCPK < Caco-2 (0 nM) < Caco-2 (10 nM) < Caco-2 (100 nM) < LMDR1 (Figure 2.11A). CL_{P-gp} in LMDR1 cells was 14.3 fold greater than in LLCPK cells, but we only see a small non-significant 1.5 fold difference between modeled CL_{P-gp} for LLCPK and Caco-2 (0 nM) cells. Similar values of CL_{P-gp} are seen between Caco-2 (0 nM) and Caco-2 (10 nM). Treatment with 100 nM of vitamin D yielded a significantly greater CL_{P-gp} , 3.0 fold higher than untreated Caco-2 cells.

In agreement with the [^{14}C]-inulin permeability data (Table 2.1), the modeled values for paracellular clearance, CL_{A-B} , were fairly consistent across all cell types, but higher in the 3 different Caco-2 cell groups (Figure 2.11D). In contrast, the modeled non-P-gp transcellular clearance was not uniform across cell types; CL_{A-C} and CL_{C-B} parameters were very similar between LLCPK and LMDR1 cells, but in Caco-2 (0 nM) cells CL_{A-C} and CL_{C-B} was around 4 fold and 2 fold greater respectively (Figure 2.11B and C). Evidently, treatment with vitamin D in the Caco-2 (10 nM) and Caco-2 (100 nM) groups reduced the CL_{A-C} and CL_{C-B} down to levels similar to that seen in LLCPK and LMDR1 cells.

Estimates of P-gp activity made by compartmental modelling as well as the estimates made by traditional permeability and efflux ratio methods for all transport experiments are summarized in Tables 2.3 and 2.4.

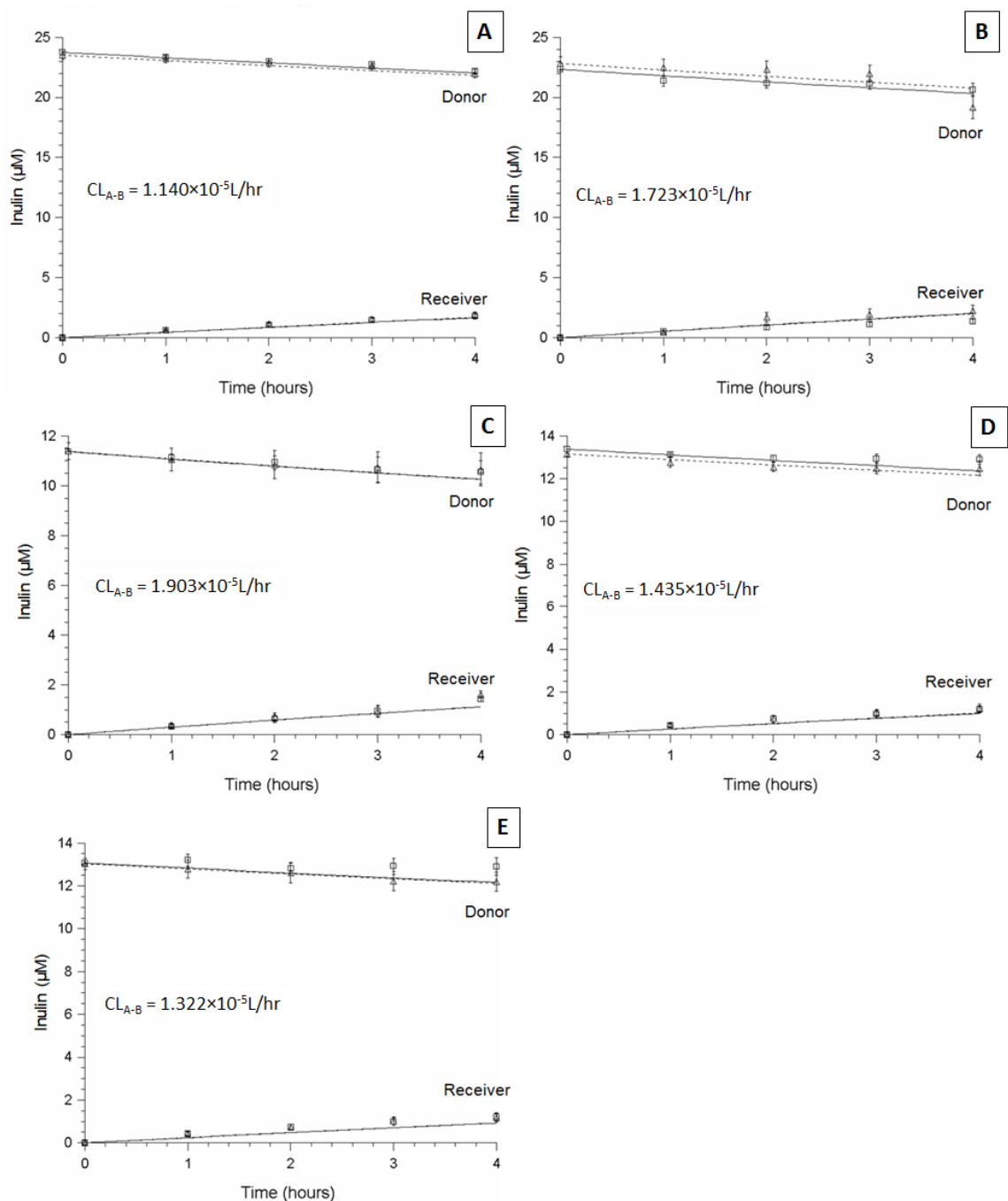


Figure 2.8. Model fits of inulin transport across LLCPK (A), LMDR1 (B), Caco-2 (0 nM) (C), Caco-2 (10 nM) (D), and Caco-2 (100 nM) (E) monolayers, using Equations 2.1-2.3, with a CL_{A-B} parameter value fit from average [14 C]-inulin transport data. *Solid lines* and *broken lines* represent simulations of the apical dosed and basolateral dosed inulin transport respectively. \blacksquare and \blacktriangle represent apical and basolateral dosed inulin data

points respectively. Data points presented are the average of 6 transport experiments \pm SE.

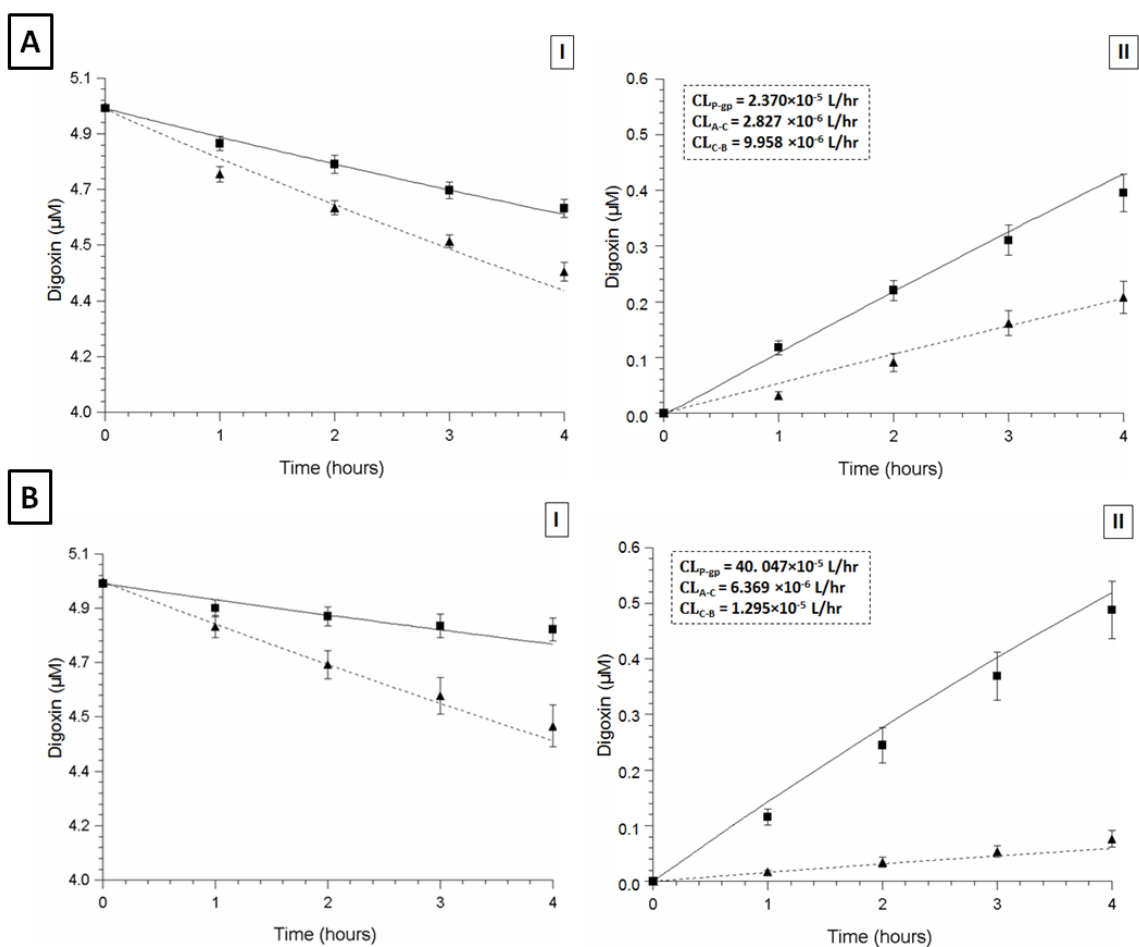


Figure 2.9. Model fits of digoxin transwell transport across **LLCPK (A)** and **LMDR1 (B)** cell monolayers out of the donor compartment (**I**) and into the receiver compartment (**II**), using Equations 2.1-2.3, with CL_{P-gp} , CL_{A-C} , and CL_{C-B} parameter values fit from average [^3H]-digoxin transport data. The *solid line* and the *broken line* represent model fits of the apical dosed and basolateral dosed digoxin transport respectively. ■ and ▲ represent apical and basolateral dosed digoxin data points respectively. Data points presented are the average of 6 transport experiment days \pm SE.

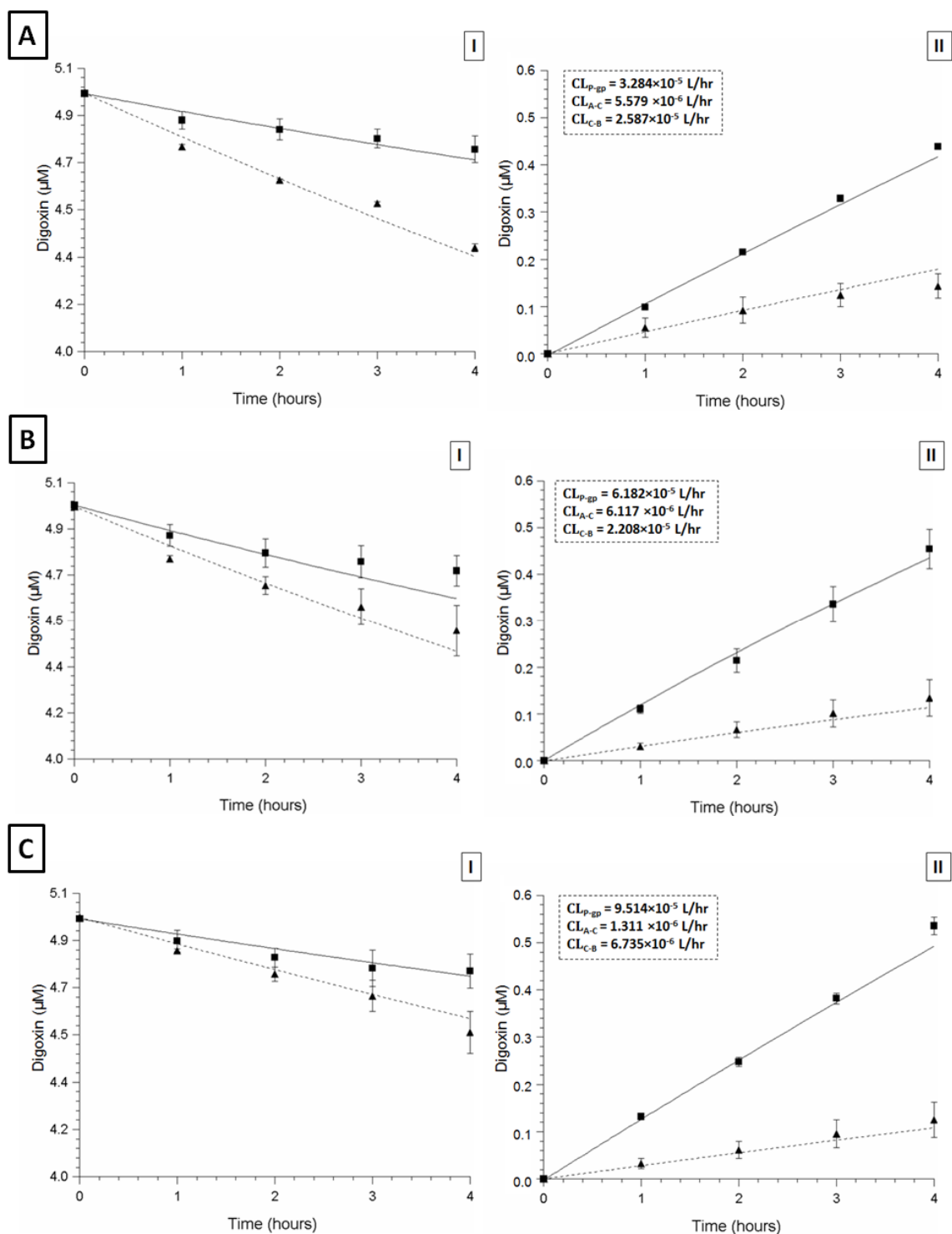


Figure 2.10. Model fits of digoxin transwell transport across **Caco-2 (0 nM) (A)**, **Caco-2 (10 nM) (B)**, and **Caco-2 (100 nM) (C)** cell monolayers out of the donor compartment (**I**) and into the receiver compartment (**II**), using Equations 2.1-2.3, with CL_{P-gp}, CL_{A-C}, and CL_{C-B} parameter values fit from average [³H]-digoxin transport data. The *solid line*

and the *broken line* represent model fits of the apical dosed and basolateral dosed digoxin transport respectively. ■ and ▲ represent apical and basolateral dosed digoxin data points respectively. Data points presented are the average of 6 transport experiment days \pm SE.

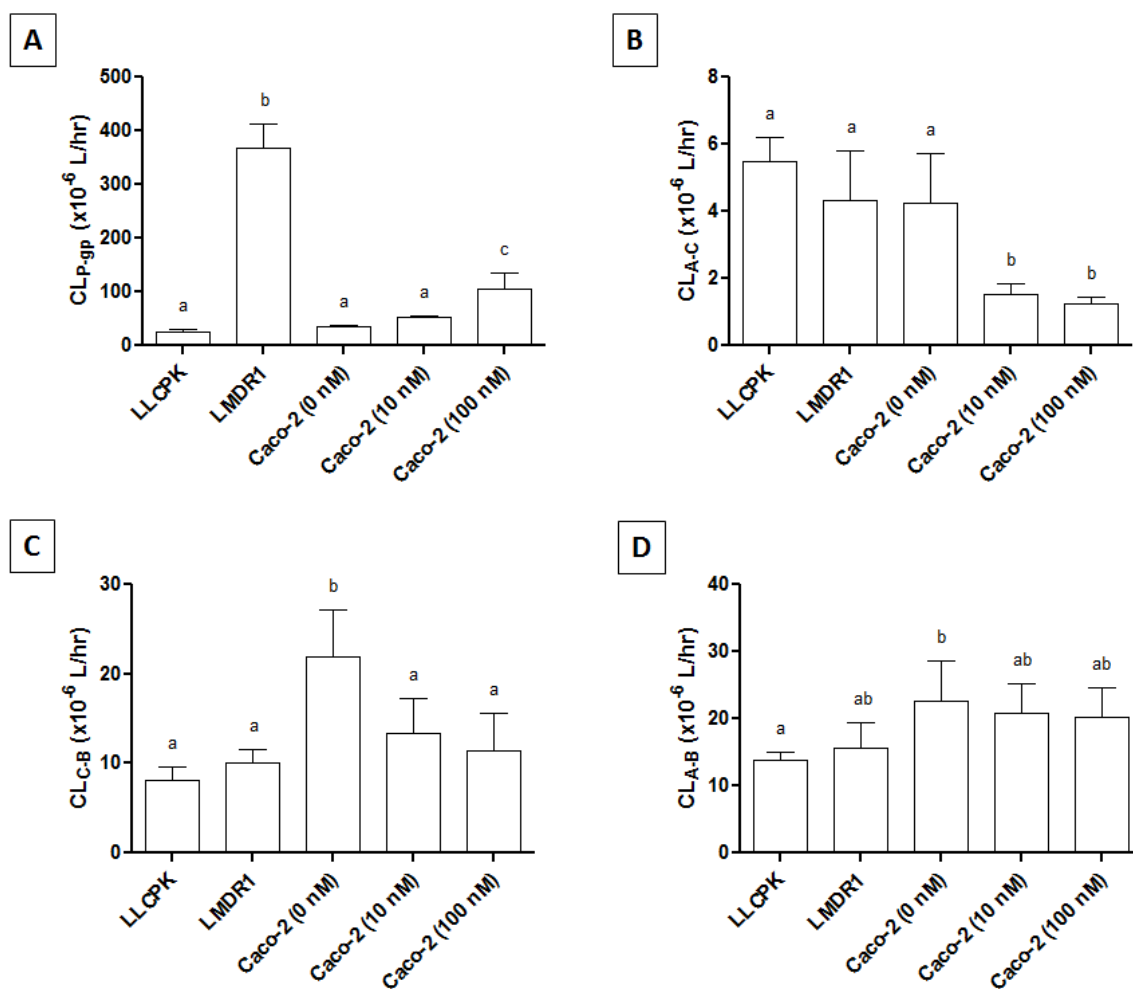


Figure 2.11. Modeled CL_{P-gp} (A), CL_{A-C} (B), CL_{C-B} (C), and CL_{A-B} (D) of bidirectional [³H]-digoxin transport for 4 hours across the different cell monolayers. Data are presented as mean \pm S.E. ($n \geq 4$). CL values with a different superscript (a, b, or c) are significantly different; $p < 0.05$.

Table 0.3. Estimates of P-gp activity in *LLCPK* and *LMDR1* cell monolayers for each experiment day, evaluated by traditional apparent permeability ($P_{app(A-B)}$, $P_{app(B-A)}$) and efflux ratio (EfR) approaches, as well as by P-gp intrinsic clearance (CL_{P-gp}) fit from our 3-compartment model. Modeled clearance values for non-P-gp transcellular flux (CL_{A-C} , CL_{C-B}) and paracellular flux (CL_{A-B}) are also included for each experiment.

Day	Traditional Estimates			Modeled Clearance			
	$P_{app(A-B)}$ $\times 10^{-6}$ cm/s	$P_{app(B-A)}$ $\times 10^{-6}$ cm/s	EfR	CL_{P-gp} $\times 10^{-6}$ L/hr	CL_{A-C} $\times 10^{-6}$ L/hr	CL_{C-B} $\times 10^{-6}$ L/hr	CL_{A-B} $\times 10^{-5}$ L/hr
LLCPK							
1	1.807	2.742	1.518	27.124	5.317	8.309	11.439
2	3.045	4.587	1.506	32.592	6.010	10.739	15.821
3	1.147	2.052	1.789	19.318	6.262	6.294	12.486
4	1.470	2.776	1.889	24.339	4.974	3.840	15.431
5	1.442	2.650	1.838	41.390	1.900	13.825	17.663
6	1.910	3.015	1.578	9.447	8.446	5.888	10.019
Avg	1.804	2.970	1.686	25.704	5.485	8.149	13.810
SD	0.272	0.349	0.070	4.482	0.715	1.484	1.201
LMDR1							
1	0.316	2.952	9.351	244.017	1.045	10.262	7.151
2	0.448	3.340	7.458	279.562	1.342	5.256	10.527
3	0.352	3.418	9.710	400.468	6.369	12.949	13.466
4	0.341	3.087	9.053	493.313	8.835	13.320	18.203
5	0.333	3.226	9.683	420.310	3.945	8.666	28.913
Avg	0.358	3.2046	9.051	367.473	4.307	10.091	15.652
SD	0.023	0.084	0.416	46.182	1.489	1.484	3.779

Table 0.4. Estimates of P-gp activity in *Caco-2* (0 nM), *Caco-2* (10 nM), and *Caco-2* (100 nM) cell monolayers for each experiment day, evaluated by traditional apparent permeability ($P_{app(A-B)}$, $P_{app(B-A)}$) and efflux ratio (EfR) approaches, as well as by P-gp intrinsic clearance (CL_{P-gp}) fit from our 3-compartment model. Modeled clearance values for non-P-gp transcellular flux (CL_{A-C} , CL_{C-B}) and paracellular flux (CL_{A-B}) are also included for each experiment.

Day	Traditional Estimates			Modeled Clearance			
	$P_{app(A-B)}$ $\times 10^{-6}$ cm/s	$P_{app(B-A)}$ $\times 10^{-6}$ cm/s	EfR	CL_{P-gp} $\times 10^{-6}$ L/hr	CL_{A-C} $\times 10^{-6}$ L/hr	CL_{C-B} $\times 10^{-6}$ L/hr	CL_{A-B} $\times 10^{-6}$ L/hr
Caco-2 (0 nM)							
1	1.234	2.939	2.383	38.64	1.055	40.80	19.16
2	0.806	3.353	4.158	29.70	3.918	20.16	10.83
3	1.485	3.304	2.224	36.71	5.861	9.76	43.52
4	0.626	3.148	5.031	31.95	9.045	23.89	28.35
5	0.799	3.110	3.891	38.98	1.324	14.64	10.83
Avg	0.990	3.171	3.537	35.20	4.240	21.85	22.54
SD	0.159	0.074	0.538	1.86	1.491	5.31	6.16
Caco-2 (10 nM)							
1	0.275	1.662	6.039	50.23	1.485	2.39	9.84
2	0.905	4.113	4.547	57.98	2.451	18.74	17.44
3	0.379	2.997	7.839	47.66	1.069	13.62	26.29
4	0.46	3.038	6.599	55.60	1.074	18.86	29.53
Avg	0.505	2.953	6.256	52.87	1.520	13.40	20.78
SD	0.139	0.502	0.683	2.37	0.325	3.87	4.45
Caco-2 (100 nM)							
1	0.182	3.442	18.912	95.63	1.068	22.67	8.40
2	0.539	4.247	7.877	94.53	1.011	6.51	15.22
3	0.36	3.761	10.46	83.22	0.951	24.01	28.09
4	0.385	3.661	9.517	148.59	1.945	12.66	28.81
Avg	0.367	3.778	11.692	105.49	1.244	11.36	20.14
SD	0.073	0.170	2.465	29.27	0.210	4.22	4.48

2.3.6 Predictive performance and sensitivity of P-gp activity metrics

Figures 2.12-2.15 show a linear regression of normalized P-gp activity versus normalized P-gp expression for each metric; Table 2.5 summarizes the outcomes of linear regression analyses. The r^2 value for the linear regression of CL_{P-gp} activity estimates was over three fold greater and the slope was over six fold greater than the $P_{app(A-B)}$ and EfR activity estimates. $P_{app(A-B)}$ and EfR estimates of P-gp activity did both fit a linear regression with P-gp expression, with p-values < 0.05 . The difference between modeled clearance and the traditional P-gp activity metrics was far less striking when we focused our analysis on only the subset of data within one cell type (Table 2.5(A) and (B)). Indeed, when we isolated Caco-2 cell expression and flux data for analysis, the r^2 values for the linear regressions of EfR and $P_{app(A-B)}$ activity estimates was less than 2 fold smaller than CL_{P-gp} and the slope was actually greater for the EfR linear regression compared to CL_{P-gp} . When we excluded the Caco-2 cell data the r^2 value for the EfR linear regression was greater than CL_{P-gp} and $P_{app(A-B)}$ was only slightly smaller than CL_{P-gp} . The slope (m) of the CL_{P-gp} regression was however, substantially larger than EfR and $P_{app(A-B)}$ by 4.7 fold and 6.8 fold respectively. CL_{P-gp} and EfR linear regressions consistently showed greater r^2 and slope compared to $P_{app(A-B)}$. $P_{app(B-A)}$ estimates of P-gp activity did not fit a linear regression with P-gp expression in any analysis; the p-value was well above 0.05 for all subsets of data analyzed (Table 2.5).

P_{app}(A-B)

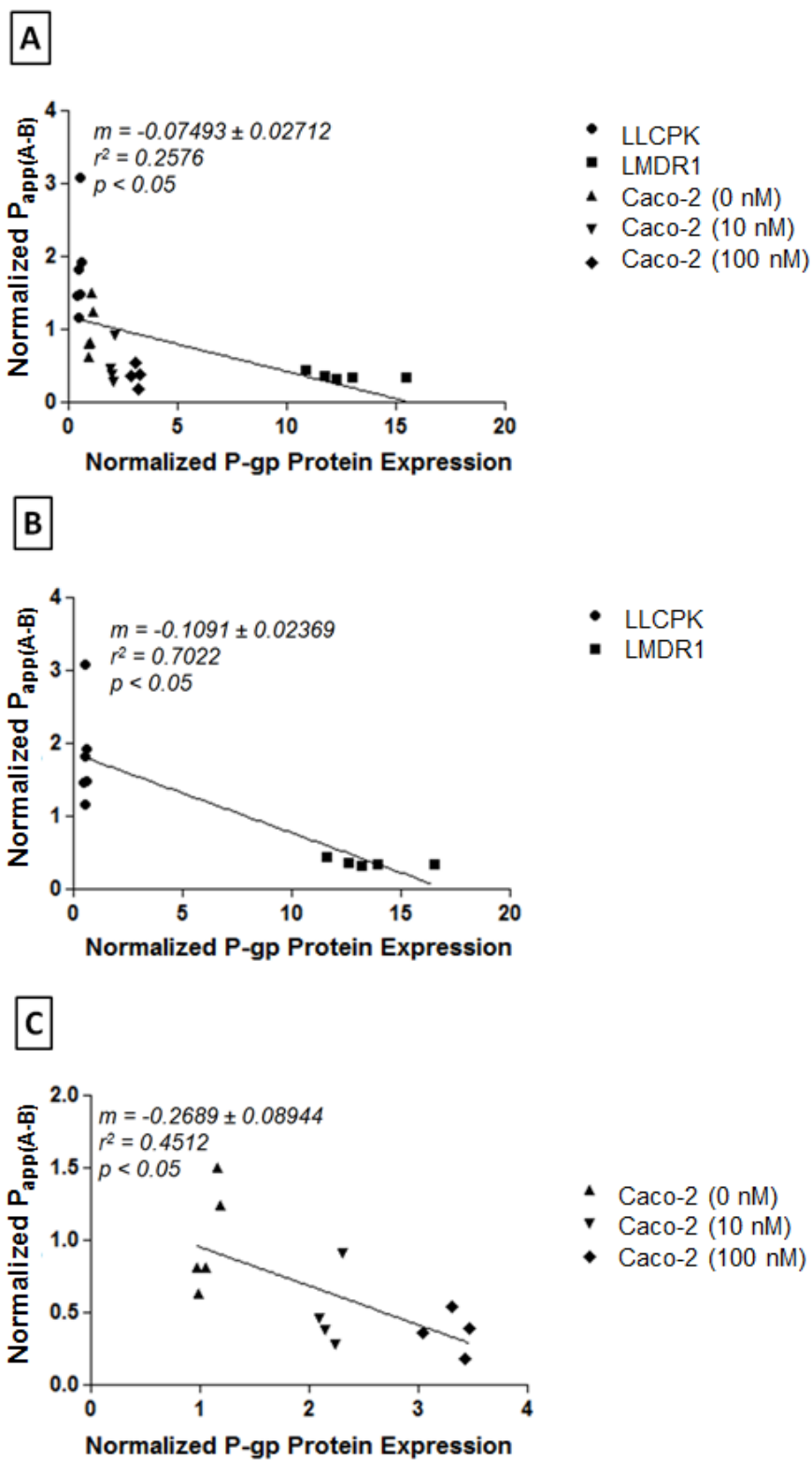


Figure 2.12. Normalized P-gp protein expression in various transwell monolayer cell types versus the corresponding normalized P-gp transport activity estimates obtained by $P_{app(A-B)}$ calculation method. P-gp expression was quantified by western blot densitometry relative to a control Caco-2 cell lysate that was loaded on each blot. Protein expression and activity estimates were normalized respectively to the averaged expression and the averaged estimated activity of the Caco-2 (0 nM) transwell monolayer cells. Slope (m) and goodness of fit (r^2) are presented for the linear regression of **all** data sets combined (A), **only LLCPK and LMDR1** data sets combined (B), and **only Caco-2 (0 nM), Caco-2 (10 nM), and Caco-2 (100 nM)** data sets combined (C). The p-value of the F-test for a non-zero slope is also presented for each linear regression.

P_{app(B-A)}

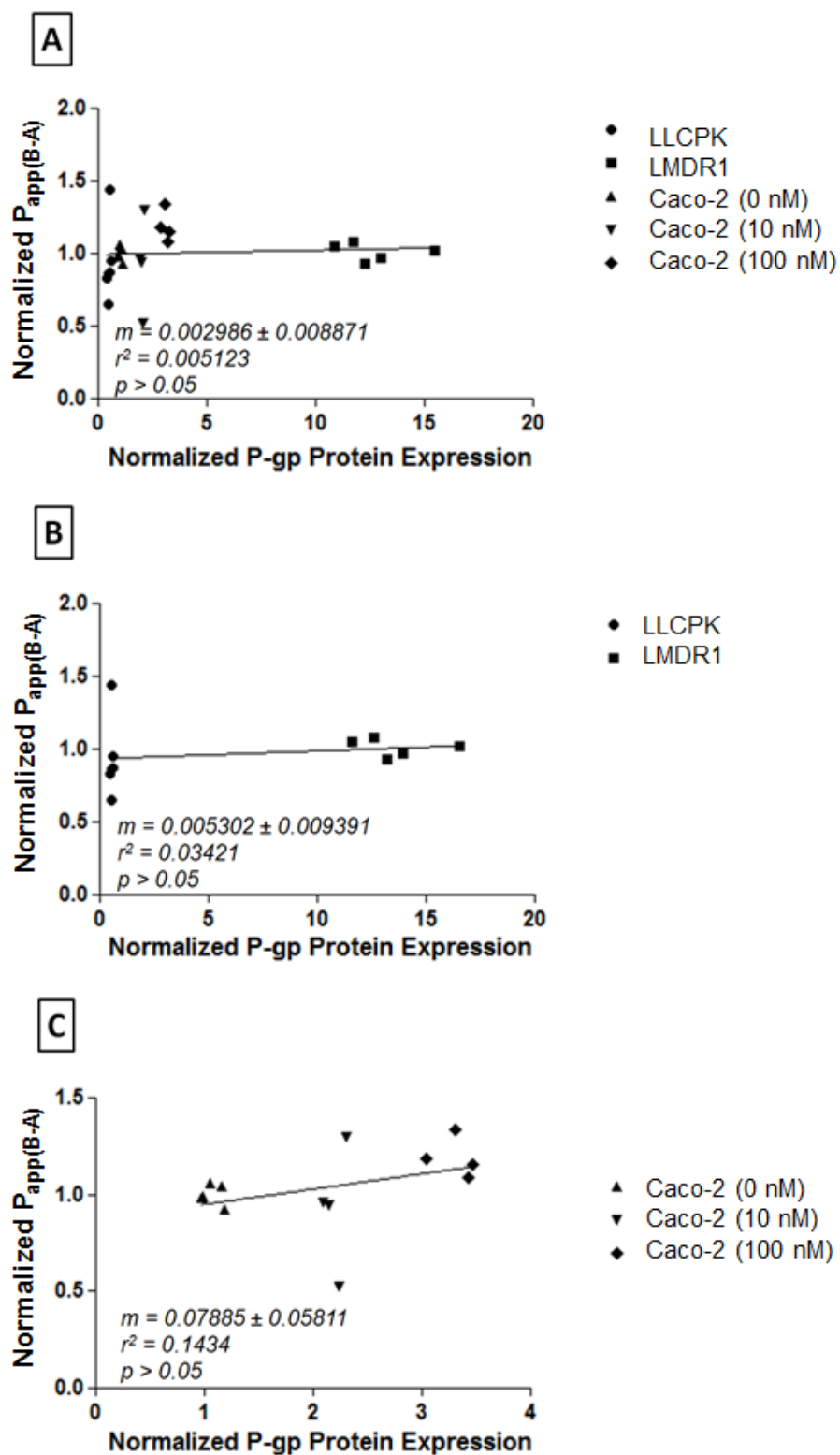


Figure 2.13. Normalized P-gp protein expression in various transwell monolayer cell types versus the corresponding normalized P-gp transport activity estimates obtained by $P_{app(B-A)}$ calculation method. P-gp expression was quantified by western blot densitometry relative to a control Caco-2 cell lysate that was loaded on each blot. Protein expression and activity estimates were normalized respectively to the averaged expression and the averaged estimated activity of the Caco-2 (0 nM) transwell monolayer cells. Slope (m) and goodness of fit (r^2) are presented for the linear regression of **all** data sets combined (A), **only LLCPK and LMDR1** data sets combined (B), and **only Caco-2 (0 nM), Caco-2 (10 nM), and Caco-2 (100 nM)** data sets combined (C). The p-value of the F-test for a non-zero slope is also presented for each linear regression.

EfR

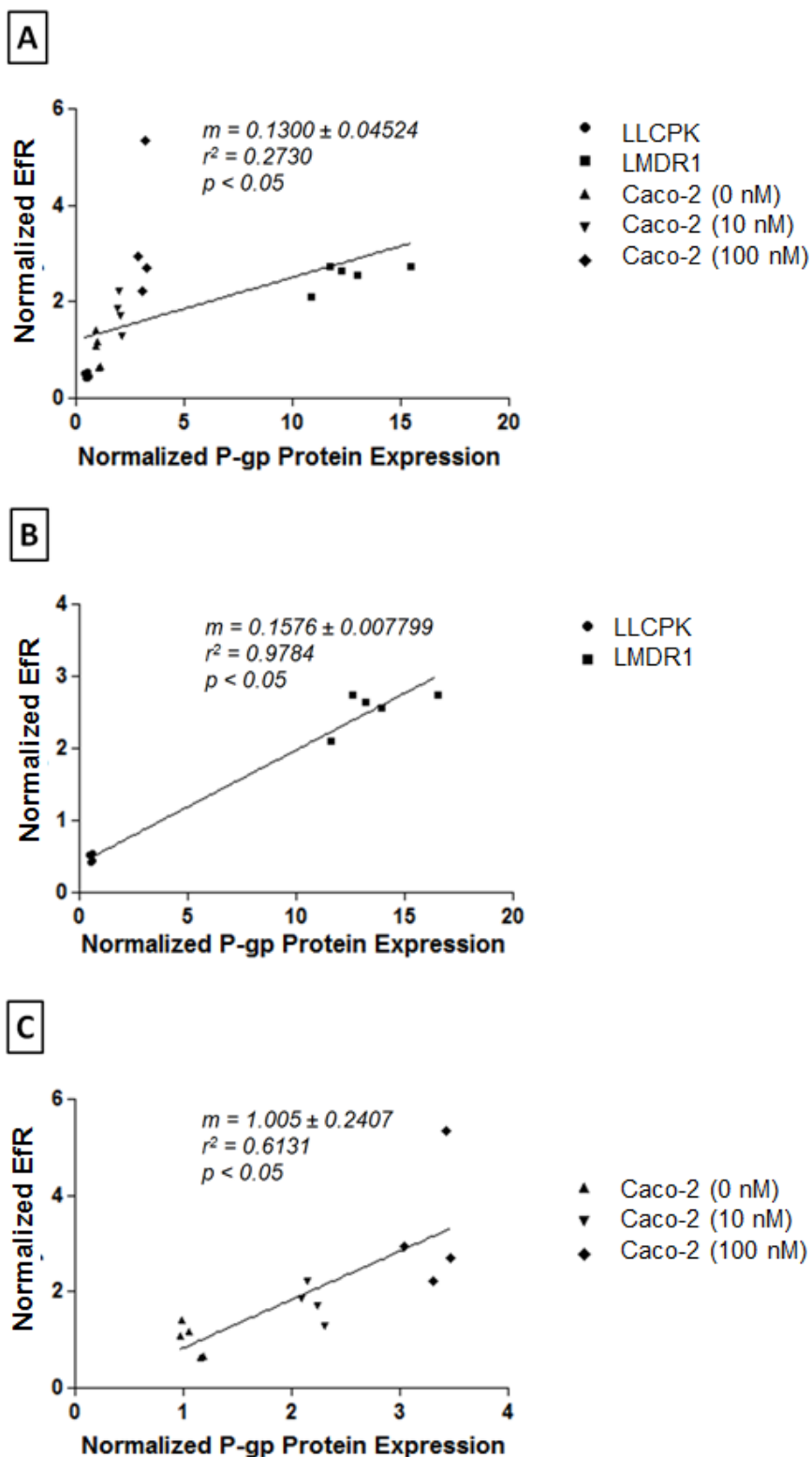
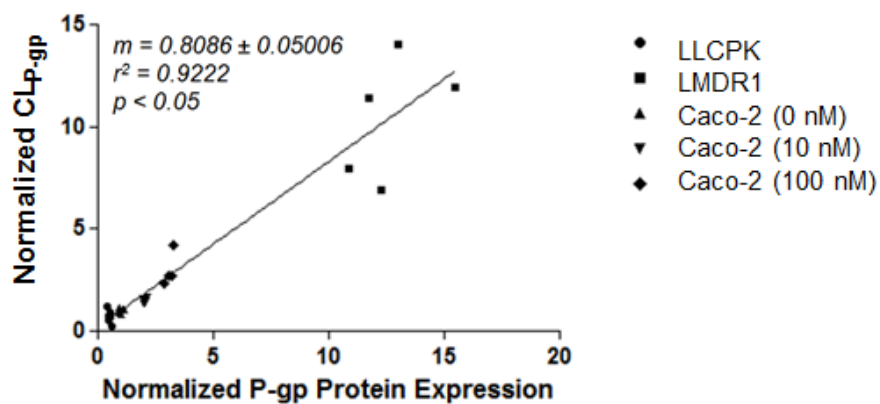


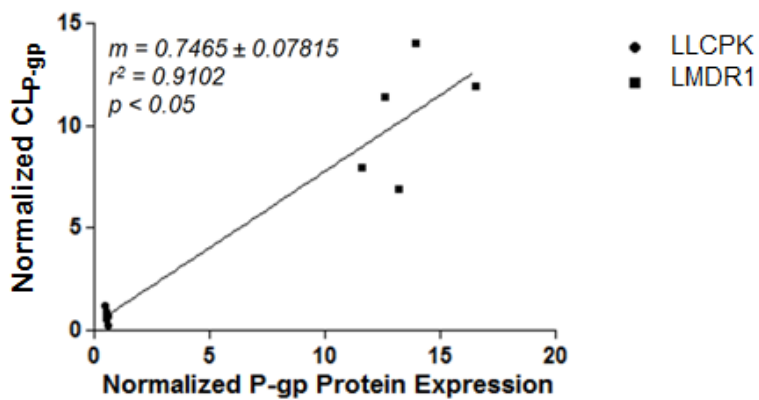
Figure 2.14. Normalized P-gp protein expression in various transwell monolayer cell types versus the corresponding normalized P-gp transport activity estimates obtained by **EfR** calculation method. P-gp expression was quantified by western blot densitometry relative to a control Caco-2 cell lysate that was loaded on each blot. Protein expression and activity estimates were normalized respectively to the averaged expression and the averaged estimated activity of the Caco-2 (0 nM) transwell monolayer cells. Slope (m) and goodness of fit (r^2) are presented for the linear regression of **all** data sets combined (A), **only LLCPK and LMDR1** data sets combined (B), and **only Caco-2 (0 nM), Caco-2 (10 nM), and Caco-2 (100 nM)** data sets combined (C). The p-value of the F-test for a non-zero slope is also presented for each linear regression.

CL_{P-gp}

A



B



C

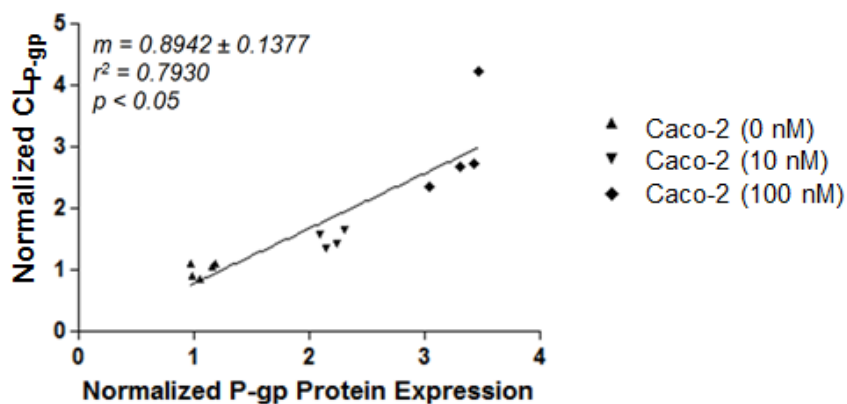


Figure 2.15. Normalized P-gp protein expression in various transwell monolayer cell types versus the corresponding normalized P-gp transport activity estimates obtained by **CL_{P-gp}** calculation method. P-gp expression was quantified by western blot densitometry relative to a control Caco-2 cell lysate that was loaded on each blot. Protein expression and activity estimates were normalized respectively to the averaged expression and the averaged estimated activity of the Caco-2 (0 nM) transwell monolayer cells. Slope (*m*) and goodness of fit (*r*²) are presented for the linear regression of **all** data sets combined (A), **only LLCPK and LMDR1** data sets combined (B), and **only Caco-2 (0 nM), Caco-2 (10 nM), and Caco-2 (100 nM)** data sets combined (C). The p-value of the F-test for a non-zero slope is also presented for each linear regression.

Table 0.5. Summary of goodness of fit (r^2) and regression slopes (m) for regression analyses of different normalized estimates of P-gp activity with P-gp expression for **LLCPK and LMDR1** data sets only (A), **Caco-2 (0 nM), (10 nM), and (100 nM)** data sets only (B), and **all** data sets combined (C).

	$P_{app(A-B)}$	$P_{app(B-A)}$	EfR	Cl_{P-gp}
(A) LLCpk and LMDR1 data sets only				
r^2	0.7022	0.03421	0.9784	0.9102
slope	-0.1091 ± 0.0237	0.0053 ± 0.0094	0.1576 ± 0.0078	0.7465 ± 0.0782
(B) Caco-2: 0 nM, 10 nM, and 100 nM data sets only				
r^2	0.4512	0.1434	0.6131	0.7930
slope	-0.2689 ± 0.0894	0.0789 ± 0.0581	1.005 ± 0.2407	0.8942 ± 0.1377
(C) All data sets				
r^2	0.2576	0.005123	0.2730	0.9222
slope	-0.0749 ± 0.0271	0.0030 ± 0.0089	0.1300 ± 0.0452	0.8086 ± 0.0501

2.4 Discussion

The objective of this study was to compare the validity and sensitivity of a modeled intrinsic clearance against unidirectional apparent permeability and efflux ratio as metrics of P-gp activity across monolayer permeability assay systems. We hypothesized that since modeled clearance measures P-gp activity more directly and specifically, it is superior to apparent permeability and efflux ratio for evaluating P-gp activity in any monolayer permeability assay.

We found that the validity and sensitivity of modeled clearance as a P-gp activity metric is generally on par with efflux ratio and superior to unidirectional apparent permeability for assays conducted in monolayers of a common cell type. But, when making P-gp activity estimates across different cell types, modeled clearance is far superior to the traditional metrics. Indeed, when we separated assays by cell type (Caco-2 (0 nM)/Caco-2 (10 nM)/Caco-2 (100 nM) or LLCPK/LMDR1), the correlation of CL_{P-gp} -estimated monolayer P-gp activity vs. measured monolayer P-gp expression had similar or greater slope (sensitivity) and r^2 value as compared to the correlations of P_{app} -estimated P-gp activity vs. P-gp expression and EfR-estimated P-gp activity vs. P-gp expression; but the r^2 and slope were respectively 3.4-fold and 6.2-fold greater for CL_{P-gp} when we evaluated the combined data from both cell types together.

Caco-2, LMDR1, and MDCK-MDR1 cells are all commonly used for cell monolayer permeability assays (11-14). Some level of polarized apical P-gp expression has been demonstrated in each of these cell types, such that they can all be used to demonstrate substrates or modulators of P-gp activity *in vitro*. Previous reports though, found that relative P-gp expression differs between Caco-2, MDCK-MDR1 (not included in our study), LLCPK, and LMDR1 cell types (15; 16), which agreed with the western blot findings in our study. Our blots also agreed with previous studies that have reported a concentration-dependent increase in P-gp expression in Caco-2 cells treated with vitamin D (17; 18). Some models of intestinal absorption and metabolism rely on vitamin D treatment to induce CYP3A4 activity in Caco-2 monolayers. So, LLCPK, LMDR1 and Caco-2 cells and Caco-2 cells treated with vitamin D are all commonly utilized in cell-based models and assays of permeability; and because of their inherent differences in P-

gp expression, our study had a suitable range of cell monolayer P-gp expression across which to examine the validity and sensitivity of P-gp activity metrics.

The level of P-gp expression in a given monolayer cell system dictates the level of P-gp efflux activity. Accordingly, from cursory assessment of our transport data there is evidence of increasing efflux transport – marked by increasing basolateral to apical disparity in bidirectional flux – in the rank orders LLCPK<LMDR1 and Caco-2 (0 nM) < Caco-2 (10 nM) < Caco-2 (100 nM), which paralleled the rank orders of cell monolayer P-gp expression. In our study though, the basolateral to apical apparent permeability did not demonstrate this relationship with cell monolayer P-gp expression. We found no correlation between $P_{app(B-A)}$ and P-gp expression in Caco-2 cells, in LLCPK/LMDR1 cells, or in Caco-2 and LLCPK/LMDR1 cells. This result conflicted with previous studies by Taipalensuu *et al.* and Hayeshi *et al.*, who reported correlation between Caco-2 cell P-gp expression and both basolateral to apical apparent permeability and efflux ratio (14; 19). Possible explanation for our conflicting results could relate to plastic adsorption in the basolateral compartment or cellular retention of drug passing through the cell from the basolateral compartment into the apical compartment. Youdim *et al.*, suggests that traditional permeability equations fail to account for cellular retention (20). The loss of drug to cellular retention and plastic adsorption during transport experiments could certainly lead to false measurements of a drug's permeability value (20-22). Our model exercise does suggest though that lack of correlation between $P_{app(B-A)}$ with P-gp expression is most likely due to the fact that digoxin permeability at the basolateral membrane is significantly lower than efflux activity at the apical membrane. This indicates that overall basolateral to apical digoxin transcellular flux is rate-limited by basolateral membrane permeation rather than P-gp activity. However, the $P_{app(A-B)}$ and EfR values calculated in our experiments did show a correlation with P-gp expression in Caco-2 cells, which agreed with previous studies (14; 19). Similarly in LLCPK/LMDR1 cells we also saw correlation between $P_{app(A-B)}$ and P-gp expression and between EfR and LLCPK/LMDR1 cells.

In explaining why CL_{P-gp} reflects P-gp activity more predictably and sensitively when comparing between cell types, we believe this relates not to difference in P-gp expression

between cell types, but to differences in non-P-gp transporters and cell morphology that also contribute to drug transit. Aside from P-gp, Caco-2 cells, LMDR1 cells, and MDCK-MDR1 cells have all been reported to show different relative expression levels of several transporters, including but not limited to: MRP2, and BCRP apical efflux transporters, peptide transporter 1 (PepT1) apical uptake transporter, multidrug resistance-associated protein 3 (MRP3), MRP1, and organic solute transporter- α and - β (OST- α and - β) basolateral efflux transporters and OATP-A (*SLC21A3*), OATP-C (*SLC21A6*), and OATP-B (*SLC21A9*) basolateral uptake transporters (23-30; 19). Many of these transporters have overlapping substrate specificities with P-gp and thus multiple transporters may contribute, to varying degrees in different monolayers, to the flux of any given drug that is being tested for specific interaction with P-gp. As Sun and Pang demonstrated in a theoretical study, the presence of other active transport has the potential to overcome the effect of P-gp apical efflux activity, which could result in the over- or under-estimation of traditional monolayer permeability metrics of P-gp activity (9). This may even apply to the prototypical P-gp probe substrate, digoxin. Some non-P-gp transporters have been previously implicated in digoxin transcellular flux across assay monolayers. Sun and Pang's theoretical study predicted the kinetic presence of a basolateral digoxin uptake transporter in Caco-2 cells and there has been evidence in MDCK cells of active basolateral uptake of digoxin that is inhibited by GF120918 (9; 31). There have also been reports that digoxin is transported by OST- α and - β (32), which is expressed in Caco-2 cells. There is a clear potential for other transporters to obscure the monolayer permeability that P_{app} and EfR attribute solely to P-gp activity. Yet, though many transporters may contribute to flux across Caco-2, LLCPK or MDCK monolayers, we are not aware of any comprehensive studies in the literature that directly compare transporter expression patterns between these cells. Difficulty assessing differences in transporter expression among these cells lines will be compounded by species-related differences in transporter activity towards specific substrates. Consequently, it is difficult even to anticipate the relative impact of different transporters on monolayer transit between cell lines; so, it is hard to know how much P_{app} or EfR measured in a given cell type may be over- or under-estimating P-gp activity.

While the non-P-gp transporter differences are overlooked in the calculation of EfR and P_{app} as estimates of P-gp activity, in our modeled clearance the general effects of non-P-gp transporter difference are imbedded within the fitted CL_{A-C} and CL_{C-B} parameters. The difference that we observed between the CL_{A-C} and CL_{C-B} parameters fitted from Caco-2 data versus LLCPK/LMDR1 data seem to reflect the reported difference in non-P-gp transport activity between Caco-2 and LLCPK/LMDR1 cells.

Although transporter differences between cell lines may not have been compared in great detail, certain morphological differences between Caco-2, LLCPK, and MDCK cells have been documented. Caco-2 cells, for example, are well known to form *in vitro* monolayers with greater integrity and lower transepithelial electrical resistance (TEER) than MDCK cells (33). In their theoretical study, Sun and Pang demonstrated the potential for paracellular flux to obscure apical efflux (9). Since paracellular transit differs between cell types, as was also demonstrated in our study by measurement of the paracellular marker [^{14}C]-inulin, the degree to which paracellular flux obscures the P_{app} and EfR estimations of P-gp also differs between cell types. For our model CL_{P-gp} however, the difference between Caco-2 and LLCPK/LMDR1 paracellular [3H]-digoxin transit is imbedded in the CL_{A-B} parameter. Therefore, the CL_{P-gp} estimate of P-gp activity derived from any monolayer assay is, theoretically, independent of the integrity characteristics of a particular monolayer.

Transporter and morphological differences between cell types, or even within a cell type, can be further complicated by differences in laboratory practice. Owing to the intrinsic heterogeneity of the parental Caco-2, LLCPK and MDCK cell lines, culture-related conditions have been shown to influence the morphological and functional characteristics of *in vitro* monolayers, by selecting for sub populations of cells in culture (34).

Variability has been previously reported in Caco-2 cell paracellular permeability and transporter expression (35; 36) and has been ascribed to difference in culture conditions, passage number and cell source (37-39; 19). This results in significant variability in the estimates of P-gp activity calculated by P_{app} or EfR, even in the same *in vitro* system and cell type (40). In effect, the value of the monolayer permeability assay for assessing P-gp activity and IVIVE becomes limited when we use P_{app} or EfR for any moderate substrate

of P-gp that has broad transporter specificity or high passive permeability. By specifically isolating the activity of P-gp transporter from the other active and passive transport processes in a monolayer permeability assay, CL_{P-gp} is able to effectively extract more widely useable data for any laboratory working with their preferred assay conditions.

2.5 References

1. McLeod HL and Evans WE (2001) Pharmacogenomics: unlocking the human genome for better drug therapy. *Annual Review of Pharmacology and Toxicology* 41: 101-21
2. Shitara Y, Horie T, Sugiyama Y (2006) Transporters as a determinant of drug clearance and tissue distribution. *European Journal of Pharmaceutical Sciences* 27(5): 425-46
3. Giacomini KM, Huang SM, Tweedie DJ, Benet LZ, Brouwer KL, Chu X, Dahlin A, Evers R, Fischer V, Hillgren KM, Hoffmaster KA, Ishikawa T, Keppler D, Kim RB, Lee CA, Niemi M, Polli JW, Sugiyama Y, Swaan PW, Ware JA, Wright SH, Yee SW, Zamek-Gliszczynski MJ, Zhang L (2010) Membrane transporters in drug development. *Nature Reviews Drug Discovery* 9: 215–236
4. Schmider J, von Moltke LL, Shader RI, Harmatz JS, Greenblatt DJ (1999) Extrapolating *in vitro* data on drug metabolism to *in vivo* pharmacokinetics: evaluation of the pharmacokinetic interaction between amitriptyline and fluoxetine. *Drug Metabolism Reviews* 31(2): 545-60
5. Kitamura S, Maeda K, Wang Y, Sugiyama Y (2008) Involvement of multiple transporters in the hepatobiliary transport of rosuvastatin. *Drug Metabolism and Disposition* 36(10): 2014–2023
6. Zhou S-F (2008) Structure, function and regulation of P-glycoprotein and its clinical relevance in drug disposition. *Xenobiotica* 38: 802–832
7. FDA Guidance for Industry (2012) Drug Interaction Studies — Study Design, Data Analysis, and Implications for Dosing and Labelin
8. Polli JW, Wring SA, Humphreys JE, Huang L, Morgan JB, Webster LO, Serabjit-Singh CS (2001) Rational use of *in vitro* P-glycoprotein assays in drug discovery. *Journal of Pharmacology and Experimental Therapeutics* 299: 620–628
9. Sun H and Pang KS (2008) Permeability, transport, and metabolism of solutes in Caco-2 cell monolayers: a theoretical study. *Drug Metabolism and Disposition* 36: 102–123
10. Ito K, Kusuhara H, and Sugiyama Y (1999) Effects of intestinal CYP3A4 and P-glycoprotein on oral drug absorption—theoretical approach. *Pharmaceutical Research (NY)* 16: 225–231
11. Hidalgo IJ, Raub TJ, Borchardt RT (1989) Characterization of the human colon carcinoma cell line (Caco-2) as a model system for intestinal epithelial permeability. *Gastroenterology* 96: 736–749

12. Hochman JH, Pudvah N, Qiu J, Yamazaki M, Tang C, Lin JH, Prueksaritanont T (2004) Interactions of human P-glycoprotein with simvastatin, simvastatin acid, and atorvastatin. *Pharmaceutical Research* 21(9): 1686-91
13. Zhu HJ, Wang JS, Markowitz JS, Donovan JL, Gibson BB, Gefroh HA, Devane CL (2006) Characterization of P-glycoprotein inhibition by major cannabinoids from marijuana. *Journal of Pharmacology and Experimental Therapeutics* 317(2): 850-7
14. Taipalensuu J, Tavelin S, Lazorova L, Svensson AC, Artursson P (2004) Exploring the quantitative relationship between the level of MDR1 transcript, protein and function using digoxin as a marker of MDR1-dependent drug efflux activity. *European Journal of Pharmaceutical Sciences* 21: 69–75
15. Tang F, Horie K, Borchardt RT (2002) Are MDCK cells transfected with the human MDR1 gene a good model of the human intestinal mucosa? *Pharmaceutical Research* 19: 773–779
16. Kuteykin-Teplyakov K, Luna-Tortós C, Ambroziak K, Löscher W (2010) Differences in the expression of endogenous efflux transporters in MDR1-transfected versus wildtype cell lines affect P-glycoprotein mediated drug transport. *British Journal of Pharmacology* 160(6): 1453-63
17. Schmiechlin-Ren P, Thummel KE, Fisher JM, Paine MF, Lown KS, Watkins PB (1997) Expression of enzymatically active CYP3A4 by Caco-2 cells grown on extracellular matrix-coated permeable supports in the presence of 1alpha, 25-dihydroxyvitamin D3. *Molecular Pharmacology* 51: 741–754
18. Thummel KE, Brimer C, Yasuda K, Thottassery J, Senn T, Lin Y, Ishizuka H, Kharasch E, Schuetz J, Schuetz E (2001) Transcriptional control of intestinal cytochrome P-4503A by 1alpha, 25-dihydroxy vitamin D3. *Molecular Pharmacology* 60: 1399–1406
19. Hayeshi R, Hilgendorf C, Artursson P, Augustijns P, Brodin B, Dehertogh P, Fisher K, Fossati L, Hovenkamp E, Korjamo T, Masungi C, Maubon N, Mols R, Müllertz A, Mönkkönen J, O'Driscoll C, Oppers-Tiemissen HM, Ragnarsson EG, Rooseboom M, Ungell AL (2008) Comparison of drug transporter gene expression and functionality in Caco-2 cells from 10 different laboratories. *European Journal of Pharmaceutical Sciences* 35: 383–396
20. Youdim KA, Avdeef A, Abbott NJ (2003) *In vitro* trans-monolayer permeability calculations: often forgotten assumptions. *Drug Discovery Today* 8: 997–1003
21. Ingels FM, Deferme S, Delbar N, Oth M, Augustijns PF (2002) Implementation of the Caco-2 cell culture model as a predictive tool for the oral absorption of drugs. In house evaluation procedures. *Journal de pharmacie de Belgique* 57: 153–158

22. Palmgren JJ, Monkkonen J, Korjamo T, Hassinen A, Auriola S (2006) Drug adsorption to plastic containers and retention of drugs in cultured cells under *in vitro* conditions. *European Journal of Pharmaceutics and Biopharmaceutics* 64: 369–378
23. Goh LB, Spears KJ, Yao D, Ayrton A, Morgan P, Roland Wolf C, Friedberg T (2002) Endogenous drug transporters in *in vitro* and *in vivo* models for the prediction of drug disposition in man. *Biochemical Pharmacology* 64: 1569–1578
24. Guo A, Hu P, Balimane PV, Leibach FH, Sinko PJ (1999) Interactions of a nonpeptidic drug, valacyclovir, with the human intestinal peptide transporter (hPEPT1) expressed in a mammalian cell line. *Journal of Pharmacology and Experimental Therapeutics* 289: 448–454
25. Kobayashi D, Nozawa T, Imai K, Nezu J, Tsuji A, Tamai I (2003) Involvement of human organic anion transporting polypeptide OATP-B (SLC21A9) in pH-dependent transport across intestinal apical membrane. *Journal of Pharmacology and Experimental Therapeutics* 306: 703–708
26. Hirohashi T, Suzuki H, Chu XY, Tamai I, Tsuji A, Sugiyama Y (2000) Function and expression of multidrug resistance-associated protein family in human colon adenocarcinoma cells (Caco-2). *Journal of Pharmacology and Experimental Therapeutics* 292: 265–270
27. Okuwaki M, Takada T, Iwayanagi Y, Koh S, Kariya Y, Fujii H, Suzuki H (2007) LXR alpha transactivates mouse organic solute transporter alpha and beta via IR-1 elements shared with FXR. *Pharmaceutical Research* 24: 390–398
28. Kullak-Ublick GA, Ismail MG, Stieger B, Landmann L, Huber R, Pizzagalli F, Fattinger K, Meier PJ, Hagenbuch B (2001) Organic anion-transporting polypeptide B (OATP-B) and its functional comparison with three other OATPs of human liver. *Gastroenterology* 120: 525–533
29. Lowes S, Cavet ME, Simmons NL (2003) Evidence for a non-MDR1 component in digoxin secretion by human intestinal Caco-2 epithelial layers. *European Journal of Pharmacology* 458: 49–56
30. Hilgendorf C, Ahlin G, Seithel A, Artursson P, Ungell AL, Karlsson J (2007) Expression of thirty-six drug transporter genes in human intestine, liver, kidney, and organotypic cell lines. *Drug Metabolism and Disposition* 35: 1333–1340
31. Acharya P, O'Connor MP, Polli JW, Ayrton A, Ellens H, Bentz J (2008) Kinetic identification of membrane transporters that assist P-glycoprotein-mediated transport of digoxin and loperamide through a confluent monolayer of MDCKII-hMDR1 cells. *Drug Metabolism and Disposition* 36: 452–460
32. Seward DJ, Koh AS, Boyer JL, Ballatori N (2003) Functional complementation between a novel mammalian polygenic transport complex and an

- evolutionarily ancient organic solute transporter, OST α -OST β . *Journal of Biological Chemistry* 278: 27473–27482
33. Irvine JD, Takahashi L, Lockhart K, Cheong J, Tolan JW, Selick HE, Grove JR (1999) MDCK (madin-darby canine kidney) cells: A tool for membrane permeability screening. *Journal of Pharmaceutical Sciences* 88: 28–33
 34. Sambuy Y, De Angelis I, Ranaldi G, Scarino ML, Stamatii A, Zucco F (2005) The Caco-2 cell line as a model of the intestinal barrier: influence of cell and culture-related factors on Caco-2 cell functional characteristics. *Cell Biology and Toxicology* 21: 1–26
 35. Walter E and Kissel T (1994) Transepithelial transport and metabolism of thyrotropin-releasing hormone (TRH) in monolayers of a human intestinal cell line (Caco-2): evidence for an active transport component? *Pharmaceutical Research* 11: 1575–1580
 36. Walter E and Kissel T (1995) Heterogeneity in the human intestinal cell line Caco-2 leads to differences in transepithelial transport. *European Journal of Pharmaceutical Sciences* 3: 215–230
 37. Behrens I and Kissel T (2003) Do cell culture conditions influence the carrier-mediated transport of peptides in Caco-2 cell monolayers? *European Journal of Pharmaceutical Sciences* 19: 433–442
 38. Volpe DA (2008) Variability in Caco-2 and MDCK cell-based intestinal permeability assays. *Journal of Pharmaceutical Sciences* 97: 712–725
 39. Miliotis T, Ali L, Palm JE, Lundqvist AJ, Ahnoff M, Andersson TB, Hilgendorf C (2011) Development of a highly sensitive method using liquid chromatography-multiple reaction monitoring to quantify membrane P-glycoprotein in biological matrices and relationship to transport function. *Drug Metabolism and Disposition* 39: 2440–2449
 40. Bentz J, O'Connor MP, Bednarczyk D, Coleman J, Lee C, Palm J, Pak YA, Perloff ES, Reyner E, Balimane P, Brännström M, Chu X, Funk C, Guo A, Hanna I, Herédi-Szabó K, Hillgren K, Li L, Hollnack-Pusch E, Jamei M, Lin X, Mason AK, Neuhoff S, Patel A, Podila L, Plise E, Rajaraman G, Salphati L, Sands E, Taub ME, Taur JS, Weitz D, Wortelboer HM, Xia CQ, Xiao G, Yabut J, Yamagata T, Zhang L, Ellens H (2013) Variability in P-glycoprotein inhibitory potency (IC₅₀) using various *in vitro* experimental systems: implications for universal digoxin drug-drug interaction risk assessment decision criteria. *Drug Metabolism and Disposition* 41(7): 1347-66

Chapter 3

General Discussion

3.1 Study Objective

The objective of this study was to compare the validity and sensitivity of unidirectional apparent permeability and efflux ratio against modeled intrinsic clearance, as metrics of P-gp activity in the monolayer permeability assay. Our rationale was that P_{app} and EfR only provide a qualitative estimate of P-gp activity from general drug flux across an assay monolayer, whereas CL_{P-gp} quantitatively estimates specific P-gp-mediated efflux from the cell compartment at the apical membrane. Therefore, the mechanistically based estimate would be expected to be more sensitive and valid across cell systems and variable laboratory assay conditions. Moreover, CL_{P-gp} provides quantitative values that can be directly applied for IVIVE, unlike P_{app} and EfR. No prior studies have compared these P-gp activity metrics across different commonly used assay cell systems. Here, our main objective was to obtain experimental data to prove that modeled clearance estimates P-gp activity better than P_{app} and EfR across monolayer permeability assay cell types.

3.2 Monolayer permeability assay metrics of P-gp activity

We compared the P-gp activity metrics across various cell types because, although Caco-2, LLCPK and MDCK cells can all form an *in vitro* monolayer with polarized P-gp expression, *in vitro* monolayers composed of these cell types differ in ways that fundamentally affect the transit of test drugs. Our experiment cells differed in P-gp expression in the rank order LLCPK < Caco-2 (0 nM) < Caco-2 (10 nM) < Caco-2 (100 nM) < LMDR1, and since, in theory, P-gp transport activity is directly proportional to P-gp expression, valid and useful transport activity metrics could be evaluated using data from all experimental groups. It would appear that $P_{app(A-B)}$, EfR and CL_{P-gp} are all valid metrics of P-gp activity when estimates are made within a common cell type (eg. in Caco-2 (0 nM)/Caco-2 (10 nM)/Caco-2 (100 nM) or LLCPK/LMDR1); we found good correlation between monolayer P-gp expression and respectively $P_{app(A-B)}$, EfR, and CL_{P-gp} estimates of monolayer P-gp activity. However, unidirectional apparent permeability and efflux ratio are not good metrics when estimating monolayer P-gp activity across

different cell types; poor correlation was shown between monolayer P-gp expression and respective P_{app} and EfR estimates of P-gp activity. Unidirectional apparent permeability and efflux ratio simplify transit across the monolayer as movement across a single barrier driven only by P-gp transport (1-4). Our investigation suggests that this approximation was adequate when estimating different P-gp activities within one cell type because the action of the P-gp transporter alone was responsible for much of the difference seen in [3 H]-digoxin bidirectional flux between Caco-2 (0 nM), Caco-2 (10 nM), and Caco-2 (100 nM) cell monolayers and between LLCPK and LMDR1 monolayers. But, difference in isolated P-gp transport activity across a single barrier was not sufficient on its own to account for the difference seen in [3 H]-digoxin flux between LLCPK, Caco-2 (0 nM), Caco-2 (10 nM), Caco-2 (100 nM), and LMDR1 monolayers. We conclude neither P_{app} nor EfR are valid metrics of P-gp activity when comparing across cell types.

Conversely, we found our modeled CL_{P-gp} is well suited to estimate P-gp activity within and across cell types; with good correlation for all linear regression analyses. Our compartmental model includes CL_{C-B} and CL_{A-C} to account for both passive and active transport processes occurring in both directions across the basolateral and apical membranes respectively. Thus, these parameters are able to account for non-P-gp transporters on either membrane, which may contribute significantly to differences in monolayer transit observed between monolayer cell types because Caco-2, LLCPK and MDCK cells all show different transporter expression *in vitro* (1; 5-12). The model fitted CL_{C-B} and CL_{A-C} parameters reflected the difference in non-P-gp transporter expression between LLCPK/LMDR1 and Caco-2 cell types. Our model also includes CL_{A-B} to account for variable paracellular transit, which results from differences in monolayer integrity that have been well documented between monolayer cell types (13; 14). By accounting for all of these confounding processes, CL_{P-gp} is able to tease out the specific contribution of P-gp-mediated transport across all assays. In our investigation, modeled clearance has proven to be a valid metric of P-gp activity between monolayer permeability assay cell types.

Another ideal property of a quantitative metric for P-gp activity is sensitivity to varying levels of P-gp expression and function. The relative sensitivity of metrics can be

evaluated by comparing the slopes (m) of the relationships between normalized P-gp activity and P-gp expression either within a cell type or with combined cell types. When considering results from combined Caco-2 and LLCPK cells, the rank order of slope values are $P_{app(B-A)} < P_{app(A-B)} < EfR < CL_{P-gp}$. This indicates that across cell systems, CL_{P-gp} is the most sensitive P-gp activity metric. However, within the LLCPK/LMDR1 system, slope values suggest that EfR is the most sensitive P-gp activity metric. CL_{P-gp} was the most sensitive measure of P-gp activity when evaluating data within the Caco-2 system.

3.3 Standardizing monolayer permeability assays

Given the importance of P-gp in the absorption, distribution, and excretion of drugs, it is essential to have *in vitro* assays that are capable of assessing potential P-gp interactions. A variety of biological systems are available to assess the potential for these interactions, including ATPase assays, fluorescent assays, and membrane vesicles. But, monolayer permeability assays are recommended as the most direct measure of P-gp activity (15-20). For this reason, academic, industry, and regulatory laboratories regularly conduct monolayer permeability assays on drugs to test for P-gp interaction using the standard transwell set-up. But, there is great potential for individual laboratories to introduce variability into this assay, which can make it challenging to draw congruent pharmacokinetic conclusions from the same assay conducted in different laboratories.

First, as previously mentioned there is not one standard cell type used to compose the monolayer; Caco-2, LLCPK, or MDCK are all commonly interchanged. Although each of these cell types will spontaneously differentiate *in vitro* to form a monolayer with polarized apical P-gp expression (21-24), we have clearly demonstrated in our study the inherent challenge of trying to draw compatible conclusions about P-gp activity from multiple monolayer cell types.

Moreover, owing to the inherent heterogeneity of the parent Caco-2, LLCPK, and MDCK cell lines, lack of standardization in laboratory practice can amplify variability in the permeability assay systems applied by different groups, regardless of chosen cell type. There is significant inter-lab variability in culture conditions, transwell equipment, cell

sources, cell passage number, seeding density, and bioanalytical techniques (25-28; 12). Many labs gauge monolayer integrity by measuring TEER, while others use mannitol, inulin, or Lucifer yellow flux. Furthermore, the monolayer integrity acceptance criteria vary substantially even for labs using the same measure. Some laboratories conduct transport experiments on a shaker, while others do not. The components of the culture media and assay buffers may vary between labs as well. Many labs also have their own protocol for seeding density and culture time of monolayer cells. Even plate and well insert sources vary, as well as insert pore size. A comparative study looking at inter-lab variability across 23 research laboratories and academic institutions found that 80% of variability in P-gp IC50 estimates was due to the use of different laboratory practices (28).

Consistency in the conclusions drawn about P-gp activity from monolayer permeability assays, performed under such diverse conditions, necessitates either strict standardization of assay protocols or a method of interpreting assay data that accounts for as much of the assay variability as possible. Sambuy *et al.* performed an interlaboratory study of mannitol permeability and TEER in Caco-2 cells with the goal of establishing a standardized protocol that would allow meaningful comparison of results obtained in different laboratories (29). We are not aware of any similar initiatives and none that address variability in non-P-gp transporter expression, which contributes to substrate transcellular flux variation. In this study though, we have explicitly demonstrated the capability of modeled clearance to yield a standard P-gp activity output, at very least, for the monolayer permeability assay variability that results from using different cell types. In principle, this model should extend to standardize P-gp activity estimation for a variety of different sources of assay variability.

3.4 Applying monolayer permeability assay data to drug discovery and development

The output of monolayer permeability assays are meant to provide information about whether a drug is a substrate of P-gp or the potential for P-gp mediated DDIs. Particularly in the DDD process, monolayer permeability assays provide important preclinical information in the early stages of drug candidate investigation that decides subsequent *in*

in vivo and clinical testing (15; 30-38). At these early stages though, the major role of monolayer permeability assay is just to provide a qualitative yes or no assessment of whether or not a drug is a substrate or inhibitor of P-gp. If yes, then more in-depth study is conducted on the PK effects and potential DDIs. For this qualitative assessment, standardization of assay cell types or conditions may not be crucial. P_{app} or EfR results may show some variation between labs, but in practice, a compound with a measured EfR of 10 in one lab that has a measured EfR of 12 in another lab will be assessed as a P-gp substrate in either case. An issue arises however, for drugs that show only moderate interaction with P-gp. For these drugs, close consensus would be required between P_{app} or EfR estimates of P-gp activity made in different labs in order for the drug-P-gp interaction to be harmoniously defined across laboratories. There have been reports of drugs that appear as P-gp substrate in a Caco-2 assay, but not in a MDCK-MDR1 assay (39). The consequence of a false negative or a false positive can be respectively, a failure to conduct appropriate follow-up tests to collect critical PK information, or performing needless subsequent studies that do not yield significant *in vivo* or clinical relevance. CL_{P-gp} is very important for its ability to bring consensus to the interpretation of P-gp interactions made using monolayer permeability assays in different laboratories.

3.5 Applying monolayer permeability assay data to IVIVE

Although the use of monolayer permeability assays recommended by regulatory agencies in the early stages of DDD focuses more on simple identification of P-gp substrates and inhibitors, there is substantial interest in industry and academia in more detailed characterization of P-gp interactions because of its important role in absorption, distribution and excretion pharmacokinetics (30; 40; 41). Therefore, monolayer permeability assays are also used as an important tool in *in vitro* to *in vivo* extrapolation (IVIVE).

A drug that is identified as a substantial P-gp substrate by P_{app} or EfR, with an EfR of 20 for example, will then qualitatively be expected to show reduced clinical oral absorption because of broad P-gp expression in the intestines. In order to make any quantitative prediction from the monolayer permeability assay though, data must be properly interpreted to characterize the P-gp activity in a physiologically relevant way.

CL_{P-gp} not only serves as a consensus metric of P-gp activity in monolayer permeability assays, but it provides a quantitative and physiologically relevant assessment of P-gp activity that can be applied directly to quantitative IVIVE. It is particularly useful for quantitative IVIVE because it specifically characterizes P-gp transport activity from the intracellular space, where P-gp accesses substrate. Characterizing P-gp transporter kinetics directly from flux data would be simplifying the system as a single barrier with only P-gp activity, which would only yield apparent kinetics for P-gp. In reality there are several other kinetic processes contributing to flux across the monolayer, the most important of which are described in our 3 compartmental model (42-47).

The physiological relevance of CL_{P-gp} makes it appropriate for application in physiologically-based pharmacokinetic (PBPK) models. These models, as we have described, incorporate chemical information about compounds and physiological and *in vitro* kinetic information into anatomically arranged compartments. Intrinsic clearance, defined as the perfusion-rate-independent clearance of a drug from a system by the cumulative intrinsic activities of the contributing drug metabolizing enzymes and/or transporters, is an essential component of these models. For drug metabolizing enzymes, intrinsic clearance can be characterized from the metabolism kinetics in isolated hepatocyte, microsomal fractions, or recombinant enzyme systems (15; 48-50). For uptake transporters, it can be described from uptake kinetics in isolated hepatocytes or recombinant cell lines (51; 50). With the modeled clearance we describe here in our study, we can produce the intrinsic clearance input for PBPK model efflux transporters from the conventional monolayer permeability assay. In the context of a PBPK, which incorporates all of the dynamically acting ADME proteins and physiological processes, we can understand drugs that appear to interact with P-gp in the monolayer permeability assay but do not necessarily demonstrate clinical P-gp interaction because of the overlapping *in vivo* activity of other ADME enzymes (52).

3.6 Limitations of the experimental approach to estimate CL_{P-gp} (model assumptions)

1. All transwell transport experiments were assumed to operate exclusively under linear conditions in our model.

2. We assumed there were no spatial variations in pH or concentration intracellularly
3. Our steady state model of transport assumes mass balance of drug in the system, when in fact drug is removed during multiple sampling
4. We assumed that digoxin is not subject to any significant metabolism
5. We assumed that neither digoxin, nor inulin were subject to any significant protein or plastic binding in the transwells
6. We simplified the complexity of the model in order to successfully fit the data, by assuming that digoxin clearance was equal in both directions across the apical membrane and equal in both directions across the basolateral membrane.

3.7 Recommendations/future studies

1. In our studies, we investigated P-gp efflux with 2 commonly used monolayer cell types (Caco-2 and LLCPK). In a future study, it would be interesting to include P-gp activity estimates made in MDCK/MDCK-MDR1 monolayers to the linear regression analysis, to confirm that the validity and sensitivity of CL_{P-gp} as a P-gp metric extends to this third commonly used monolayer cell type.
2. Similarly, it would be interesting to include monolayer assays conducted with varied protocols to the linear regression analysis, to see how well our model isolates P-gp activity and accounts for monolayer difference produced by variable laboratory practices.
3. We used the gold standard P-gp probe drug, digoxin, for our study, but future studies may investigate P_{app} , EfR and CL_{P-gp} monolayer permeability assay metrics for other P-gp substrates that may show different permeability or may be less specific to the P-gp transporter.
4. It would be interesting as well to consider effects of P-gp inhibition by drugs and effects on P-gp activity metrics. For example, examining which activity metric is

most sensitive in estimating the inhibitory constant (K_i) for P-gp for a given test drug whose co-administration affects the flux of digoxin in a transwell system.

5. Finally, estimation of absolute P-gp intrinsic activity of P-gp with digoxin using absolute quantification of P-gp by LC-MS/MS would provide critical information for IVIVE.

3.8 Overall conclusion

In conclusion, our findings support our hypothesis that CL_{P-gp} offers a more valid and sensitive estimate of P-gp activity in the monolayer permeability assay, particularly for comparison across different monolayer cell types. The traditional metrics, P_{app} and EfR do not relate well across the many variations of monolayer permeability assay that exist and thus the conclusions drawn by these metrics have limited global value. Conversely, we found that modeled clearance, CL_{P-gp} , seems to account for non-P-gp transcellular and paracellular processes that contribute to monolayer transit, thus providing a more physiologically relevant characterization of P-gp transporter activity. Many efflux transporters, particularly P-glycoprotein, play an important role in drug pharmacokinetics and disposition and *in vitro* characterization of P-gp activity is very important to understanding drug PK and DDIs (30; 40; 41). Modeled clearance provides more physiologically relevant information that can be used for understanding and predicting clinical pharmacokinetics for more successful drug therapy.

3.9 References

1. Guo A, Hu P, Balimane PV, Leibach FH, Sinko PJ (1999) Interactions of a nonpeptidic drug, valacyclovir, with the human intestinal peptide transporter (hPEPT1) expressed in a mammalian cell line. *Journal of Pharmacology and Experimental Therapeutics* 289: 448–454
2. Williams GC, Liu A, Knipp G, Sinko PJ (2002) Direct evidence that saquinavir is transported by multi-drug resistance-associated protein (MRP1) and canalicular multispecific organic anion transporter (MRP2). *Antimicrobial Agents and Chemotherapy* 46: 3456–3462
3. Troutman MD and Thakker DR (2003) Efflux ratio cannot assess P-glycoprotein-mediated attenuation of absorptive transport: asymmetric effect of P-glycoprotein on absorptive and secretory transport across Caco-2 cell monolayers. *Pharmaceutical Research* 20: 1200–1209
4. Tran TT, Mittal A, Gales T, Maleeff B, Aldinger T, Polli JW, Ayrton A, Ellens H, Bentz J (2004) Exact kinetic analysis of passive transport across a polarized confluent MDCK cell monolayer modeled as a single barrier. *Journal of Pharmaceutical Sciences* 93: 2108–2123
5. Goh LB, Spears KJ, Yao D, Ayrton A, Morgan P, Roland Wolf C, Friedberg T (2002) Endogenous drug transporters in *in vitro* and *in vivo* models for the prediction of drug disposition in man. *Biochemical Pharmacology* 64: 1569–1578
6. Kobayashi D, Nozawa T, Imai K, Nezu J, Tsuji A, Tamai I (2003) Involvement of human organic anion transporting polypeptide OATP-B (SLC21A9) in pH-dependent transport across intestinal apical membrane. *Journal of Pharmacology and Experimental Therapeutics* 306: 703–708
7. Hirohashi T, Suzuki H, Chu XY, Tamai I, Tsuji A, Sugiyama Y (2000) Function and expression of multidrug resistance-associated protein family in human colon adenocarcinoma cells (Caco-2). *Journal of Pharmacology and Experimental Therapeutics* 292: 265–270
8. Okuwaki M, Takada T, Iwayanagi Y, Koh S, Kariya Y, Fujii H, Suzuki H (2007) LXR alpha transactivates mouse organic solute transporter alpha and beta via IR-1 elements shared with FXR. *Pharmaceutical Research* 24: 390–398
9. Kullak-Ublick GA, Ismail MG, Stieger B, Landmann L, Huber R, Pizzagalli F, Fattinger K, Meier PJ, Hagenbuch B (2001) Organic anion-transporting polypeptide B (OATP-B) and its functional comparison with three other OATPs of human liver. *Gastroenterology* 120: 525–533
10. Lowes S, Cavet ME, Simmons NL (2003) Evidence for a non-MDR1 component in digoxin secretion by human intestinal Caco-2 epithelial layers. *European Journal of Pharmacology* 458: 49–56

11. Hilgendorf C, Ahlin G, Seithel A, Artursson P, Ungell AL, Karlsson J (2007) Expression of thirty-six drug transporter genes in human intestine, liver, kidney, and organotypic cell lines. *Drug Metabolism and Disposition* 35: 1333–1340
12. Hayeshi R, Hilgendorf C, Artursson P, Augustijns P, Brodin B, Dehertogh P, Fisher K, Fossati L, Hovenkamp E, Korjamo T, Masungi C, Maubon N, Mols R, Müllertz A, Mönkkönen J, O'Driscoll C, Oppers-Tiemissen HM, Ragnarsson EG, Rooseboom M, Ungell AL (2008) Comparison of drug transporter gene expression and functionality in Caco-2 cells from 10 different laboratories. *European Journal of Pharmaceutical Sciences* 35: 383–396
13. Walter E and Kissel T (1994) Transepithelial transport and metabolism of thyrotropin-releasing hormone (TRH) in monolayers of a human intestinal cell line (Caco-2): evidence for an active transport component? *Pharmaceutical Research* 11: 1575–1580
14. Walter E and Kissel T (1995) Heterogeneity in the human intestinal cell line Caco-2 leads to differences in transepithelial transport. *European Journal of Pharmaceutical Sciences* 3: 215–230
15. FDA Guidance for Industry (2012) Drug Interaction Studies — Study Design, Data Analysis, and Implications for Dosing and Labeling
16. Zhang L, Strong JM, Qiu W, Lesko LJ, Huang SM (2006) Scientific perspectives on drug transporters and their role in drug interactions. *Molecular Pharmaceutics* 3: 62–69
17. Balimane PV, Han YH, Chong S (2006) Current industrial practices of assessing permeability and P-glycoprotein interaction. *AAPS Journal* 8: E1–E13
18. Keogh JP and Kunta JR (2006) Development, validation and utility of an *in vitro* technique for assessment of potential clinical drug-drug interactions involving P-glycoprotein. *European Journal of Pharmaceutical Sciences* 27: 543–554
19. Polli JW, Wring SA, Humphreys JE, Huang L, Morgan JB, Webster LO, Serabjit-Singh CS (2001) Rational use of *in vitro* P-glycoprotein assays in drug discovery. *Journal of Pharmacology and Experimental Therapeutics* 299: 620–628
20. Rautio J, Humphreys JE, Webster LO, Balakrishnan A, Keogh JP, Kunta JR, Serabjit-Singh CJ, Polli JW (2006) *In vitro* p-glycoprotein inhibition assays for assessment of clinical drug interaction potential of new drug candidates: a recommendation for probe substrates. *Drug Metabolism and Disposition* 34: 786–792

21. Hidalgo IJ, Raub TJ, Borchardt RT (1989) Characterization of the human colon carcinoma cell line (Caco-2) as a model system for intestinal epithelial permeability. *Gastroenterology* 96: 736–749
22. Hochman JH, Pudvah N, Qiu J, Yamazaki M, Tang C, Lin JH, Prueksaritanont T (2004) Interactions of human P-glycoprotein with simvastatin, simvastatin acid, and atorvastatin. *Pharmaceutical Research* 21(9): 1686-91
23. Zhu HJ, Wang JS, Markowitz JS, Donovan JL, Gibson BB, Gefroh HA, Devane CL (2006) Characterization of P-glycoprotein inhibition by major cannabinoids from marijuana. *Journal of Pharmacology and Experimental Therapeutics* 317(2): 850-7
24. Taipalensuu J, Tavelin S, Lazorova L, Svensson AC, Artursson P (2004) Exploring the quantitative relationship between the level of MDR1 transcript, protein and function using digoxin as a marker of MDR1-dependent drug efflux activity. *European Journal of Pharmaceutical Sciences* 21: 69–75
25. Behrens I and Kissel T (2003) Do cell culture conditions influence the carrier-mediated transport of peptides in Caco-2 cell monolayers? *European Journal of Pharmaceutical Sciences* 19: 433–442
26. Volpe DA (2008) Variability in Caco-2 and MDCK cell-based intestinal permeability assays. *Journal of Pharmaceutical Sciences* 97: 712–725
27. Miliotis T, Ali L, Palm JE, Lundqvist AJ, Ahnoff M, Andersson TB, Hilgendorf C (2011) Development of a highly sensitive method using liquid chromatography-multiple reaction monitoring to quantify membrane P-glycoprotein in biological matrices and relationship to transport function. *Drug Metabolism and Disposition* 39: 2440–2449
28. Bentz J, O'Connor MP, Bednarczyk D, Coleman J, Lee C, Palm J, Pak YA, Perloff ES, Reyner E, Balimane P, Brännström M, Chu X, Funk C, Guo A, Hanna I, Herédi-Szabó K, Hillgren K, Li L, Hollnack-Pusch E, Jamei M, Lin X, Mason AK, Neuhoff S, Patel A, Podila L, Plise E, Rajaraman G, Salphati L, Sands E, Taub ME, Taur JS, Weitz D, Wortelboer HM, Xia CQ, Xiao G, Yabut J, Yamagata T, Zhang L, Ellens H (2013) Variability in P-glycoprotein inhibitory potency (IC₅₀) using various *in vitro* experimental systems: implications for universal digoxin drug-drug interaction risk assessment decision criteria. *Drug Metabolism and Disposition* 41(7): 1347-66
29. Sambuy Y, De Angelis I, Ranaldi G, Scarino ML, Stamatii A, Zucco F (2005) The Caco-2 cell line as a model of the intestinal barrier: influence of cell and culture-related factors on Caco-2 cell functional characteristics. *Cell Biology and Toxicology* 21: 1–26
30. International Transporter Consortium, Giacomini KM, Huang SM, Tweedie DJ, Benet LZ, Brouwer KL, Chu X, Dahlin A, Evers R, Fischer V, Hillgren KM,

- Hoffmaster KA, Ishikawa T, Keppler D, Kim RB, Lee CA, Niemi M, Polli JW, Sugiyama Y, Swaan PW, Ware JA, Wright SH, Yee SW, Zamek-Gliszczynski MJ, Zhang L (2010). Membrane transporters in drug development. *Nature Reviews Drug Discovery* 9(3): 215–236
31. Bjornsson TD, Callaghan JT, Einolf HJ, Fischer V, Gan L, Grimm S, Kao J, King SP, Miwa G, Ni L, Kumar G, McLeod J, Obach RS, Roberts S, Roe A, Shah A, Snikeris F, Sullivan JT, Tweedie D, Vega JM, Walsh J, Wrighton SA (2003) The conduct of *in vitro* and *in vivo* drug-drug interaction studies: a Pharmaceutical Research and Manufacturers of America (PhRMA) perspective. *Drug Metabolism and Disposition* 31: 815–832
 32. Hsiao P, Bui T, Ho RJ, Unadkat JD (2007) *In vitro* to *in vivo* prediction of p-glycoprotein based drug interactions at the human and rodent blood-brain barrier. *Drug Metabolism and Disposition* 34: 786–792
 33. Miners JO, Smith PA, Sorich MJ, McKinnon RA, Mackenzie PI (2004) Predicting human drug glucuronidation parameters: application of *in vitro* and *in silico* modeling approaches. *Annual Review of Pharmacology and Toxicology* 44: 1–25
 34. Hidalgo I (2001) Assessing the absorption of new pharmaceuticals. *Current Topics in Medicinal Chemistry* 1: 385–401
 35. Marchetti S, Mazzanti R, Beijnen JH, Schellens JH (2007) Concise review: Clinical relevance of drug-drug and herb-drug interactions mediated by the ABC transporter ABCB1 (MDR1, P-glycoprotein). *Oncologist* 12: 927–941
 36. Huang C, Zheng M, Yang Z, Rodrigues AD, Marathe P (2008) Projection of exposure and efficacious dose prior to first-in-human studies: how successful have we been?. *Pharmacology Research* 25: 713–726
 37. Zhang L, Reynolds KS, Zhao P, Huang SM (2010) Drug interactions evaluation: an integrated part of risk assessment of therapeutics. *Toxicology and Applied Pharmacology* 243: 134–145
 38. Yengi LG, Leung L, Kao J (2007) The evolving role of drug metabolism in drug discovery and development. *Pharmaceutical Research* 24(5): 842–58
 39. Taub ME, Podila L, Ely D, Almeida I (2005) Functional assessment of multiple P-glycoprotein (P-gp) probe substrates: influence of cell line and modulator concentration on P-gp activity. *Drug Metabolism and Disposition* 33(11): 1679–87
 40. Shitara Y, Horie T, Sugiyama Y (2006) Transporters as a determinant of drug clearance and tissue distribution. *European Journal of Pharmaceutical Sciences* 27(5): 425–46

41. Giacomini KM, Huang SM, Tweedie DJ, Benet LZ, Brouwer KL, Chu X, Dahlin A, Evers R, Fischer V, Hillgren KM, Hoffmaster KA, Ishikawa T, Keppler D, Kim RB, Lee CA, Niemi M, Polli JW, Sugiyama Y, Swaan PW, Ware JA, Wright SH, Yee SW, Zamek-Gliszczynski MJ, Zhang L (2010) Membrane transporters in drug development. *Nature Reviews Drug Discovery* 9: 215–236
42. Ito K, Kusuhara H, and Sugiyama Y (1999) Effects of intestinal CYP3A4 and P-glycoprotein on oral drug absorption—theoretical approach. *Pharmaceutical Research (NY)* 16: 225–231
43. González-Alvarez I, Fernández-Teruel C, Garrigues TM, Casabo VG, Ruiz-García A, Bermejo M (2005) Kinetic modelling of passive transport and active efflux of a fluoroquinolone across Caco-2 cells using a compartmental approach in NONMEM. *Xenobiotica* 35(12): 1067-88
44. Bourdet DL, Pollack GM, Thakker DR (2006) Intestinal absorptive transport of the hydrophilic cation ranitidine: a kinetic modeling approach to elucidate the role of uptake and efflux transporters and paracellular vs. transcellular transport in Caco-2 cells. *Pharmaceutical Research* 23: 1178–1187
45. Ho NFH, Raub TJ, Burton PS, Barsuhn CL, Adson A, Audus KL, Borchardt RT (2000) Quantitative approaches to delineate passive transport mechanisms in cell culture monolayers, in *Transport Processes in Pharmaceutical Systems* (Amidon GL, Lee PI, and Topp EM eds) pp 219–317, Marcel Dekker, New York
46. Tran TT, Mittal A, Aldinger T, Polli JW, Ayrton A, Ellens H, Bentz J (2005) The elementary mass action rate constants of P-gp transport for a confluent monolayer of MDCKII-hMDR1 cells. *Biophysical Journal* 88: 715–738
47. Sun H, Pang KS (2008) Permeability, Transport, and Metabolism of Solutes in Caco-2 Cell Monolayers: A Theoretical Study. *Drug Metabolism and Disposition* 36(1): 102–123
48. Kedderis GL. (2007). *In vitro* to *in vivo* extrapolation of metabolic rate constants for physiologically based pharmacokinetic models. In: Lipscomb, JC, Ohanian EV. (eds.) *Toxicokinetics and risk assessment*. New York: Informa healthcare
49. Gómez-Lechón MJ, Donato MT, Castell JV, Jover R (2003) Human hepatocytes as a tool for studying toxicity and drug metabolism. *Current Drug Metabolism* 4(4): 292-312
50. Hewitt NJ, Lecluyse EL, Ferguson SS (2007) Induction of hepatic cytochrome P450 enzymes: methods, mechanisms, recommendations, and *in vitro-in vivo* correlations. *Xenobiotica* 37: 1196–1224
51. Shitara Y, Itoh T, Sato H, Li AP, Sugiyama Y (2003) Inhibition of transporter-mediated hepatic uptake as a mechanism for drug-drug interaction between

cer- ivastatin and cyclosporin A. *Journal of Pharmacology and Experimental Therapeutics* 304: 610–616

52. Cummins CL, Jacobsen W, Benet LZ (2002) Unmasking the dynamic interplay between intestinal P-glycoprotein and CYP3A4. *Journal of Pharmacology and Experimental Therapeutics* 300: 1036–1045

Curriculum Vitae

Name: Alex D. Morgan

Post-secondary Education and Degrees: University of Western Ontario
London, Ontario, Canada
2005-2009 B.MSc.

The University of Western Ontario
London, Ontario, Canada
2009-2015 M.Sc.

Honours and Awards: Frederick Banting and Charles Best Canada Graduate
Scholarship
Awards: 2010-2011

Abstracts Submitted:

Morgan, Alex D. (2012). Absolute quantification of P-glycoprotein drug transport activity for *in vitro* to *in vivo* pharmacokinetic prediction. Poster presented at the 2012 annual meeting of the Canadian Society of Pharmacology and Therapeutics, Toronto, Ontario.

Morgan, Alex D. (2011, July). Quantitative *in vitro* to *in vivo* prediction of P-glycoprotein-mediated drug transport. Invited to give an oral presentation and poster presentation for the 41st annual Gordon Research Conferences on Drug Metabolism, Holderness, New Hampshire.

Morgan, Alex D. (2011, May). Quantitative *in vitro* to *in vivo* prediction of P-glycoprotein-mediated drug transport. Poster presented at the 2011 annual meeting of the Canadian Society of Pharmacology and Therapeutics, Montreal, Quebec.

Morgan, Alex D. (2011, May). Quantitative *in vitro* to *in vivo* prediction of P-glycoprotein-mediated drug transport. Poster presented at the 2011 University of Western Ontario, Department of Medicine Research Day, London, Ontario.

Morgan, Alex D. (2010, June). Quantitative *in vitro* to *in vivo* prediction of P-glycoprotein-mediated drug transport. The 2010 annual meeting of the Canadian Society of Pharmacology and Therapeutics, Toronto, Ontario.

Morgan, Alex D. (2010, March). Quantitative *in vitro* to *in vivo* prediction of P-glycoprotein-mediated drug transport. The 2010 Lawson Research Day, London, Ontario.